

Copyright Warning & Restrictions

The copyright law of the United States (Title 17, United States Code) governs the making of photocopies or other reproductions of copyrighted material.

Under certain conditions specified in the law, libraries and archives are authorized to furnish a photocopy or other reproduction. One of these specified conditions is that the photocopy or reproduction is not to be “used for any purpose other than private study, scholarship, or research.” If a user makes a request for, or later uses, a photocopy or reproduction for purposes in excess of “fair use” that user may be liable for copyright infringement,

This institution reserves the right to refuse to accept a copying order if, in its judgment, fulfillment of the order would involve violation of copyright law.

Please Note: The author retains the copyright while the New Jersey Institute of Technology reserves the right to distribute this thesis or dissertation

Printing note: If you do not wish to print this page, then select “Pages from: first page # to: last page #” on the print dialog screen

The Van Houten library has removed some of the personal information and all signatures from the approval page and biographical sketches of theses and dissertations in order to protect the identity of NJIT graduates and faculty.

EFFECT OF LIQUID VISCOSITY ON PERFORMANCE
OF WIRE MESH ENTRAINMENT SEPARATORS

BY

RAYMOND P. VOGEL

A THESIS

PRESENTED IN PARTIAL FULFILLMENT OF

THE REQUIREMENTS FOR THE DEGREE

OF

MASTER OF SCIENCE IN CHEMICAL ENGINEERING

AT

NEWARK COLLEGE OF ENGINEERING

This thesis is to be used only with due regard to the rights of the author(s). Bibliographical references may be noted, but passages must not be copied without permission of the College and without credit being given in subsequent written or published work.

Newark, New Jersey
1964

2625-2-6

ABSTRACT

The knitted wire mesh entrainment separator, commonly referred to as a demister*, is in common use to separate entrained liquid from vapor streams. However, little quantitative information is available concerning the effect of physical properties of the entrained liquid on allowable gas velocities.

Studies were made on two demister styles to determine the effect of liquid viscosity on demister performance. Liquid viscosities from 0.9 to 12 centipoise were investigated using water, glycerine-water mixtures and heavy no. 2 fuel oil as the test liquids. Air was used as the gas medium in all cases.

Regression analysis of the test data indicates that by increasing viscosity from 0.9 to 12 centipoise the allowable vapor velocity is decreased by only 10%. The effects of other liquid and demister properties on flooding velocity can be approximated by the following proposed equation:

$$V_{\text{FLOOD}} = \frac{5.45 (P_L)^{0.47} (\gamma)^{0.20}}{(a/\epsilon^3)^{0.30} (\mu_L)^{0.036} (G_L)^{0.11}}$$

* Registered trademark of Otto York Company.

APPROVAL OF THESIS

FOR

DEPARTMENT OF CHEMICAL ENGINEERING
NEWARK COLLEGE OF ENGINEERING

BY

FACULTY COMMITTEE

APPROVED:

NEWARK, NEW JERSEY

FEBRUARY, 1964

ACKNOWLEDGEMENTS

The author expresses his appreciation to the following individuals for their contributions to this research project:

Prof. J.J. Salamone, Chemical Engineering Department, Newark College of Engineering, for his guidance and encouragement as well as the supply of various items of equipment.

Mr. H.F. Schroeder, Esso Research and Engineering Company, who constructed the original test apparatus for his earlier studies.

Messrs. S.W. Clark, A.J. Schilling, A.A. Giacobbe, J. Keil California Oil Company, Perth Amboy, N.J., for the supply of additional items of test equipment, laboratory determination of test liquid physical properties and the processing of test data for regression analysis on the IBM 7094 digital computer of Standard Oil of California.

Mr. E.W. Poppele, Otto York Company, Inc., for supplying the essential test demisters as well as for his valuable comments on his earlier experiments and industrial experience.

Mrs. R.P. Vogel, for her many contributions, the latest of which is typing this report.

TABLE OF CONTENTS

	<u>Page No.</u>
Abstract	11
Acknowledgements	1V
List of Figures	V11
List of Tables	V111
Introduction	1
Theory	3
Description of Test Apparatus	6
Air Handling Section	6
Liquid Handling System	8
Test Column	9
Experimental Procedure	11
Test Column Preparation	11
Air Section Startup	12
Experimental Data	12
Determination of Load and Flood Points	12
Liquid Properties	15
Experimental Results	17
Data Correlation	27
Published Correlations	27
Linear Regression Analysis	30
Conclusions	37
Recommendations	39
Nomenclature	40

TABLE OF CONTENTS (Cont'd)

		<u>Page No.</u>
Appendix A	Equipment Details	41
Appendix B	Experimental Data	53
Appendix C	Physical Properties of Test Liquids	95
Appendix D	Data Correlation	98
References		103

LIST OF FIGURES

<u>Figure No.</u>	<u>Title</u>	<u>Page No.</u>
1	Equipment Schematic Diagram	7
2	Flooding Velocity, 421 Demister	20
3	Loading Velocity, 421 Demister	21
4	Flooding Velocity, 931 Demister	22
5	Loading Velocity, 931 Demister	23
6	Demister Pressure Drop At Flood Point	25
7	Demister Entrainment Factor (K_F) At The Flood Point	28
8	Data Correlation Using Proposal Of Poppelo	29
9	Regression Equation For Flooding Velocity	33
10	Regression Equation For Loading Velocity	34
A-1	Orifice Calibration	48
A-2	Air Density	49
A-3	Calculated Air Velocities	50
A-4	Rotometer Calibration, Water-Glycerine	51
A-5	Rotometer Calibration, Heavy No. 2 Fuel Oil	52
B-1 Thru B-32	Experimental Determination Of Demister Load Point And Flood Point	63-94
C-1	Surface Tension Of Test Liquids	96
C-2	Viscosity Of Glycerine-Water Mixtures	97

LIST OF TABLES

		<u>Page No.</u>
Table 1	Data Summary	18
Table 3-1 Thru 3-9	Experimental Data	54-62
Table D-1	Calculated Data For Figures 7 And 8	99
Table D-2	Regression Coefficients From Stepwise Linear Regression Analysis	100
Table D-3	Regression Output, Step 6, Flooding Velocity	101
Table D-4	Regression Output, Step 6, Loading Velocity	102

INTRODUCTION

Demisters are commonly used to separate entrained liquid from a vapor stream in equipment such as distillation columns, separator drums and evaporators. Although demisters have proven effective in this service, the effect of variables on demister performance have not been completely defined.

York and Poppele⁽⁴⁾ have summarized the variables which affect allowable gas velocities through mesh demisters. These factors are: (a) gas density, (b) liquid surface tension, viscosity and entrainment loading rate, and (c) specific surface of the wire mesh demister. York⁽³⁾ has proposed application of the Souders-Brown⁽⁶⁾ expression to define the effects of liquid and gas densities on allowable vapor velocities. This expression (equation 1) considers only the variables of gas and liquid densities and is inadequate to predict demister performance in systems where the other variables may have significant effects.

Poppele⁽²⁾ established the effect of liquid entrainment loading on two demister styles using the water/air system. Schroeder⁽¹⁾ studied the effects of surface tension by using surfactants in the water/air system and verified the work of Poppele⁽²⁾. Liquid viscosity was the remaining liquid property to evaluate.

The purpose of this study was to study the effect of liquid viscosity on allowable demister vapor velocity. Viscosities ranging from 0.9 to 12 centipoises were studied using systems of water/air, glycerine-water/air and heavy no. 2 fuel oil/air. Two demister styles were used and the liquid loading rates were varied from 25 to 400 #/hr.-ft.². Since the density and surface tension of the test liquids were not constant, the effects of these variables as well as viscosity were determined by stepwise linear regression analysis of the experimental results.

THEORY

The benefits derived from the use of a demister result from its ability to coalesce small entrained particles. The larger particles thus formed have entrainment velocities which are higher than the originally entrained particle and can, therefore, settle through the vapor stream to the bulk of the liquid phase.

A dry demister has a very high void fraction and can tolerate high velocities with only small pressure drop. As entrained liquid is coalesced, the free flow area for the vapor decreases and velocities within the demister are higher than the superficial velocity based on total column area. By increasing the vapor velocity through a demister we will eventually reach a point where the upward frictional force of the air on the particle is equal to the downward gravitational force on the particle. Further increase in velocity will result in a net upward force which will carry the particle through the top demister surface. This carryover is called flooding. The flooding velocity is defined as the superficial vapor velocity at which flooding starts.

Equation (1) shows the theoretical velocity at which the net vertical force is zero on a freely suspended liquid droplet.

$$V = K \sqrt{(\rho_L - \rho_G) / \rho_G} \quad (1)$$

This equation has been applied by York(3) to define the effect of liquid and gas density on demister

flooding velocity. This equation is not rigorous for direct application to demisters, and values of the entrainment factor (K) must be determined experimentally. The need for experimental evaluation of K is obvious when we consider the following:

- (1) Equation (1) was derived for freely falling suspended droplets. In demisters the droplets are suspended on wire mesh. Therefore, forces between the liquid and wire resulting from surface tension and viscosity will affect the velocity at which a particle will be entrained above the demister.
- (2) The velocity (V) in equation (1) is the superficial vapor velocity based on column diameter. Local velocity within the demister is higher than the superficial vapor velocity depending upon demister properties, liquid load and particle size of the coalesced liquid.
- (3) The value of the entrainment factor (K) is not constant as implied by the equation form. K is directly related to the diameter of the coalesced particle and inversely related to the drag coefficient. Particle diameter is a function of liquid surface tension, liquid density, to a lesser extent of liquid viscosity, and of the relative

volumes of vapor and liquid(7). The drag coefficient is a function of Reynolds number and particle sphericity. Reynolds number, in turn, is dependent upon particle diameter.

Until a more rigorous equation is developed for demisters, the effects of variables on allowable vapor velocity must be determined experimentally. Actual performance of demisters and the procedure used to determine demister flooding velocities are discussed in detail under EXPERIMENTAL PROCEDURE.

DESCRIPTION OF TEST APPARATUS

A schematic drawing of the test apparatus is shown in Figure 1. The apparatus is comprised of three basic sections, namely, (1) air handling section, (2) liquid handling system and (3) the test column. Each of these sections is discussed separately below. Additional equipment details are given in Appendix A.

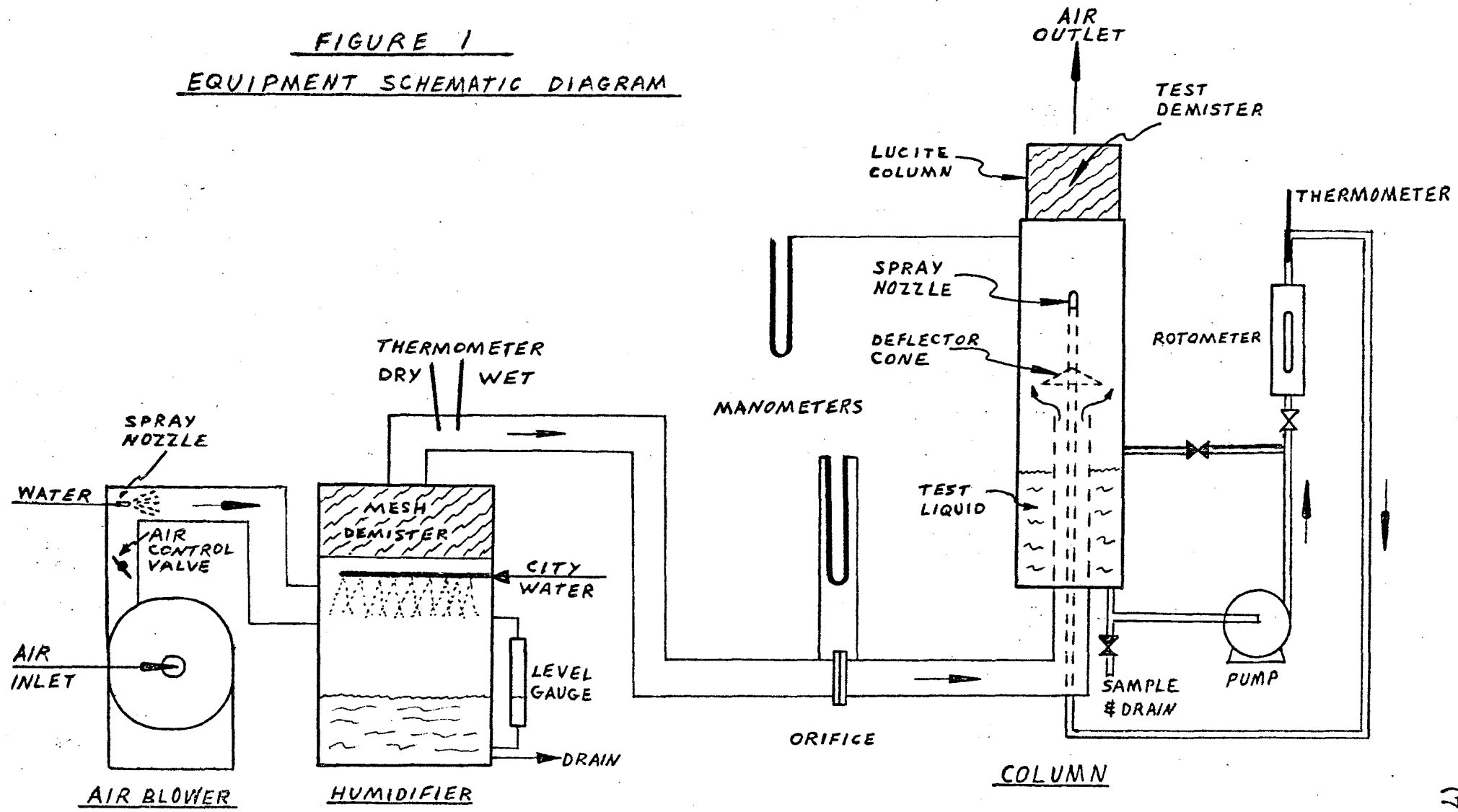
AIR HANDLING SECTION

The purpose of this equipment is to provide a measured quantity of air to the test column. Control of both the temperature and humidity of the air is necessary to minimize vaporization losses of the test liquid.

Air is compressed in turbo blowers (two in parallel) which results in substantial increase in temperature and decrease in humidity. Primary cooling and humidification is obtained by a water spray into the blower discharge line. Secondary humidification is accomplished in the humidifier (55 gallon drum) where the air is contacted with additional water sprays. The air leaves the humidifier through a wire mesh demister to prevent water carryover into the test column. This treatment results in air to the test column at 80-100°F and 80% humidity.

Air flow is regulated by a butterfly valve in the

FIGURE 1
EQUIPMENT SCHEMATIC DIAGRAM



blower discharge line. Flow rate is calculated by standard orifice calculation methods (8) from orifice pressure drop measurements. Details of orifice plate and manometer are given in Appendix A, page 44.

The air lines are 4 inch diameter sheet metal pipe. All seams are sealed with furnace pipe cement to prevent any air leakage.

LIQUID HANDLING SYSTEM

The purpose of this equipment is to deliver the desired quantity of test liquid to the bottom surface of the test demister in a full cone spray.

The bottom section of the test column is used as a reservoir for the test liquid. The liquid is pumped through a nozzle so as to completely impinge upon the bottom surface of the test demister. Liquid temperature is measured with a mercury thermometer inserted into the rotometer outlet line. The liquid which drains from the demister drops back to the reservoir and is recirculated.

A bypass line is available between the pump discharge and reservoir. Between runs this line is used to mix test liquid to maintain as uniform a composition as possible (particularly for water-glycerine mixtures). A connection is available for sampling between runs and draining the test liquid when required.

Test liquid is prevented from draining into the air inlet line by a deflector cone mounted to the liquid line 3 inches above the air inlet line.

TEST COLUMN

The test column is comprised of a long bottom section of 9 inch diameter stove pipe upon which is attached (air tight) a short 8 inch O.D. lucite tube. The test demister is contained in the lucite tube about 28 inches above the end of the air inlet line. The liquid spray nozzle is about 8 inches below the test demister. Slight adjustment is made to get complete impingement of liquid on the bottom demister surface.

The demister performance is determined almost entirely on observation of pressure drop. A water manometer is used to measure demister pressure drop.

The major equipment in the air handling section and test column are those constructed by H. F. Schroeder (1).

Modifications to his equipment include:

- (1) Piping a second blower in parallel to the first to obtain required air rates to test the 931 demister.
- (2) Installation of the water spray into the blower discharge.

- (3) Cementing seams in air system to replace tape which had deteriorated with time.
- (4) Revise humidifier water flow scheme.
- (5) Install deflector cone in test column.

EXPERIMENTAL PROCEDURE

TEST COLUMN PREPARATION

The spray nozzle was selected based on the desired liquid loading rate. It was found that the best liquid spray was obtained when the liquid pump was operated at full capacity and control valve wide open. Changes in liquid rate from run to run were therefore accomplished by nozzle changes. After installing the nozzle, liquid was circulated to check spray impingement on the bottom of the demister.

The test demister was then placed in position in the lucite column. To minimize nozzle changes the test runs on the 931 and 421 demisters were usually made consecutively at a given liquid rate. After each test run the demister was removed either to change the nozzle or to change to the other demister.

Test liquid circulation was started. Slight adjustment (closing) of the liquid control valve was usually required to stabilize rotometer reading. This also provided sufficient control to maintain constant liquid rates throughout the run to compensate for reduction in liquid rate due to slight fouling of the nozzle filter.

AIR SECTION STARTUP

Water rate to the secondary spray was adjusted to establish a constant water level in the bottom of the humidifier. The air blower was started with the air control valve in the closed position. Air rate was increased to obtain a small orifice differential pressure. The wet bulb thermometer was moistened with water and the air system was brought to equilibrium (80-100°F dry bulb temperature and 80% humidity).

EXPERIMENTAL DATA

Air rate was varied from velocities below the load point to velocities beyond the flooding point. At each air rate the system was allowed to attain equilibrium. Data recorded includes (1) time, (2) liquid rate and temperature, (3) orifice and demister differential pressure, (4) air wet and dry bulb temperature. Experimental data are included in Appendix B.

DETERMINATION OF LOAD AND FLOOD POINTS.

For each air rate the orifice pressure drop (function of air velocity) was plotted against the demister pressure drop on log-log paper. These plots are shown in Appendix B, Figures B1 thru B32. Plots were made during the run to assure that sufficient data points were available to define

loading and flooding velocities. These plots were also a good indication whether or not equilibrium was obtained.

At air rates below the loading point the log-log plot yields a linear relation with gradual increase in demister pressure drop as air is increased up to loading velocity. The increase is attributed to that associated with increased velocity as well as the accumulation of a larger quantity of liquid within the demister.

Increasing velocity beyond the load point results in a more rapid increase of demister pressure drop as the quantity of liquid accumulation increases and the liquid level in the demister increases more rapidly. A linear relation is still obtained but with higher slope.

Further increases in air rate eventually resulted in liquid carryover and reentrainment above the demister. A number of pressure drops were recorded beyond the point of liquid carryover. It was found that these points also formed a straight line plot but the slope of this line was much lower than the slope obtained below the load point. The quantity of liquid within the demister had reached an equilibrium value and the increased demister pressure drop was due to air velocity increases only.

It was decided to define this second break in the curve as the demister flooding point. This appeared to be

a more quantitative method of defining the flood point which would result in greater repeatability. Earlier investigations by Schroeder (1) and Poppele (2) defined flooding as the inception of liquid break through. Inception of liquid breakthrough can mean different things to different experimenters whereas a break in a curve is quantitative.

After flooding the demister additional data points were obtained between load and flood points as well as below the load point. The data between load and flood points fell along the original curve and aided in defining the flood point.

At velocities below the load point there was a tendency for demister pressure drop to be slightly above the original curve. This is best illustrated in the curves for Runs 33 thru 36 (Figures B-29 thru B-32). This higher demister pressure drop is most likely due to the presence of a small quantity of liquid remaining in the demister resulting in less flow area for the air. The load point (velocity) could be affected by as much as 5% depending on whether the data was obtained on a wet or dry demister. Flooding velocity would not be significantly affected.

Worthy of mention is an observation on Run No. 1,

Figure B-1. At very low velocities (less than 5 ft/sec.) there seems to be a fourth linear portion to the demister pressure drop curve. The effect of air velocity on pressure drop is very small most likely due to the absence of liquid in the test demister.

Equilibrium conditions were reached quickly, usually within one minute, for air rates below the load point and above the flood point. However, demister pressure drop changed very slowly between flood and load points particularly for low liquid rates (55 #/hr-ft^2) on the 931 demister. At times it was necessary to allow thirty minutes to attain steady state.

LIQUID PROPERTIES

Densities of test liquids were obtained between each run. Some evaporation of water from water glycerine mixtures was apparent.

Samples were taken occasionally for determination of surface tension and viscosity. Densities were also obtained, and checked favorably with the first determination.

Surface tension of water was found to decrease with time. Fresh water gave surface tension equivalent to that contained in standard reference books. However, prolonged

testing of the same water sample resulted in decrease in surface tension.

The surface tensions of water-glycerine mixtures were below the surface tension stated in various reference books of physical properties. The most likely cause of lower surface tension is the presence of some unknown contamination. Measurements are considered accurate since checks were made on both distilled water and glycerine. Very good agreement was obtained on these checks with published surface tensions.

The measured surface tensions were plotted as a function of the time on a particular sample. Surface tensions for the other runs were then estimated from this curve (see Figure C-1)

Because of water evaporation from the water-glycerine mixtures, the density and viscosity increased slightly with time. Average densities were used and the viscosity of the mixture was determined from Figure C-2 which are published viscosities. Viscosities of samples agreed closely with published data.

EXPERIMENTAL RESULTS

A total of 36 runs was performed covering the following range of variables:

Demister Style	York styles 421 and 931
Liquid Density	52-73 #/ft ³
Liquid Viscosity	0.9-12 centipoise
Liquid Loading Rates	25-400 #/hr-ft ²
Liquid Surface Tension	31-72 dynes/cm.
Air Density	0.071 #/ft ³
Air Velocity	5-24 ft./sec.

Flooding velocities, loading velocities, and liquid properties were determined as previously discussed in "EXPERIMENTAL PROCEDURE". These variables for each test run are summarized in Table 1. Runs No. 3, 4, 7, 15 and 29 are not included in the summary. Runs 3 and 7 were inconclusive because test liquid entered the demister manometer lead line. Run 4 was performed using a smaller orifice which was not used in other runs and therefore was not calibrated. Run 15 was a partial run which checked run no. 10. Run 29 was not completed since it was not possible to obtain adequate spray with 85% glycerine (50 centipoise).

Dimensional units of FT./Sec. are used for flooding and loading velocities for the purpose of discussion of test results. Evaluation of the variables which affect demister

TABLE 1
DATA SUMMARY

D E S C R I B E R	R U N N O.	TEST LIQUID					AIR				
		LIQUID	T _L	P _L	M _L	G _L	Y	P _G	V _L	V _F	
	1	421	Water	78	62.3	0.89	400	70.5	.0702	9.8	11.3
	2	421	"	76	62.3	0.92	380	69.1	.0714	10.1	11.0
	5	421	"	79	62.3	0.88	385	68.6	.0713	11.0	12.0
	6	931	"	78	62.3	0.89	385	70.4	.0716	9.1	15.5
	8	421	"	72	62.3	0.96	110	70.3	.0721	12.4	13.3
	9	931	"	81	62.3	0.86	110	68.7	.0717	14.3	15.8
	10	931	"	80	62.3	0.87	410	67.3	.0715	13.8	14.3
	11	931	"	82	62.3	0.85	55	68.7	.0712	13.4	16.3
	12	931	"	84	62.3	0.83	55	67.8	.0714	13.0	16.6
	13	421	"	85	62.3	0.82	55	65.0	.0708	12.0	14.1
	14	421	"	76	62.3	0.92	400	69.8	.0719	10.4	10.7
	16	931	25% glyc.	80	66.1	1.8	390	58.0	.0718	13.1	14.6
	17	421	33% "	81	67.1	2.3	360	58.6	.0715	9.3	9.9
	18	421	33% "	84	67.1	2.2	85	57.2	.0713	10.6	11.7
	19	931	33% "	86	67.2	2.1	85	55.5	.0710	12.1	15.1
	20	931	41% "	86	68.8	2.8	107	53.8	.0720	14.5	17.0
	21	421	43% "	81	69.4	3.4	142	52.8	.0716	10.9	12.2
	22	421	52% "	82	70.4	5.1	135	58.1	.0715	11.3	11.9
	23	931	57% "	85	71.3	6.2	120	56.4	.0713	14.9	16.8
	24	931	65% "	84	72.5	10.3	40	58.6	.0714	14.8	17.2
	25	931	65% "	81	72.5	11.5	55	57.1	.0722	13.5	17.3
	26	931	65% "	88	72.5	9.5	265	56.0	.0716	14.4	16.0
	27	421	68% "	87	73.1	12.0	230	54.5	.0717	9.2	9.8
	28	421	68% "	86	73.1	12.3	162	53.0	.0718	9.8	10.6
	30	421	38% "	81	68.2	2.8	145	58.2	.0722	10.1	12.6
	31	421	Hvy. 2 Oil	85	52.5	3.7	280	31.5	.0717	7.0	7.7
	32	931	"	92	52.5	3.7	270	31.5	.0719	9.1	10.9
	33	421	"	85	52.5	3.7	25	31.5	.0715	11.2	12.3
	34	421	"	91	52.5	3.7	95	31.5	.0711	8.4	9.3
	35	931	"	88	52.5	3.7	95	31.5	.0713	11.0	12.8
	36	421	"	90	52.5	3.7	107	31.5	.0712	8.6	10.3

performance should not be affected since all test runs were made at constant air density. However, it is recognized that vapor mass velocity may ultimately provide the best definition of demister performance for systems which either use other than air or are operated above or below atmospheric pressure.

The flooding and loading velocities for the 421 and 931 style demisters are plotted in Figures 2 thru 5 as a function of liquid loading. For convenience of presentation the water-glycerine data are presented in only two groups, 25-52 wt. % glycerine and 65-68 wt. % glycerine. The data of Poppele⁽²⁾ is shown for comparison of results for the air/water system.

All plots show the same general trend in the effect of liquid properties on flooding and loading velocities. Velocities for water are 3-4 ft./sec. above those for Heavy No. 2 Fuel Oil. Velocities for water-glycerine on the 421 demister give intermediate velocities which decrease with increasing wt. % glycerine. On the 931 demister the water and water-glycerine velocities are about the same. The flooding and loading velocities decrease with increased liquid load at about the same slope for each test liquid and for each demister. The relative effects of the variables which affect flooding and loading velocities are discussed in

FIGURE 3
LOADING VELOCITY
421 DEMISTER

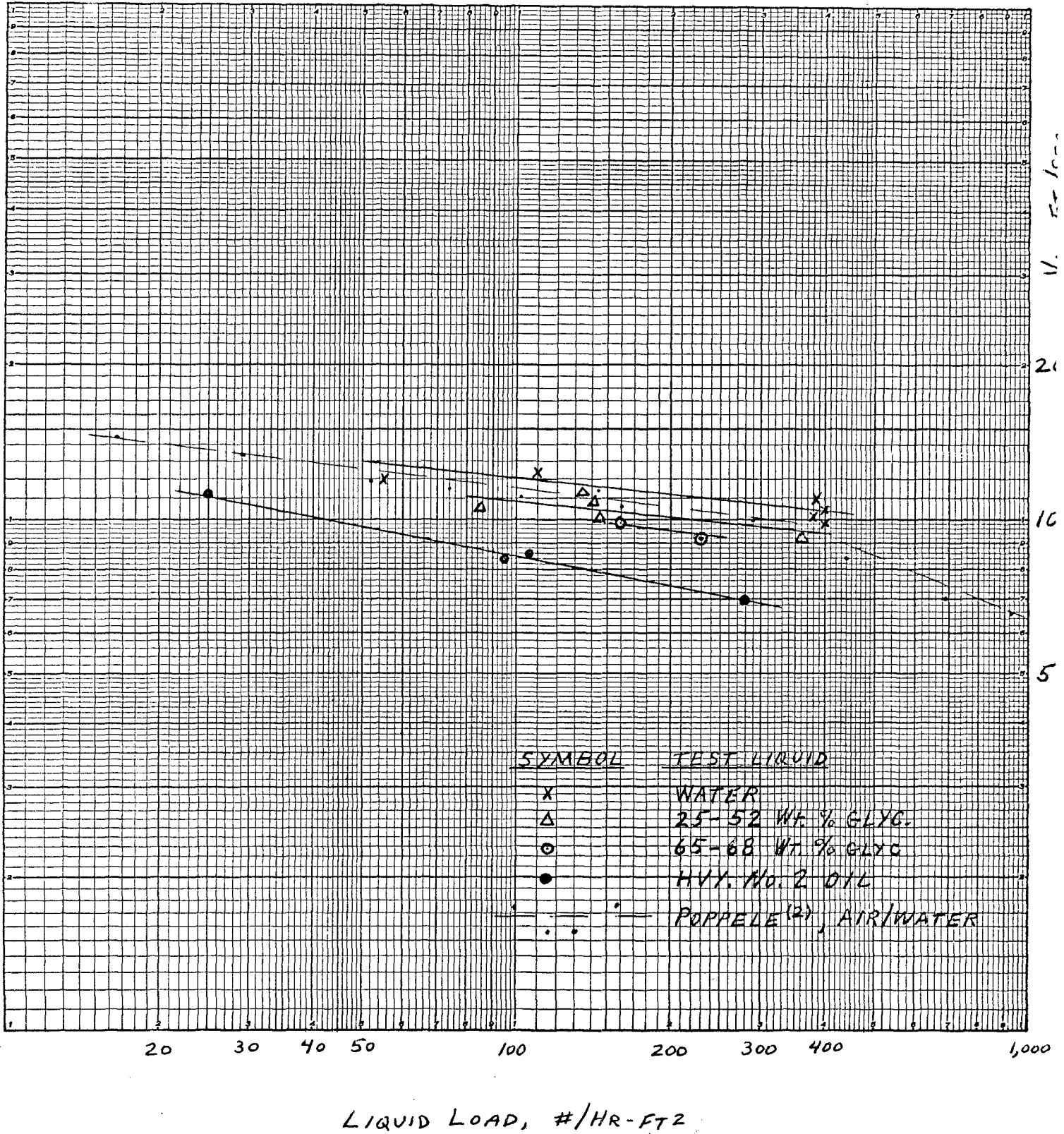
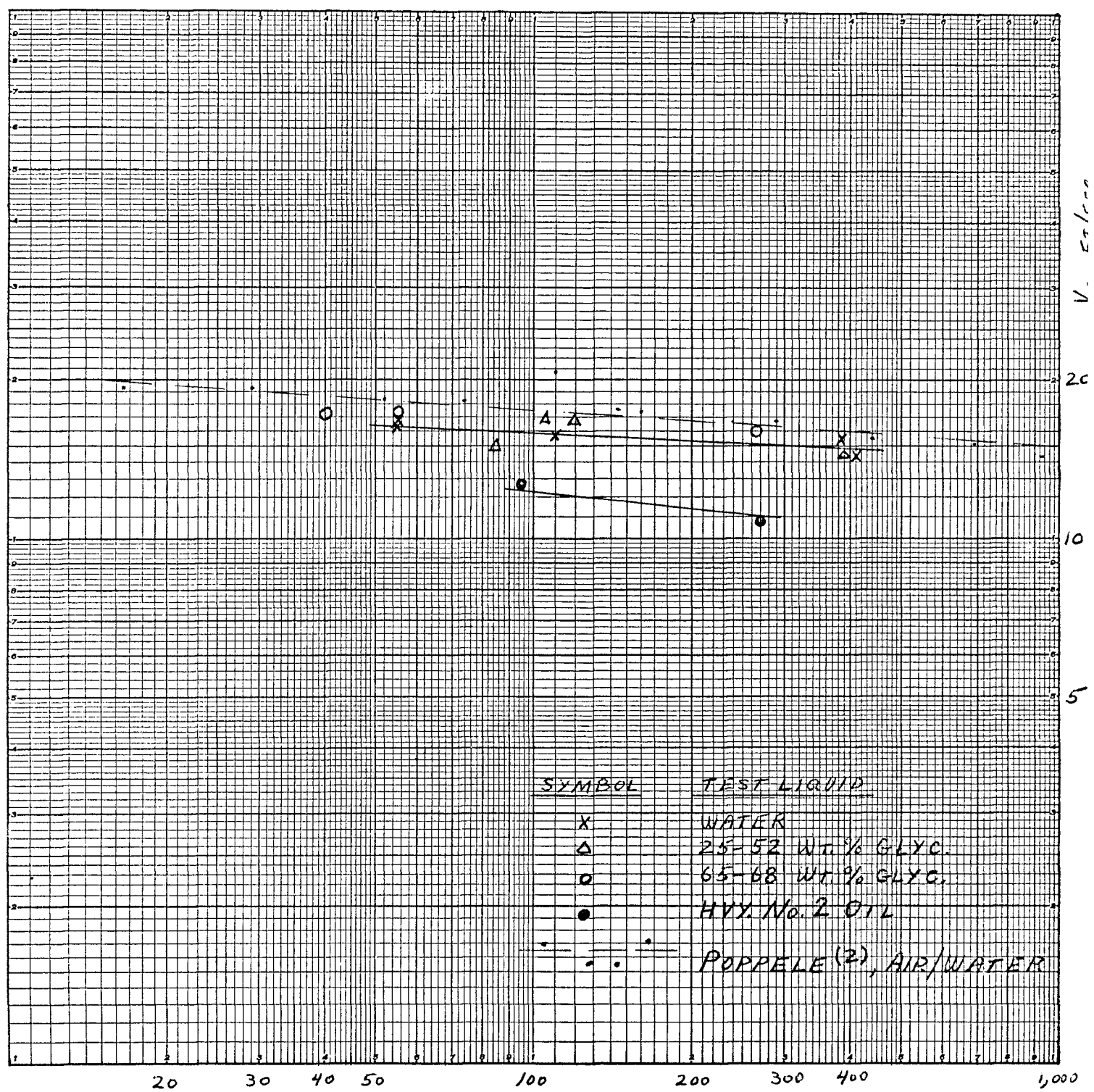


FIGURE 4

FLOODING VELOCITY

931 DEMISTER

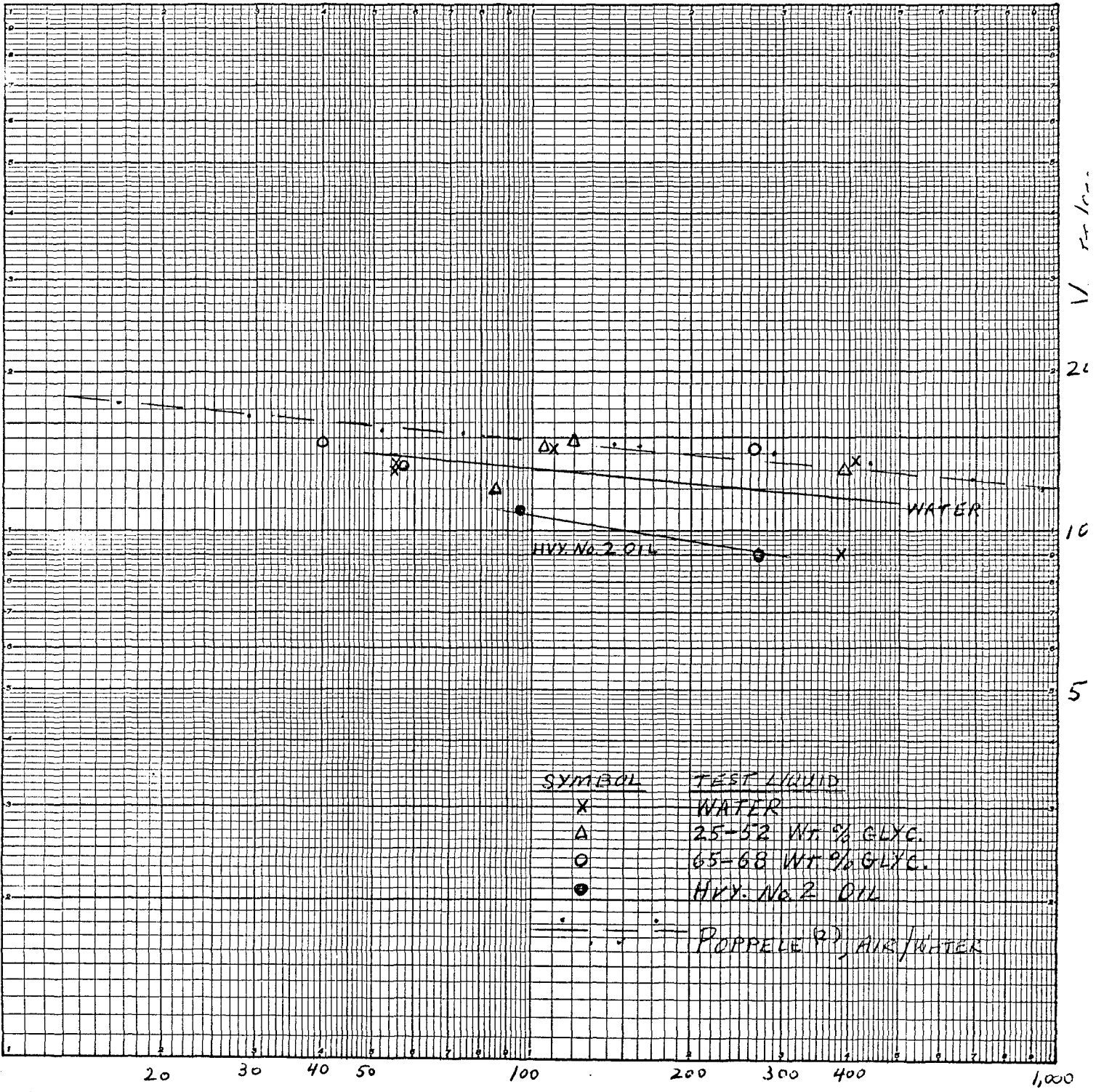


LIQUID LOAD, #/HR-FT²

FIGURE 5

LOADING VELOCITY

931 DEMISTER



SYMBOL	TEST LIQUID
X	WATER
Δ	25-52 WT % GLYC.
O	65-68 WT % GLYC.
●	HVY. No. 2 OIL
- - -	POPPELE'S AIR/WATER

LIQUID LOAD, #/HR-FT²

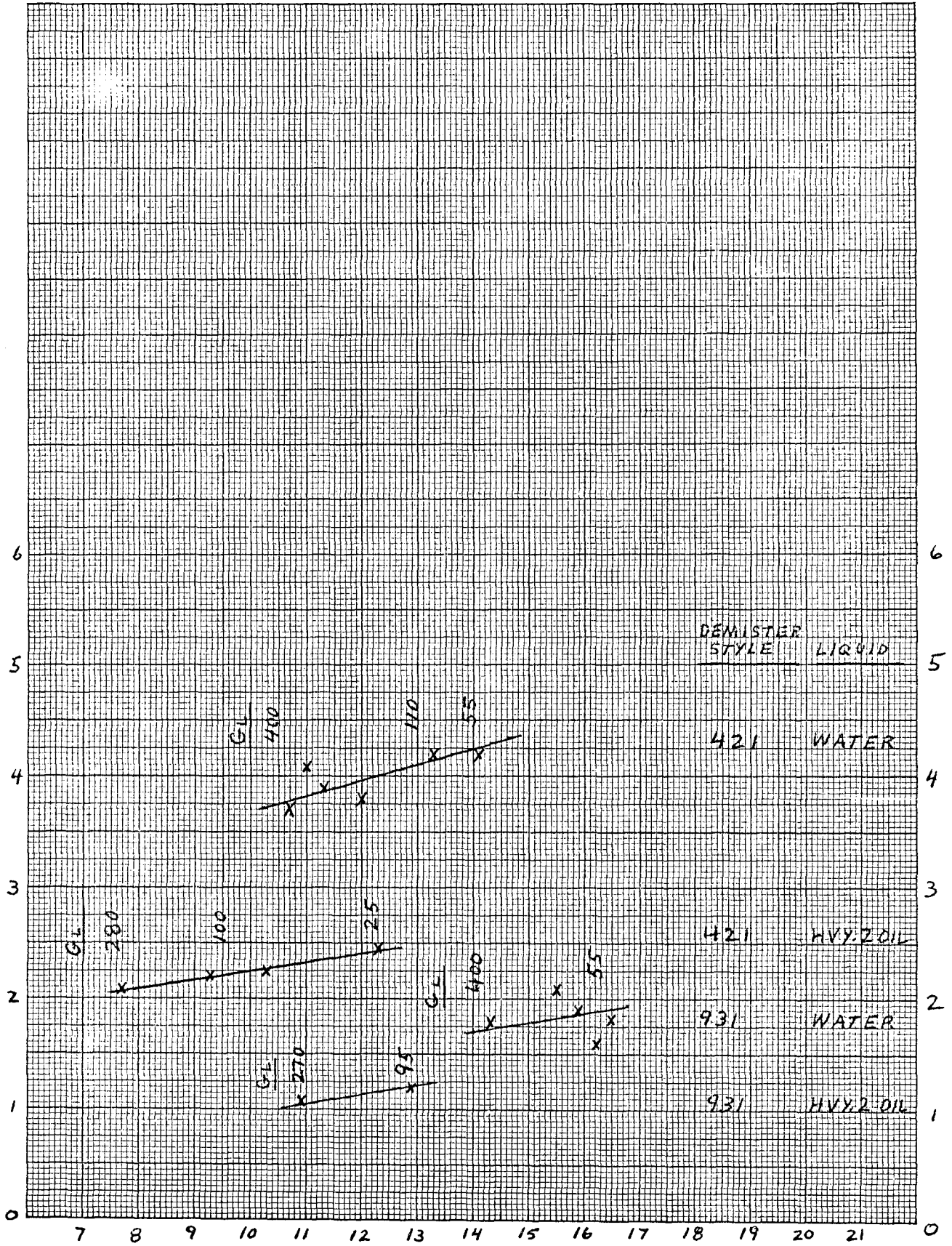
detail in the next section entitled "DATA CORRELATION".

These results for air/water system show reasonable agreement with the work of Poppele(2). Velocities are within 5-15% of those of Poppele. The effect of liquid load on velocities are almost identical with the exception of the 421 flooding velocity (Figure 2) where Poppele shows a much higher effect of liquid load on velocity.

This difference in the effect of liquid load on flooding velocity is attributed to the difference in the methods used in determining flood points. Poppele relied on visual observation of incipient flood, whereas, the author studied velocities above the flood point and redefined flooding as discussed under EXPERIMENTAL PROCEDURE. This new definition of flood point is expected to give better agreement among experimental results. It is essential that velocities between load and flood point be redetermined after the flooding point is exceeded to assist in obtaining a more exact location of the flood point.

Demister pressure drop at the flood point was found to be dependent on the demister style and the test liquid. Liquid load had only a slight effect on demister pressure drop. This is illustrated in Figure 6. This relation provides additional guidance in determining flood point in future experiments.

FIGURE 6
 DEMISTER PRESSURE DROP
 AT THE FLOOD POINT



FLOODING VELOCITY, FT./SEC.

ΔP_D , IN. WATER

Flooding and loading velocities were relatively easy to determine at high liquid load rates on the denser demister (Style 421). Determinations became increasingly more difficult as liquid load was decreased and as demister void fraction increased (Style 931). This accounts somewhat for the greater variability of data for the 931 style demister (Figure 4 and 5).

Both the 421 and 931 demister were very effective in removing liquid from the air. Below the load point there was no visible sign of liquid breakthrough. At very high air velocities (low liquid load on 931 demister) a few drops of liquid were carried through as the flood point was approached. However, this is not the normal operating range of the demister (near flood). Flooding and loading velocities for the 931 demister were about 20% higher than those for the 421 demister.

DATA CORRELATION

PUBLISHED CORRELATIONS

The most popular method of expressing allowable demister vapor velocity was proposed by York(3). His equation is as follows:

$$V = K \sqrt{(p_L - p_G) / p_G} \quad (1)$$

Values of K at the flood point have been calculated from the test data in Table 1 and are plotted in Figures 7A and 7B as a function of demister liquid load. Calculated data are tabulated in Table D-1.

The values of K_F , and therefore the value of flooding velocity, differ by as much as 30% on the 421 demister at constant liquid loading primarily as a result of variations in liquid properties. A difference of 30% is also obtained between the 421 and 931 demister at constant liquid rate and constant liquid properties. These differences illustrate the need to determine the effects of each variable on demister performance.

Poggele(4) has proposed the following relation which is similar to the equations used in defining the flooding point in packed columns:

$$\frac{V^2 a p_G (\mu_L)^{0.2}}{g_c \epsilon^3 \rho_L} = f \left(\frac{G_L}{G_G} \sqrt{\frac{\rho_G}{\rho_L}} \right) \quad (2)$$

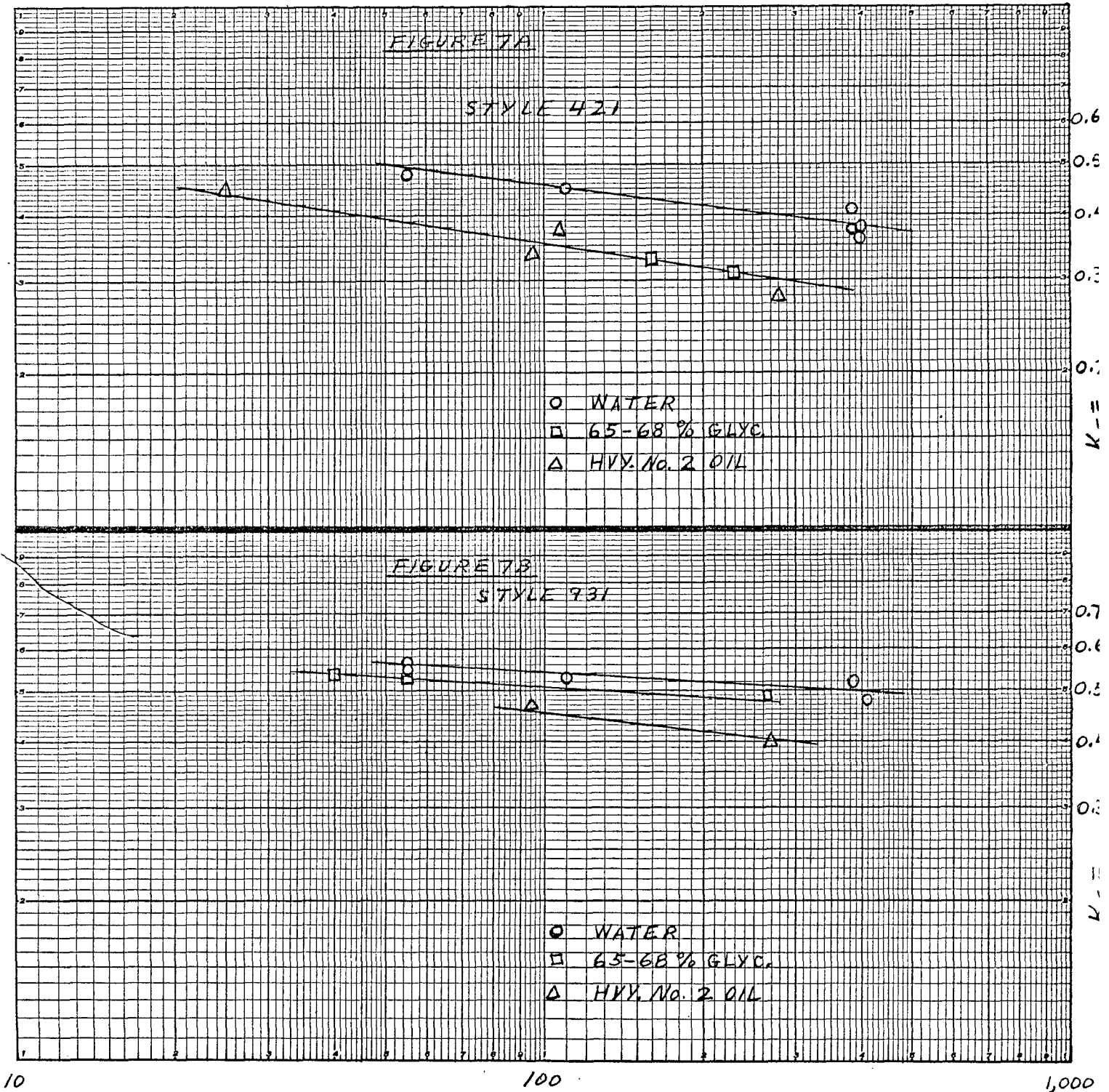
These variables have been calculated for the test data in Table D-1 and plotted in Figure 8.

Curves A and B in Figure 8 show a straight line relation between variables but there is a distinct line for each demister style. Lines A and B are made to coincide into line C in Figure 8 by using $(a/\epsilon^3)^{0.5}$ as the correlating

FIGURE 7A AND 7B

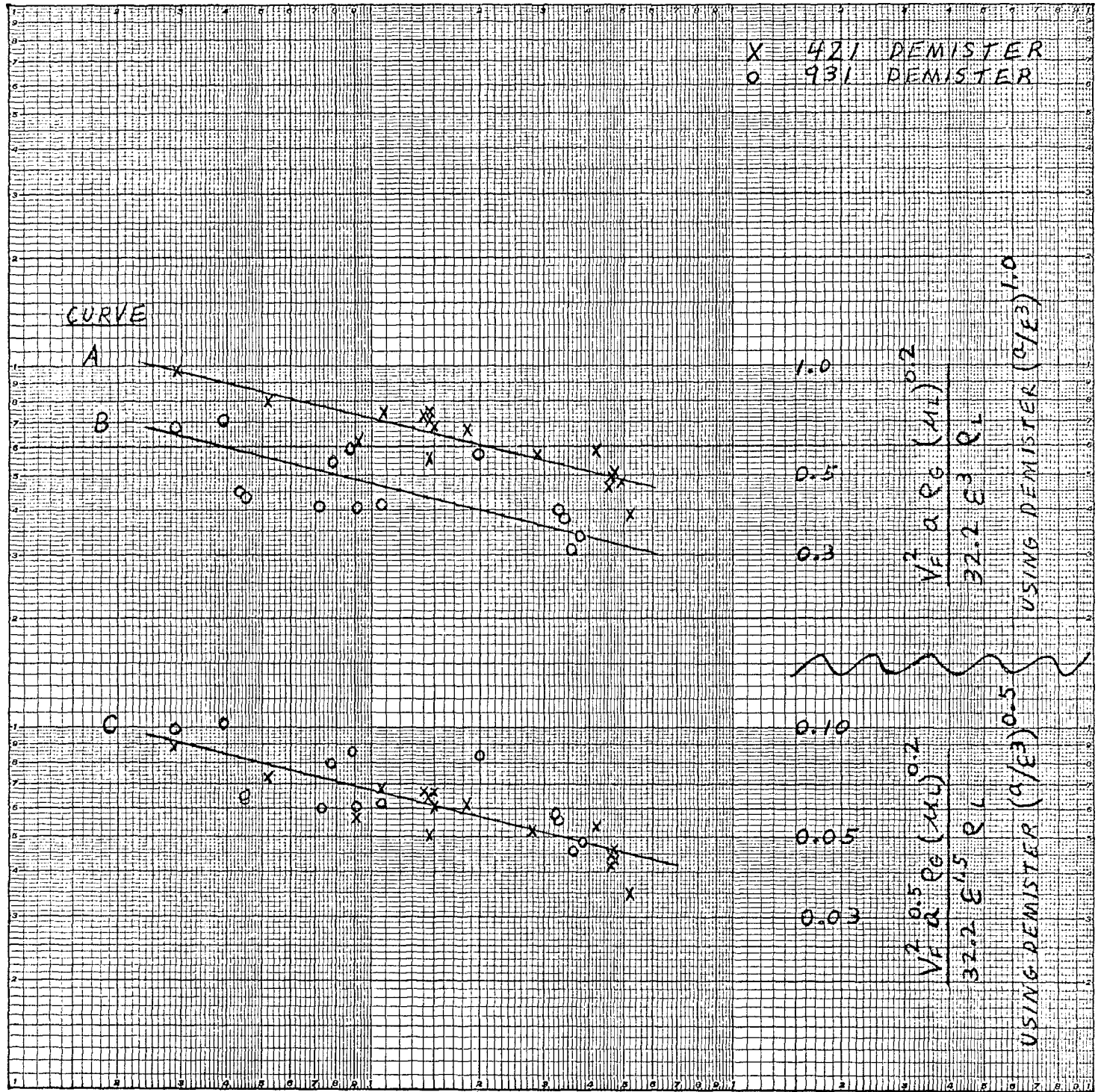
DEMISTER ENTRAINMENT FACTOR (K_F)

AT THE FLOOD POINT



LIQUID LOAD, #/HR-FT²

FIGURE 8
DATA CORRELATION USING
PROPOSAL OF POPPELE



0.001 0.001 0.01 0.1

$$\frac{G_L}{G_G} \sqrt{\rho_G / \rho_L}$$

variable rather than $(a/\epsilon^3)^{1.0}$. There is still considerable variation of the data either from variables not included or from variables not adequately represented.

Curve C in Figure 6 can be considerably simplified by assuming a linear relationship. The equation is as follows:

$$\text{LOG} \left[\frac{V_F^2 \left(\frac{a}{\epsilon^3}\right)^{0.5} \rho_G (\mu_L)^{0.2}}{32.2 \rho_L} \right] = -0.251 \text{LOG} \left(\frac{G_L}{G_G} \sqrt{\frac{\rho_G}{\rho_L}} \right) + \text{LOG}(0.0122) \quad (3)$$

By substituting $G_G = 3,600 \rho_G V_F$ in equation (3) and solving for V_F we obtain:

$$V_F = \frac{1.90 (\rho_L)^{0.64}}{(G_L)^{0.14} \left(\frac{a}{\epsilon^3}\right)^{0.29} (\mu_L)^{0.11} (\rho_G)^{0.50}} \quad (4)$$

This equation is a clearer illustration of the effect of variables on flooding velocity and is a more convenient form for adding other variables such as surface tension.

LINEAR REGRESSION ANALYSIS

Stepwise Linear Regression analyses were run on the IBM 7094 Digital Computer of Standard Oil Company of California. V_F and V_L were dependent variables. The equation form was as follows:

$$\left. \begin{array}{l} \ln(V_F) \\ \text{or } \ln(V_L) \end{array} \right\} = \begin{array}{l} K_1 \ln(\alpha/\epsilon^3) + K_2 \ln(\rho_e) + K_3 \ln(\mu_L) \\ + K_4 \ln(\rho_L) + K_5 \ln(G_L) + K_6 \ln(Y) + K_7 \ln(e) \end{array} \quad (5)$$

where; $K_7 \ln(e) = \text{constant}$

and $\ln(e) = 1.0$

Regression coefficients (K_1 thru K_7) are summarized for each regression step in Table D-2. Coefficient (K_2) for vapor density (ρ_e) was not determined since this variable was practically constant for all tests and could not be recognized as a significant variable. Coefficients for the remaining variables are complete in Step 6 of each regression analysis. The resultant equations for V_F and V_L are as follows:

$$V_F = \frac{5.45 (\rho_L)^{0.47} (Y)^{0.20}}{(\alpha/\epsilon^3)^{0.30} (\mu_L)^{0.036} (G_L)^{0.11}} \quad (6)$$

Standard Error = ± 1 ft./sec. at $V_F = 15$ ft./sec.

$$V_L = \frac{2.34 (\rho_L)^{0.61} (Y)^{0.12}}{(\alpha/\epsilon^3)^{0.22} (\mu_L)^{0.033} (G_L)^{0.089}} \quad (7)$$

Standard Error = ± 1.3 ft./sec. at $V_F = 13$ ft./sec.

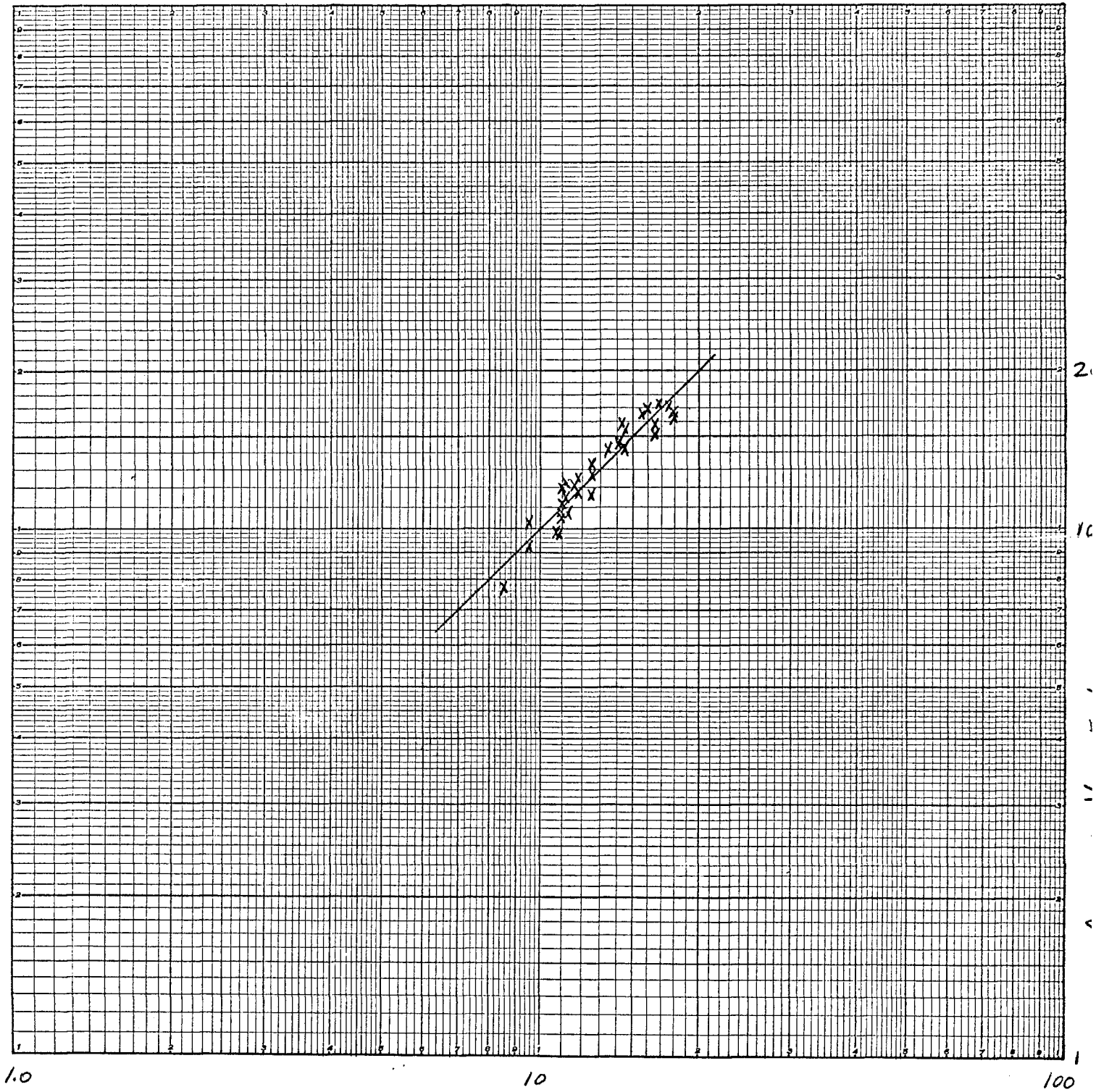
These equations can be modified to include the variables of vapor density by multiplying the constant term by $(0.0715)^{0.5}$ and including $(\rho_c)^{0.5}$ in the denominator. This inverse relation between V_F or V_L with the square root of vapor density was proposed by York and Poppele in equations (1) and (4). This relation however requires future substantiation.

Computer output solutions for equations (6) and (7) are presented in Tables L-3 and L-4. The data are plotted in Figures 9 and 10. These equations predict the value of V_F within ± 1 ft./sec. for 65% of the test data and within ± 2 ft./sec. for 95% of the test data. The error in predicting V_L is 30% higher than that for V_F . Note that the standard error of correlation in Table L-2 is based on $\ln V_F$ or V_L and must be converted to the corresponding velocity values.

Table L-2 shows correlation coefficients for seven steps of the stepwise regression for V_F and six steps of the stepwise regression on V_L . After step no. 4 in each case there is little improvement (decrease) in the standard error of correlation. This indicates that for the test liquids used in these experiments the flooding and loading velocities can be defined by the variables of liquid density, demister

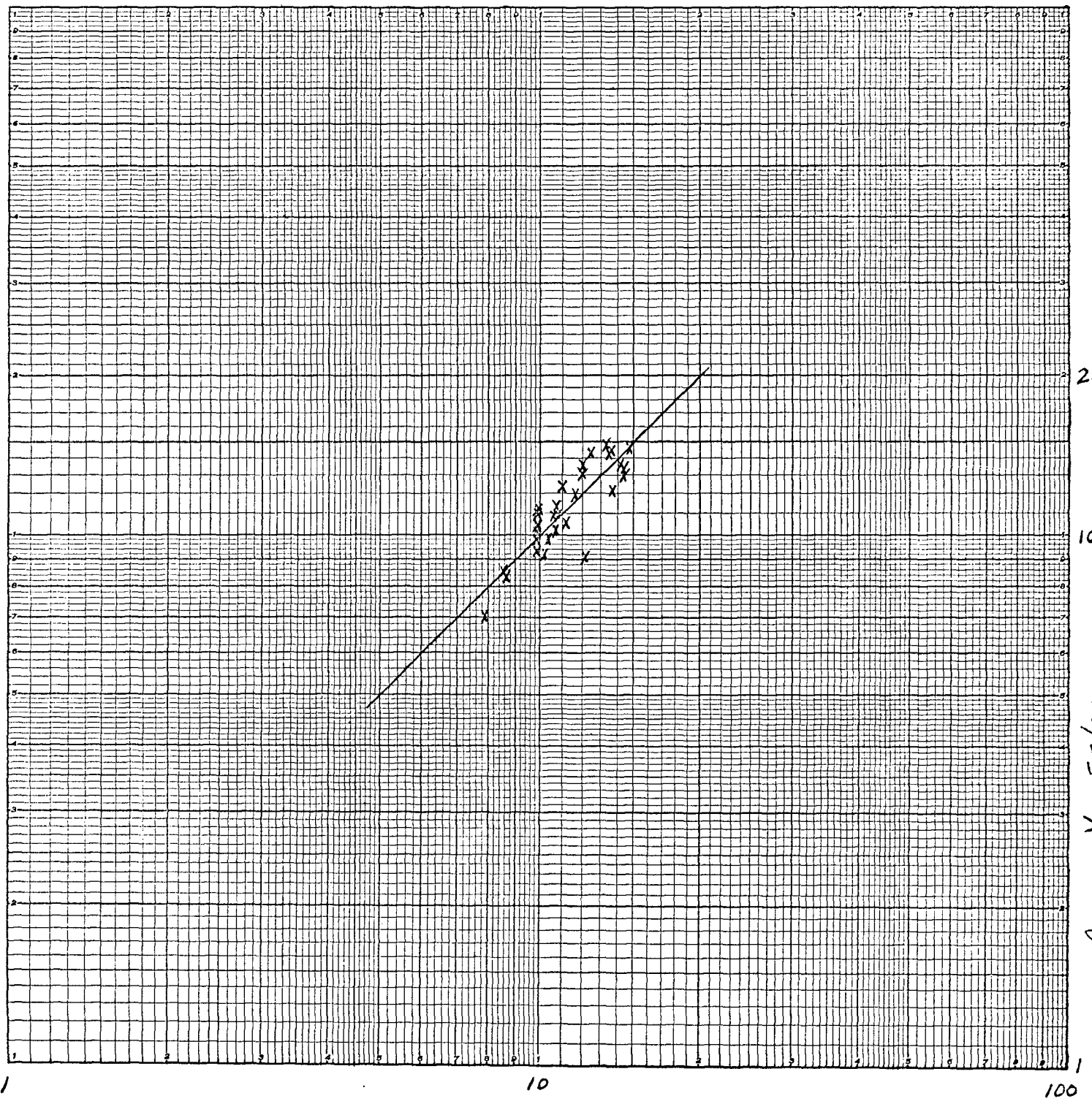
(55)

FIGURE 9
REGRESSION EQUATION FOR
FLOODING VELOCITY



$$\frac{5.45 (P_L)^{0.47} (\gamma)^{0.20}}{(\rho/\rho_3)^{0.30} (\mu_L)^{0.036} (G_L)^{0.11}} = \text{CALCULATED } V_F$$

FIGURE 10
REGRESSION EQUATION FOR
LOADING VELOCITY



$$\frac{2.34 (P_L)^{0.61} (Y)^{0.12}}{(a/E^3)^{0.22} (\mu_L)^{0.033} (G_L)^{0.089}} = \text{CALCULATED } V_L$$

specific surface, liquid load and liquid viscosity. Addition of a constant term and surface tension effects add nothing to the accuracy of prediction. However, step no. 6 was chosen for presentation because it includes all variables and shows effects of liquid density similar to that proposed by York(3) and Roppole(4).

Note that in Table D-2 the standard error of the regression coefficients is small through step 5. However, the addition of the surface tension variable resulted in a large increase in the standard error of regression coefficients for liquid properties of viscosity, density and surface tension. The following are suspected reasons for the increase in coefficient standard errors:

- (1) A high correlation existed between two of the three liquid properties or among all three properties. Plots of any two variables do not show a high correlation. However, it is likely that a high correlation could exist among all three liquid properties of the various test liquids. Selection of test liquids was limited by considerations of toxicity and flammability due to the nature of the test gas (air) and test apparatus (open system vented to laboratory atmosphere).

- (2) The effects of liquid properties on demister performance could vary with demister properties. The regression of data found the best fit of experimental data for two demisters. Therefore, any variation due to demister properties would result in greater error of the regression coefficients.
- (3) Ranges in physical properties were not large enough to determine effects with a high degree of certainty. For example, liquid density ranged from 52 to 73 #/ft.³ or $\pm 17\%$ around the average of 62.5 #/ft.³. However, the $\ln(\rho_L)$ which was used in the regression analysis ranges from 3.95 to 4.3 or $\pm 4\%$ around the average value.

The effect of surface tension was previously studied by Schroeder by using surfactants in water. Schroeder's results show a considerably larger effect of surface tension on demister performance than those shown by the author. Schroeder showed that by reducing surface tension of water from 72 dynes/cm to 36 dynes/cm the flooding velocity at the lower surface tension was only 40% of the original value. In contrast, the regression correlation would predict only a 15% reduction in flooding velocity.

CONCLUSIONS

1. Allowable demister velocities increase with increase in liquid density and liquid surface tension.
2. Allowable demister velocities decrease with increases in demister specific surface area, liquid viscosity and liquid load.
3. Liquid viscosity has only a small effect on allowable demister velocity. The allowable velocity is decreased by only 10% when viscosity is increased from 1 to 12 centipoise.
4. The effect of liquid loading on the performance of the 421 and 931 demisters show good agreement with the work of Poppele. It is expected that better agreement would have been obtained if the method had been standardized for determining the flood point.
5. The effect of liquid density on demister velocity is in close agreement with work of York and Poppele.
6. The effect of surface tension varies considerably from the work of Schroeder. The correlations developed in this study are obviously not applicable to the use of surfactants to reduce surface tension of liquids.

7. Velocities beyond the flood point were explored. This gives useful data for determining the flood point.
8. The quantitative effects of variables which affect demister performance have been determined with the exception of gas density. The application of these correlations should be limited to the ranges of experimental data used in these experiments.

RECOMMENDATIONS

The equations developed in this thesis represent the first step in defining a generalized correlation for demister performance. Most significant variables are included with the exception of vapor density. With slight modification this latter variable can be included based on earlier proposals. Application of these equations should be limited to the range of variables studied. Extrapolation beyond experimental data could result in significant error. It is expected that these equations are best suited for application to hydrocarbon liquids, water and liquids mixed with water.

The major shortcoming of these equations in application to other systems is the undetermined effect of vapor density. Most experiments have been performed with air at atmospheric pressure. No doubt there are numerous systems where vapor density is substantially different than the density of air. In future studies major emphasis should be placed on defining the effect of vapor density.

The method used by the author in determining flood points is considered an improvement over earlier definitions. This procedure should be used in future experiments to improve reproducibility of results.

NOMENCLATURE

a	Demister specific surface, ft. ² /ft. ³
g_c	Acceleration of gravity, ft./sec. ²
G_G	Vapor mass velocity, #/hr.-ft. ²
G_L	Liquid entrainment mass velocity, #/hr.-ft. ²
K	Demister entrainment factor
K_F	Demister entrainment factor at the flood point
K_1 thru K_7	Regression coefficients
ΔP_D	Demister pressure drop, inches of water
ΔP_O	Orifice pressure drop, inches of water
T_D	Air temperature to demister, °F dry bulb
T_L	Liquid temperature to demister, °F
T_W	Air temperature to demister, °F wet bulb
V	Gas velocity, ft./sec.
V_F	Gas velocity at demister flood point, ft./sec.
V_L	Gas velocity at demister load point, ft./sec.
ϵ	Demister void fraction
ρ_g	Gas density, #/ft. ³
ρ_L	Liquid density, #/ft. ³
γ	Liquid surface tension, dynes/cm.
μ_L	Liquid viscosity, centipoise

APPENDIX A
EQUIPMENT DETAILS

AIR BLOWERS

No. of units	2 in parallel
Type	Spencer Turbo Compressor, model no. 5010-H
Rated capacity	250 SCFM at 80 oz./in ² .
Horsepower	10 at 3500 RPM

Comments - These air blowers are equipped so that if the rated capacity is exceeded the motor is turned off automatically. Because of the low back pressure of the test apparatus it was necessary to operate the control butterfly valve in the 0-40% open range. If more than 40% control position was used the blower would stop. In order to run tests at low liquid loads on the 931 type demister it was necessary to use two blowers in parallel. All leaks in the test apparatus were cemented to obtain maximum blower output.

HUMIDIFIER

Chamber	55 gallon drum (open top type).
Mesh demister	Manufactured by Otto York Co, 22 inch diameter, 6 inch thick.
Secondary spray	
Construction	Stainless steel tube, 2 feet long with 1/32 inch holes along bottom of tube.
Assembly	Two tubes mounted radially at right angles just above air inlet line.
Level Gauge	One two foot section of semi-transparent, semi-flexible plastic tubing (bottom attached to lead line below water level and top attached to lead line in humidifier vapor space).
Water supply	Water was supplied by hose from city water supply line. Water rate was limited by the drainage rate to the sewer. City water rate was

adjusted to maintain about an 8 inch water level in the level gage (above bottom of barrel). Air cooling and humidification were limited by the rate of water. This setup gave 100°F air temperature at 40% humidity. The addition of the spray into the compressor discharge resulted in temperature of 80-100°F and 80% humidity leaving the humidifier.

THERMOMETERS

Three mercury thermometers (0-130°F) were used. Wet bulb temperature was obtained by tying gauze to one thermometer and moistening with water at required intervals.

Air temperature from the humidifier and liquid temperature to the test column were measured throughout the run. Temperatures of the air leaving the test demister were not obtained on a regular basis because it was found that this air temperature was very close to the test liquid temperature. Also, the air leaving the test demister was at 100% humidity for test liquids that contained water.

MANOMETERS

Pressure drop across the orifice and static pressure below the demister were measured with a water filled manometer.

ORIFICE PLATE

The orifice plate is the same one used by H.F. Schroeder⁽¹⁾ in his earlier experiments. The calibration curve (Figure A-1) is calculated by standard methods⁽⁸⁾ for an air density of 0.0695 #/ Ft.³ upstream of the orifice. Figure A-1 includes corrections for (1) the effect of Reynolds Number on orifice flow coefficient and (2) gas expansion factor. However the combined effect of these corrections is small, being only one percent or less of the uncorrected flow rate at the load and flood points.

Details of the orifice plate are as follows:

Pipe diameter	4 inches
Orifice diameter	2.628 inches
Beta	0.657
Plate thickness	1/16 inch
Taps	Flange

A plot of air density as a function of dry bulb temperature and percent humidity is shown in Figure A-2. This Figure is used to obtain densities for air rate correction factor and velocity calculations. Figure A-3

shows calculated air velocity at flood point (at actual operating conditions) as a function of orifice pressure drop. Note that variations in velocity over the range of temperature and pressure experienced is very small (0.2 ft./sec.). Therefore, velocities at demister load point were obtained directly from Figure A-3 instead of by direct calculation.

ROTOMETER

One 0-50 GPH (water) rotometer was satisfactory over the entire liquid flow range. Rotometer calibration curves are shown in Figures A-4 and A-5 for water, water - glycerine mixtures and heavy No.2 fuel oil.

LIQUID PUMP

Type	Eastern model A-1
Capacity	4.5 GPM maximum at zero pressure maximum output pressure of 11 psig.

The capacity of this pump was a major limit to the range of flow rates and fluid properties that could be studied. Liquid loadings of 25-400 #/hr-ft² were obtained and were adequate for the intent of this study. However, the nozzles were designed for liquid pressures of 20-40 psig. It was therefore not possible to study viscosities of water - glycerine mixtures above 12 centipoise. At higher viscosities no adequate spray

could be obtained.

TEST DEMISTERS

York style 931 and 421 were both studied. The 931 demister was supplied by Otto York Company. The style 421 was the same demister used by Schroeder⁽¹⁾. The 421 demister also had been supplied by Otto York Company.

Demister properties used in correlation work are:

<u>Demister</u> <u>Style</u>	<u>Void</u> <u>Fraction</u>	<u>Specific Surface,</u> <u>ft²/ft³</u>
931	0.99	46
421	0.977	110

Both demisters were 6 inches thick with diameter of 7.45 inches. The outer surface was wrapped with nylon mesh to obtain adequate seal between lucite column and demister.

SPRAY NOZZLES

The following spray nozzles, made by Spraying Systems Co., were used:

<u>Nozzle</u>	<u>Maximum Water Rate, GPH (a)</u>
TN-1	Less than 0.5
TN-2	0.5
TN-3	1.0

<u>Nozzle</u>	<u>Maximum Water Rate, GPH (a)</u>
TN-6	2.5
TN-8	4.0
TN-10	5.0
TN-12	5.5
TN-14	6.0
TN-26	11.5
G-3	15.0

(a) with available pump.

PHYSICAL PROPERTY MEASUREMENTS

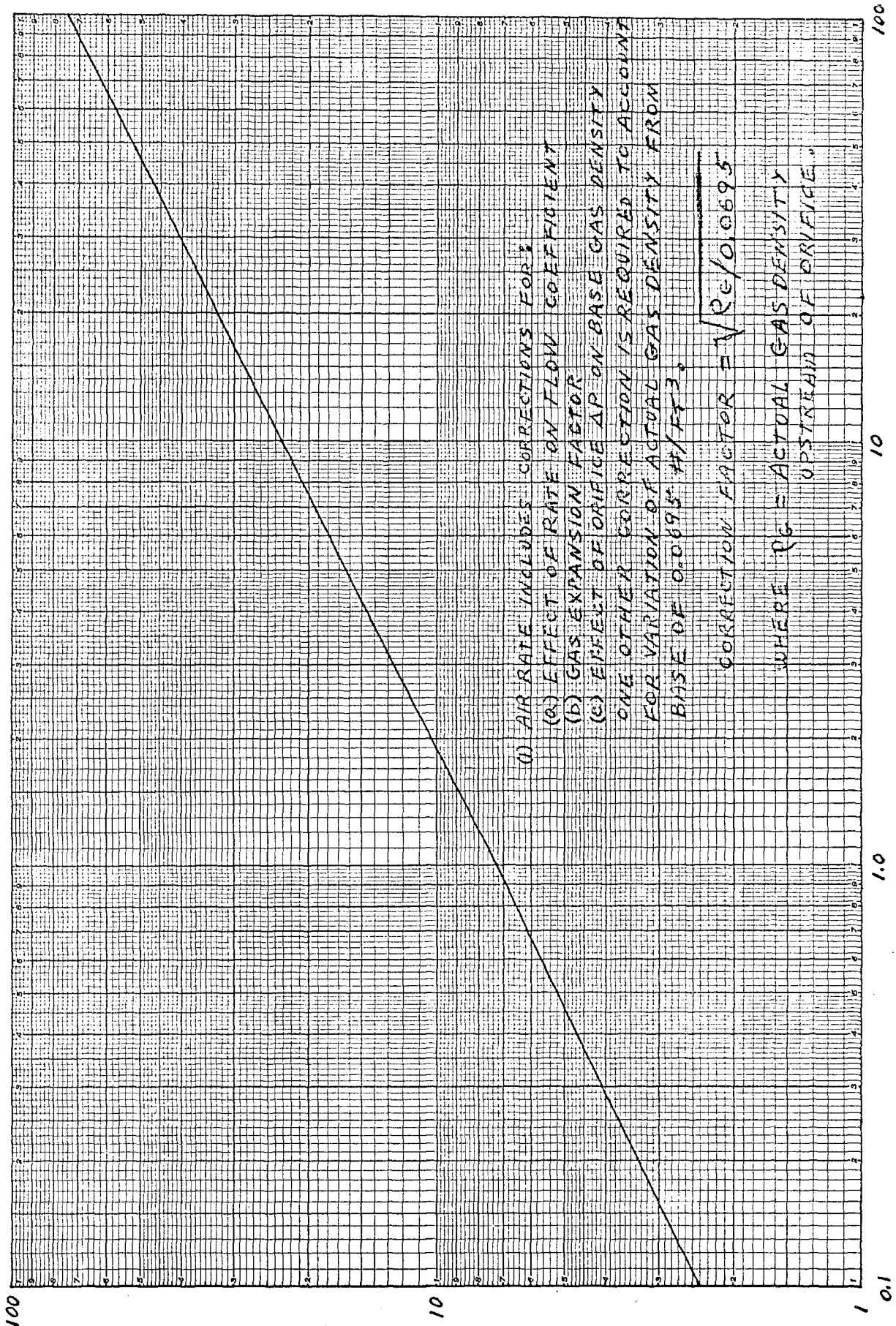
Densities were determined by weight of a volume of liquid in a graduated cylinder. Densities were measured during the tests and later checked in the laboratory at California Oil Company, Perth Amboy, N.J.

Viscosities and surface tensions were determined by laboratory personnel of California Oil Company.

DATA CORRELATION

A stepwise linear regression analysis was run on the IBM 7094 Digital Computer at the Standard Oil Company of California Computer Center in San Francisco, California.

FIGURE A-1 ORIFICE CALIBRATION



- (1) AIR RATE INCLUDES CORRECTIONS FOR:
 - (a) EFFECT OF RATE ON FLOW COEFFICIENT
 - (b) GAS EXPANSION FACTOR
 - (c) EFFECT OF ORIFICE ΔP ON BASE GAS DENSITY
- ONE OTHER CORRECTION IS REQUIRED TO ACCOUNT FOR VARIATION OF ACTUAL GAS DENSITY FROM BASE OF 0.0695 #/FT³.

CORRECTION FACTOR = $\sqrt{R_c / 0.0695}$

WHERE R_c = ACTUAL GAS DENSITY UPSTREAM OF ORIFICE

AIR RATE, #/MIN. (1)

ORIFICE PRESSURE DROP (ΔP_0), INCHES WATER

FIGURE A-2

AIR DENSITY

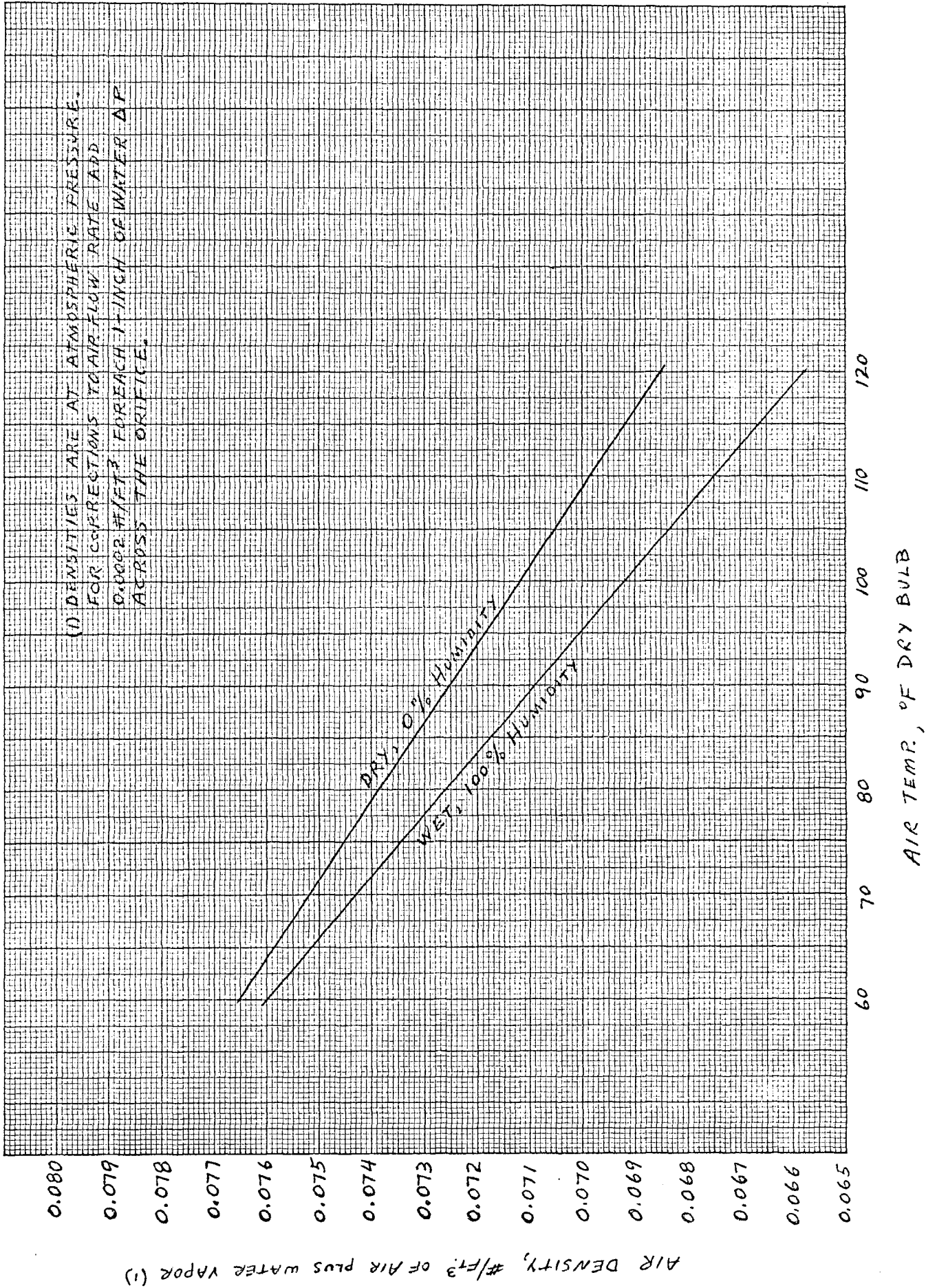
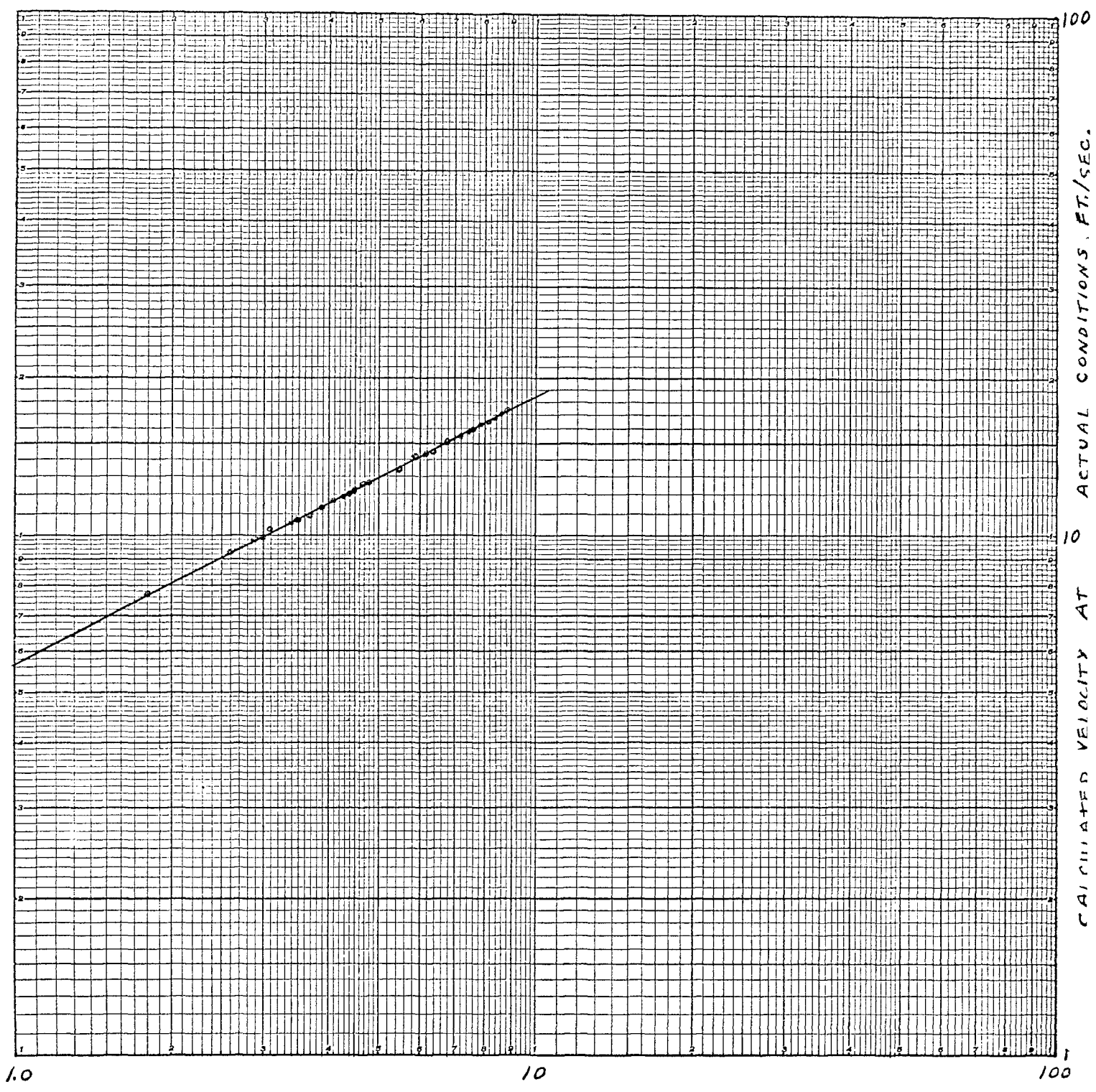


FIGURE A-3
CALCULATED AIR VELOCITIES



ΔP_0 , INCHES WATER

FIGURE A-4
 ROTOMETER CALIBRATION
 0-50 GPH - U-88
 WATER - GLYCERINE MIXTURES

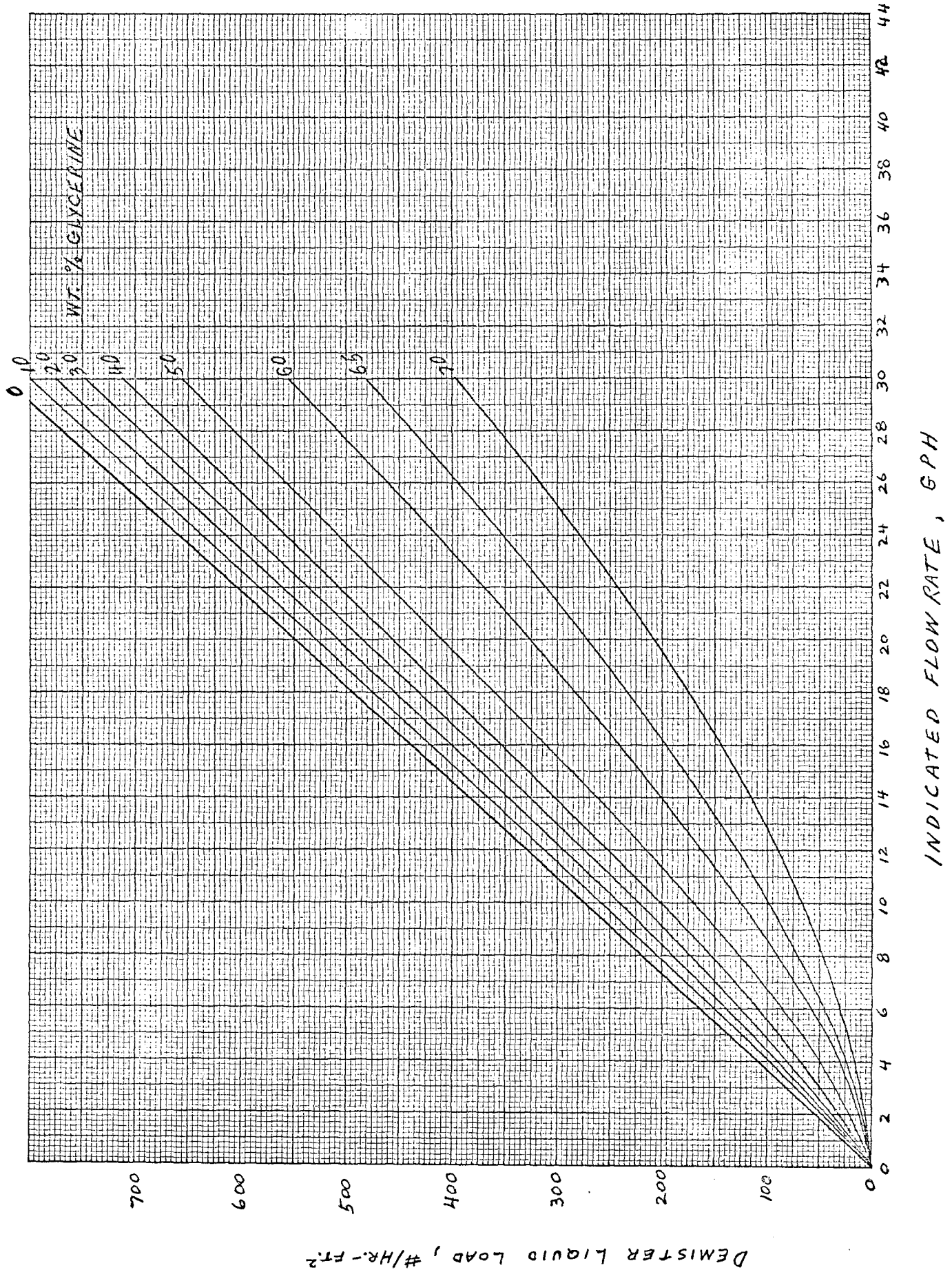
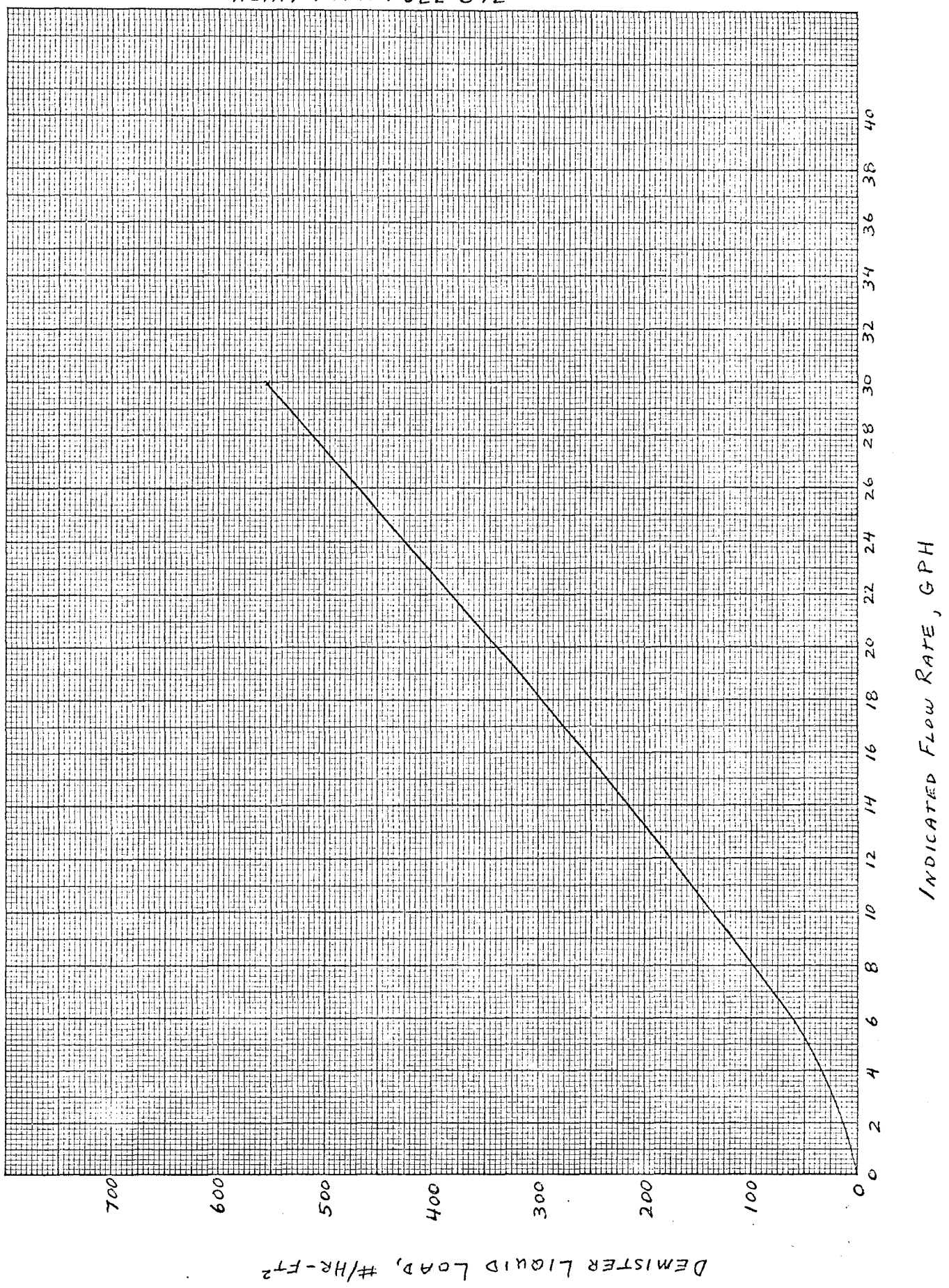


FIGURE A-5
ROTOMETER CALIBRATION
0-50 GPH - U-88
HEAVY NO. 2 FUEL OIL



APPENDIX B

EXPERIMENTAL DATA

TABLE B-1
EXPERIMENTAL DATA

Run No. - 1
System - Air/Water
Liquid Load - 400 #/hr-ft²
Demister No. - 421
Orifice Diam. - 2.628 In.
Nozzle - G-3

Run No. - 2
System - Air/Water
Liquid Load - 380 #/hr-ft²
Demister No. - 421
Orifice Diam. - 2.628 In.
Nozzle - G-3

ΔP_O	ΔP_D	T_W	T_D	T_L
0.60	0.22	-	-	-
0.23	0.19	-	-	70
0.11	0.18	-	-	-
0.40	0.19	-	-	-
0.71	0.23	-	-	71
0.92	0.25	-	-	-
1.20	0.34	-	-	-
1.55	0.47	85	116	72
1.95	0.60	-	-	-
2.17	0.70	-	-	-
2.95	1.15	92	120	76
4.50	4.05F	-	-	78
3.85	3.70	-	-	-
3.40	2.25	-	-	78
5.10	4.30F	-	-	-
5.90	4.45	-	-	78
3.55	2.05	99	104	-
3.23	1.63	-	-	-

ΔP_O	ΔP_D	T_W	T_D	T_L
0.61	0.20	68	69	68
1.29	0.52	68	78	70
0.10	0.09	70	81	71
0.44	0.17	69	82	70
0.90	0.27	70	86	70
1.35	0.52	73	96	70
2.06	0.86	78	112	71
2.94	1.43	79	114	74
3.63	3.85	79	113	74
4.55	4.34F	79	110	-
5.65	4.55F	80	108	77

Run No. - 4
System - Air/Water
Liquid Load - 370 #/hr-ft²
Demister No. - 421
Orifice Diam. - 1.789 In.
Nozzle - G-3

Run No. - 5
System - Air/Water
Liquid Load - 385 #/hr-ft²
Demister No. - 421
Orifice Diam. - 2.628 In.
Nozzle - G-3

ΔP_O	ΔP_D	T_W	T_D	T_L
0.59	0.07	70	70	70
1.53	0.10	67	67	70
1.84	0.16	69	72	70
5.50	0.31	74	84	70
8.57	0.52	77	94	71
11.4	0.74	78	100	75
15.6	1.18	80	101	76
19.7	1.85	80	100	77
20.9	2.15	80	100	-
22.3	2.83	80	99	78
22.9	3.25	82	98	78
23.8	3.85	84	98	78
25.7	4.2 F	85	98	78
30.5	4.4 F	85	97	-

ΔP_O	ΔP_D	T_W	T_D	T_L
0.60	0.22	69	77	73
1.14	0.37	72	88	73
2.27	0.90	76	98	74
2.63	1.16	78	104	75
3.10	1.40	79	106	77
3.95	2.34	79	106	78
4.45	3.80	79	105	79
5.6	4.50 F	79	104	79
3.47	1.82	79	102	79
4.06	1.90	79	103	78
4.23	2.93	80	102	78

TABLE B-2
EXPERIMENTAL DATA

Run No. - 6
System - Air/Water
Liquid Load - 385 #/hr-ft²
Demister No. - 931
Orifice Diam. - 2.628 In.
Nozzle - G-3

Run No. - 8
System - Air/Water
Liquid Load - 110 #/hr-ft²
Demister No. - 421
Orifice Diam. - 2.628 In.
Nozzle - TN-8

ΔP_O	ΔP_D	T_W	T_D	T_L
1.45	0.24	76	101	
3.25	0.48	79	108	
5.70	1.29	80	108	
6.55	1.71	80	105	
7.80	2.10	79	102	
2.95	0.50	75	95	
4.70	1.55	78	104	
5.02	1.29	79	105	
6.40	1.75	79	104	
1.92	0.29	79	105	
2.37	0.36	80	101	
0.70	0.21	81	102	
0.25	0.11	72	72	
8.80	2.05F	75	90	
9.00	2.17F	80	95	

ΔP_O	ΔP_D	T_W	T_D	T_L
1.32	0.38	69	70	68
3.57	1.05	75	78	68
5.60	4.34F	80	102	71
6.80	4.45F	80	101	72
5.23	2.40	81	102	78
4.70	1.55	75	90	79
4.96	1.75	78	94	79
2.56	0.98	78	95	80

Run No. - 9
System - Air/Water
Liquid Load - 110 #/hr-ft²
Demister No. - 931
Orifice Diam. - 2.628 In.
Nozzle - TN-8

Run No. - 10
System - Air/Water
Liquid Load - 410 #/hr-ft²
Demister No. - 931
Orifice Diam. - 2.628 In.
Nozzle - G-3

ΔP_O	ΔP_D	T_W	T_D	T_L
2.06	0.33	79	98	90
3.98	0.54	80	100	80
5.20	0.67	81	100	80
6.60	1.03	82	97	81
6.87	1.47	79	92	81
7.12	1.59	79	93	81
7.40	1.85	80	94	81
7.74	1.96F	80	95	81
8.60	1.95F	80	94	81

ΔP_O	ΔP_D	T_W	T_D	T_L
1.02	0.36	74	85	76
2.12	0.47	76	92	76
3.01	0.58	79	100	77
4.1	0.85	81	102	80
4.6	0.95	81	102	81
5.4	1.16	80	101	81
5.9	1.48	79	96	80
6.2	1.82F	-	99	-
6.5	1.82F	-	99	80

TABLE B-3
EXPERIMENTAL DATA

(56)

Run No. - 11
System - Air/Water
Liquid Load - 55 #/hr-ft²
Demister No. - 931
Orifice Diam. - 2.628 In.
Nozzle - TN-3

Run No. - 12
System - Air/Water
Liquid Load - 55 #/hr-ft²
Demister No. - 931
Orifice Diam. - 2.628 In.
Nozzle - TN-3

ΔP_0	ΔP_D	T_W	T_D	T_L
2.21	0.52	77	95	80
4.50	0.60	80	103	79
5.70	0.82	81	103	77
6.07	0.91	80	102	77
6.37	1.00	80	101	77
6.80	1.10	81	101	79
7.86	1.62F	-	101	81
8.80	1.70F	-	101	-
3.30	0.70	-	102	82
1.90	0.40	-	101	82
2.90	0.53	-	106	-
4.90	0.74	-	-	-

ΔP_0	ΔP_D	T_W	T_D	T_L
1.35	0.19	81	109	79
3.65	0.44	84	115	80
5.47	0.75	84	110	80
6.43	0.97	-	102	81
6.64	1.06	79	92	83
7.20	1.21	80	95	-
7.84	1.51	82	96	84
8.15	1.72F	83	95	84
8.93	1.80F	-	-	-

Run No. - 13
System - Air/Water
Liquid Load - 55 #/hr-ft²
Demister No. - 421
Orifice Diam. - 2.628 In.
Nozzle - TN-6

Run No. - 14
System - Air/Water
Liquid Load - 400 #/hr-ft²
Demister No. - 421
Orifice Diam. - 2.628 In.
Nozzle - G-3

ΔP_0	ΔP_D	T_W	T_D	T_L
1.36	0.35	76	83	78
2.09	0.55	80	92	82
3.52	0.95	81	96	82
4.65	1.56	81	95	83
2.88	0.78	-	94	84
4.35	1.28	-	94	84
4.80	1.92	81	104	84
5.26	2.16	85	105	85
5.70	3.95	-	103	85
6.45	4.40F	-	103	85
7.40	4.60F	-	103	85

ΔP_0	ΔP_D	T_W	T_D	T_L
0.70	0.29	69	71	73
1.96	0.52	74	85	73
3.45	1.37	79	100	74
3.90	3.90F	-	-	77
3.20	1.45	79	100	78
3.50	1.70	-	-	-
3.75	3.80F	78	98	78
3.35	1.80F	78	98	-
3.48	3.70F	78	98	-
3.36	2.20	-	-	78
2.90	1.60	-	-	79
2.45	1.04	78	97	79
1.95	0.83	78	96	79
1.35	0.65	76	94	-
0.63	0.45	75	88	79
0.36	0.22	73	85	-
0.60	0.25	73	85	78

TABLE B-4
EXPERIMENTAL DATA

Run No. - 15
System - Air/Water
Liquid Load - 410 #/hr/ft²
Demister No. - 931
Orifice Diam. - 2.628 In.
Nozzle - G-3

Run No. - 16
System - Air/25wt.% Glyc.
Liquid Load - 390 #/hr-ft²
Demister No. - 931
Orifice Diam. - 2.628 In.
Nozzle - G-3

ΔP_0	ΔP_D	T_W	T_D	T_L
3.80	0.78	80	98	79
4.75	1.03	76	85	77
5.90	1.50	-	-	-

ΔP_0	ΔP_D	T_W	T_D	T_L
1.44	0.37	74	85	76
3.65	0.59	78	97	77
4.96	1.00	78	94	78
5.45	1.20	77	94	78
5.95	1.43	78	93	78
6.30	1.95	-	-	79
6.71	2.15F	-	-	80
4.90	1.05	-	96	-
4.60	0.98	-	98	82
4.60	1.00	-	-	-
4.10	0.90	80	99	82
3.16	0.72	80	99	-
2.13	0.61	79	97	82
2.10	0.54	-	-	-
1.20	0.43	-	-	-

Check on Run No. 10
Data are plotted with Run no.10

Run No. - 17
System - Air/33wt.%Glyc.
Liquid Load - 360 #/hr-ft²
Demister No. - 421
Orifice Diam. - 2.628 In.
Nozzle - G-3

Run No. - 18
System - Air/33wt.%Glyc.
Liquid Load - 35 #/hr-ft²
Demister No. - 421
Orifice Diam. - 2.628
Nozzle - TN-8

ΔP_0	ΔP_D	T_W	T_D	T_L
1.94	0.95	81	103	78
3.00	4.14F	79	98	81
3.40	4.50F	79	98	81
2.80	2.00	81	98	82
2.90	2.63	79	98	82
2.50	1.27	79	98	82
1.72	0.98	79	95	-
1.26	0.76	-	95	82

ΔP_0	ΔP_D	T_W	T_D	T_L
2.60	1.00	79	99	84
4.12	3.26	-	98	84
4.30	4.45F	-	-	84
4.80	4.60F	-	-	-
3.60	1.64	-	92	84
2.95	1.12	78	97	84
1.16	0.65	77	90	84

TABLE B-5
EXPERIMENTAL DATA

Run No. - 19
System - Air/33wt.%Glyc.
Liquid Load - 85 #/hr-ft²
Demister No. - 931
Orifice Diam. - 2.628 In.
Nozzle - TN-8

Run No. 20
System Air/41wt.%Glyc.
Liquid Load 107#/hr-ft²
Demister No. 931
Orifice Diam. 2.628 In.
Nozzle TN-14

ΔP_O	ΔP_D	T_W	T_D	T_L
2.36	0.43	-	100	85
3.57	0.58	79	100	85
4.46	0.77	80	100	85
4.80	0.98	-	100	86
5.05	1.01	80	100	86
5.70	1.20	80	100	86
9.00	1.82F	-	-	-
7.95	1.60	-	-	-
11.0	1.87F	-	-	-
9.0	1.80F	-	-	-
7.1	1.55	-	-	-
6.0	1.40	-	-	-
5.1	1.00	-	-	-
3.4	0.60	-	-	-

ΔP_O	ΔP_D	T_W	T_D	T_L
3.4	0.60	78	92	87
5.1	0.90	78	92	86
6.0	1.10	78	83	-
7.3	1.48	-	-	-
8.5	1.85F	-	-	-
9.5	2.00F	-	-	-

Run No. - 21
System - Air/43wt.%Glyc.
Liquid Load - 142 #/hr-ft²
Demister No. - 421
Orifice Diam. - 2.628 In.
Nozzle - TN-14

Run No. - 22
System - Air/52wt.%Glyc.
Liquid Load - 135 #/hr-ft²
Demister No. - 421
Orifice Diam. - 2.628 In.
Nozzle - TN-14

ΔP_O	ΔP_D	T_W	T_D	T_L
1.57	0.67	76	88	77
3.55	1.25	80	98	78
5.3	4.8 F	78	94	80
4.5	4.6 F	81	98	82
3.9	1.80	-	98	82
1.90	0.90	-	-	84
2.85	1.00	-	-	-
3.35	1.26	-	103	84
4.5	4.2	-	103	-

ΔP_O	ΔP_D	T_W	T_D	T_L
1.45	0.53	76	90	80
3.30	1.62	79	98	80
4.30	2.97	80	100	81
4.80	4.90F	-	-	82
4.20	4.90F	80	99	82
3.80	1.85	80	100	84
4.06	3.90	80	100	85
3.90	3.65	-	-	85
2.50	1.10	80	100	86

TABLE B-6
EXPERIMENTAL DATA

Run No. - 23
System - Air/57wt.%Glyc.
Liquid Load - 120 #/hr-ft²
Demister No. - 931
Orifice Diam. - 2.628 In.
Nozzle - TN-14

Run No. - 24
System - Air/65wt.%Glyc.
Liquid Load - 40 #/hr-ft²
Demister No. - 931
Orifice Diam. - 2.628 In.
Nozzle - TN-6

ΔP_O	ΔP_D	T_W	T_D	T_L
2.0	0.25	-	-	84
4.1	0.65	80	98	85
6.5	1.10	-	-	85
7.3	1.45	-	95	85
8.0	1.85	-	96	85
9.1	2.2 F	-	96	85
8.4	2.2 F	-	95	85
4.2	0.80	-	-	-
3	-	-	-	-
2.8	0.50	-	-	-

ΔP_O	ΔP_D	T_W	T_D	T_L
2.7	0.35	-	-	84
4.9	0.65	-	-	-
7.6	1.35	79	96	84
9.2	2.1 F	-	95	84
10.0	2.2 F	-	-	-
8.6	2.0	-	-	85
7.1	1.50	-	-	-
3.5	0.80	-	-	85
2.5	0.40	-	-	-
4.7	0.65	-	-	-
7.1	1.15	-	-	-
8.0	1.50	-	-	-

Run No. - 25
System - Air/65wt.%Glyc.
Liquid Load - 55 #/hr-ft²
Demister No. - 931
Orifice Diam. - 2.628 In.
Nozzle - TN-6

Run No. - 26
System - Air/65wt.%Glyc.
Liquid Load - 265 #/hr-ft²
Demister No. - 931
Orifice Diam. - 2.628 In.
Nozzle - G-3

ΔP_O	ΔP_D	T_W	T_D	T_L
1.87	0.27	80	84	76
3.70	0.55	81	86	78
5.40	0.88	80	83	78
6.20	1.05	79	82	79
5.90	0.95	79	82	79
7.6	1.40	81	88	79
8.6	1.95	81	85	80
9.2	2.10F	-	-	-
8.2	1.84	81	85	81
7.2	1.45	81	86	82
6.9	1.35	-	-	-
6.5	1.22	-	-	-
4.7	0.83	79	87	82

ΔP_O	ΔP_D	T_W	T_D	T_L
1.70	0.25	80	86	84
3.90	0.66	80	87	84
4.80	0.86	-	-	-
5.90	1.07	80	87	86
6.30	1.23	81	88	88
6.65	1.37	-	-	88
6.95	1.50	-	-	88
7.30	1.80	81	86	-
7.75	2.20F	80	85	88
6.95	1.60	-	-	-
4.30	0.78	80	85	88

TABLE B-7
EXPERIMENTAL DATA

(60)

Run No. - 27
System - Air/68wt.%Glyc.
Liquid Load - 230 #/hr-ft²
Demister No. - 421
Orifice Diam. - 2.628 In.
Nozzle - G-3

Run No. - 28
System - Air/68wt.%Glyc.
Liquid Load - 162 #/hr-ft²
Demister No. - 421
Orifice Diam. - 2.628 In.
Nozzle - TN-26

ΔP_0	ΔP_D	T_W	T_D	T_L	ΔP_0	ΔP_D	T_W	T_D	T_L
1.70	0.57	-	-	87	1.8	0.60	-	-	-
2.53	0.87	77	80	86	2.5	1.05	79	85	84
3.70	5.10F	-	-	-	2.9	1.30	-	-	-
3.00	5.15F	-	-	-	3.5	2.50F	80	85	86
2.60	1.75	79	84	87	3.2	2.10	80	85	88
2.75	2.20	-	-	-	3.0	1.80	-	-	-
2.90	5.00F	80	-	88	2.7	1.50	-	85	-
2.30	1.10	-	82	88	2.2	1.20	-	-	-
1.00	0.45	-	-	-	1.7	0.90	-	-	-

Run No. - 30
System - Air/38wt.%Glyc.
Liquid Load - 145 #/hr-ft²
Demister No. - 421
Orifice Diam. - 2.628 In.
Nozzle - G-3

Run No. - 31
System - Air/Hvy. No. 2 Oil
Liquid Load - 280 #/hr-ft²
Demister No. - 421
Orifice Diam. - 2.628 In.
Nozzle - G-3

ΔP_0	ΔP_D	T_W	T_D	T_L	ΔP_0	ΔP_D	T_W	T_D	T_L
3.5	1.4	78	79	-	0.85	0.52	72	77	83
1.5	0.65	78	79	-	1.90	2.10	75	84	-
2.5	0.85	-	-	-	1.35	0.70	77	86	-
2.9	1.05	-	-	-	0.56	0.35	-	-	-
3.2	1.25	79	85	81	0.23	0.17	-	-	-
3.5	1.50	80	86	-	1.20	0.65	-	-	-
4.1	3.0	-	-	-	1.65	1.21	-	85	-
4.3	3.4	-	-	-	1.55	0.87	-	-	-
4.7	4.95F	-	-	-	1.82	2.10F	83	94	86
3.8	1.80	80	85	-	1.62	1.20	-	-	86
3.2	1.05	-	-	-	1.60	1.10	-	-	-
2.5	0.90	-	-	-	1.75	1.60	83	85	86
1.5	0.65	-	-	82					

TABLE B-8
EXPERIMENTAL DATA

(61)

Run No. - 32
System - Air/Hvy. No.2 Oil
Liquid Load - 270 #/hr-ft²
Demister No. - 931
Orifice Diam. - 2.628 In.
Nozzle - G-3

Run No. - 33
System - Air/Hvy.No.2 Oil
Liquid Load - 25 #/hr-ft²
Demister No. - 421
Orifice Diam. - 2.628
Nozzle - TN-3

ΔP_O	ΔP_D	T_W	T_D	T_L
1.00	0.18	82	90	-
3.00	0.65	-	-	-
2.00	0.45	-	95	92
4.00	1.15F	-	-	-
3.40	1.13F	-	-	-
2.95	0.65	-	-	92
3.05	0.74	-	-	-
3.15	0.75	-	-	-
3.25	0.87	-	-	-
3.45	1.10F	82	87	92
1.00	0.25	-	-	-

ΔP_O	ΔP_D	T_W	T_D	T_L
1.50	0.37	73	78	86
2.80	0.82	-	-	-
3.60	1.10	80	84	85
4.20	1.75	-	-	85
4.30	2.15	84	89	-
4.50	2.45F	-	90	85
4.00	1.90	-	-	-
3.60	1.60	82	91	85
3.00	1.00	82	91	85
2.00	0.65	-	-	-
1.10	0.42	81	87	-
4.00	1.60	83	93	-
3.50	1.35	84	93	85
5.10	2.55F	-	-	-

Run No. - 34
System - Air/Hvy. No.2 Oil
Liquid Load - 95 #/hr-ft²
Demister No. - 421
Orifice Diam. - 2.628 In.
Nozzle - TN-14

Run No. - 35
System - Air/Hvy.No.2 Oil
Liquid Load - 95 #/hr-ft²
Demister No. - 931
Orifice Diam. - 2.628 In.
Nozzle - TN-14

ΔP_O	ΔP_D	T_W	T_D	T_L
1.0	0.33	-	82	-
2.0	0.70	-	-	-
3.0	2.30F	80	90	91
2.6	2.20F	82	88	91
2.25	1.20	-	-	-
2.4	1.30	-	-	-
2.5	1.60	-	-	-
1.2	0.55	-	82	-
1.8	0.75	-	84	91
2.3	1.00	-	-	91

ΔP_O	ΔP_D	T_W	T_D	T_L
1.3	0.25	-	-	-
3.1	0.47	80	86	91
3.9	0.63	80	87	91
5.0	1.20F	-	-	-
4.6	1.00	83	92	90
2.3	0.45	-	-	-
1.2	0.28	87	81	90
4.0	0.70	-	-	-
4.3	0.80	-	-	-

TABLE B-9
EXPERIMENTAL DATA

Run No. - 36
 System - Air/Hvy. No. 2 Oil
 Liquid Load - 107 #/hr-ft²
 Demister No. - 421
 Orifice Diam. - 2.628 In.
 Nozzle - TN-14

ΔP_0	ΔP_D	T_M	T_D	T_L
0.70	0.22	77	84	81
1.3	0.40	-	-	-
2.35	0.86	83	87	-
2.75	1.25	83	88	82
3.00	2.15	83	89	86
3.4	2.35F	83	89	89
3.0	2.10	-	-	-
2.7	1.20	-	-	-
2.0	0.80	-	-	-
1.2	0.50	-	-	-

FIGURE B-1

EXPERIMENTAL DETERMINATION OF DEMISTER
LOAD POINT AND FLOOD POINT

RUN No. 1

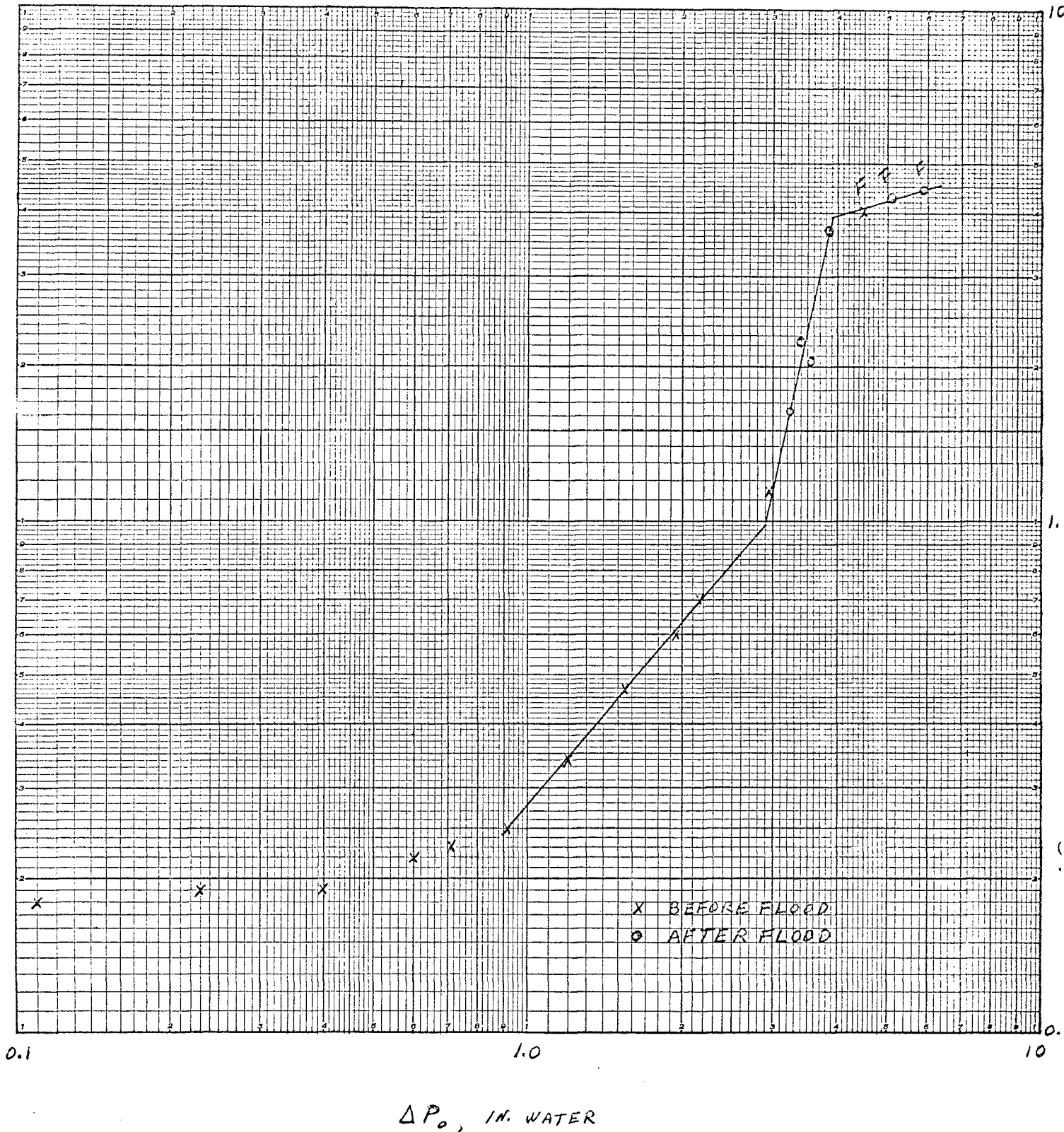
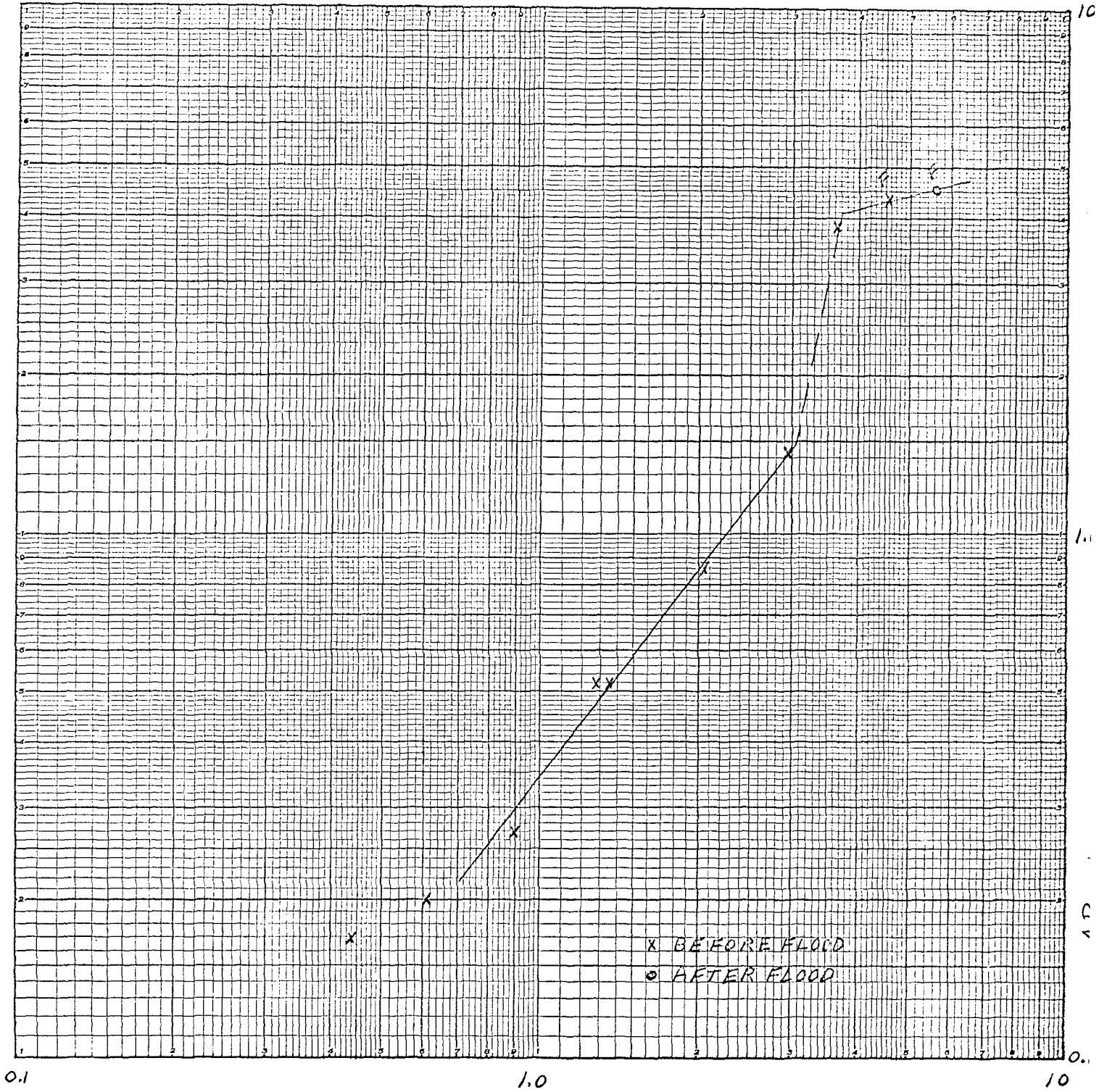


FIGURE B-2
EXPERIMENTAL DETERMINATION OF DEMISTER
LOAD POINT AND FLOOD POINT

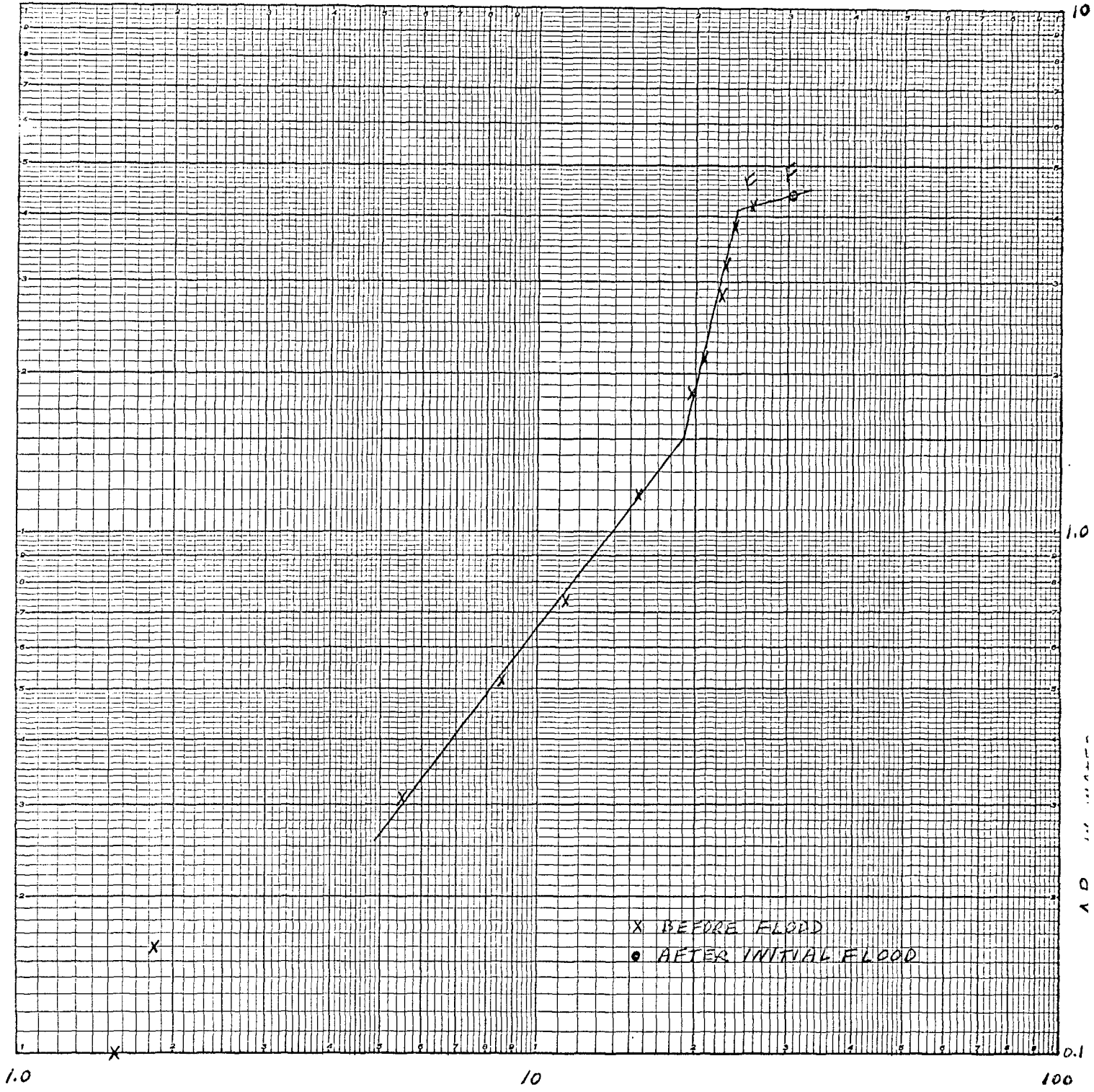
RUN No. 2



ΔP_0 , IN. WATER

EXPERIMENTAL DETERMINATION OF DEMISTER
LOAD POINT AND FLOOD POINT

RUN NO. 4



$\Delta P_o, \text{ IN. WATER}$

FIGURE B-4

EXPERIMENTAL DETERMINATION OF DEMISTER
LOAD POINT AND FLOOD POINT

RUN NO. 5

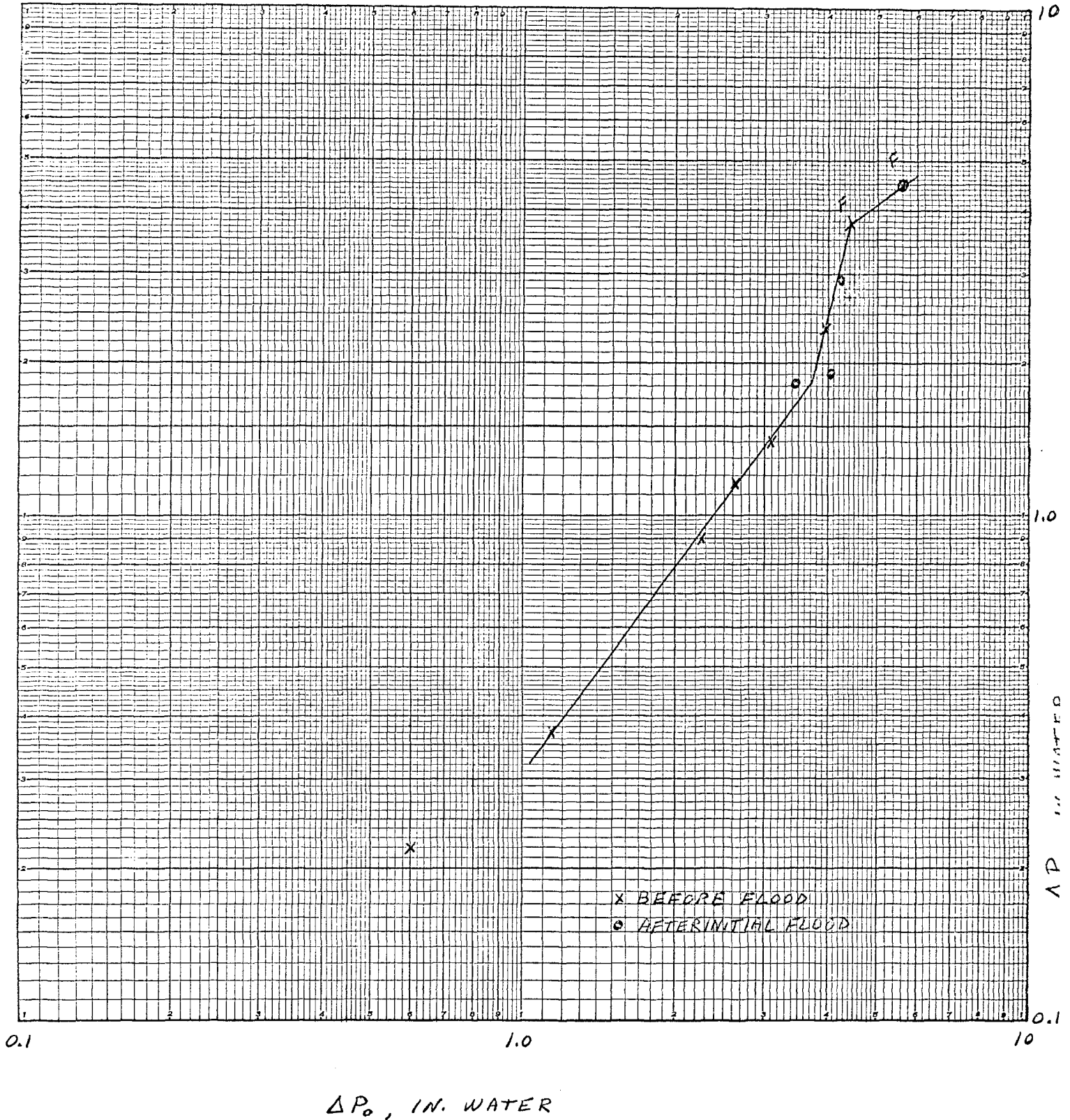
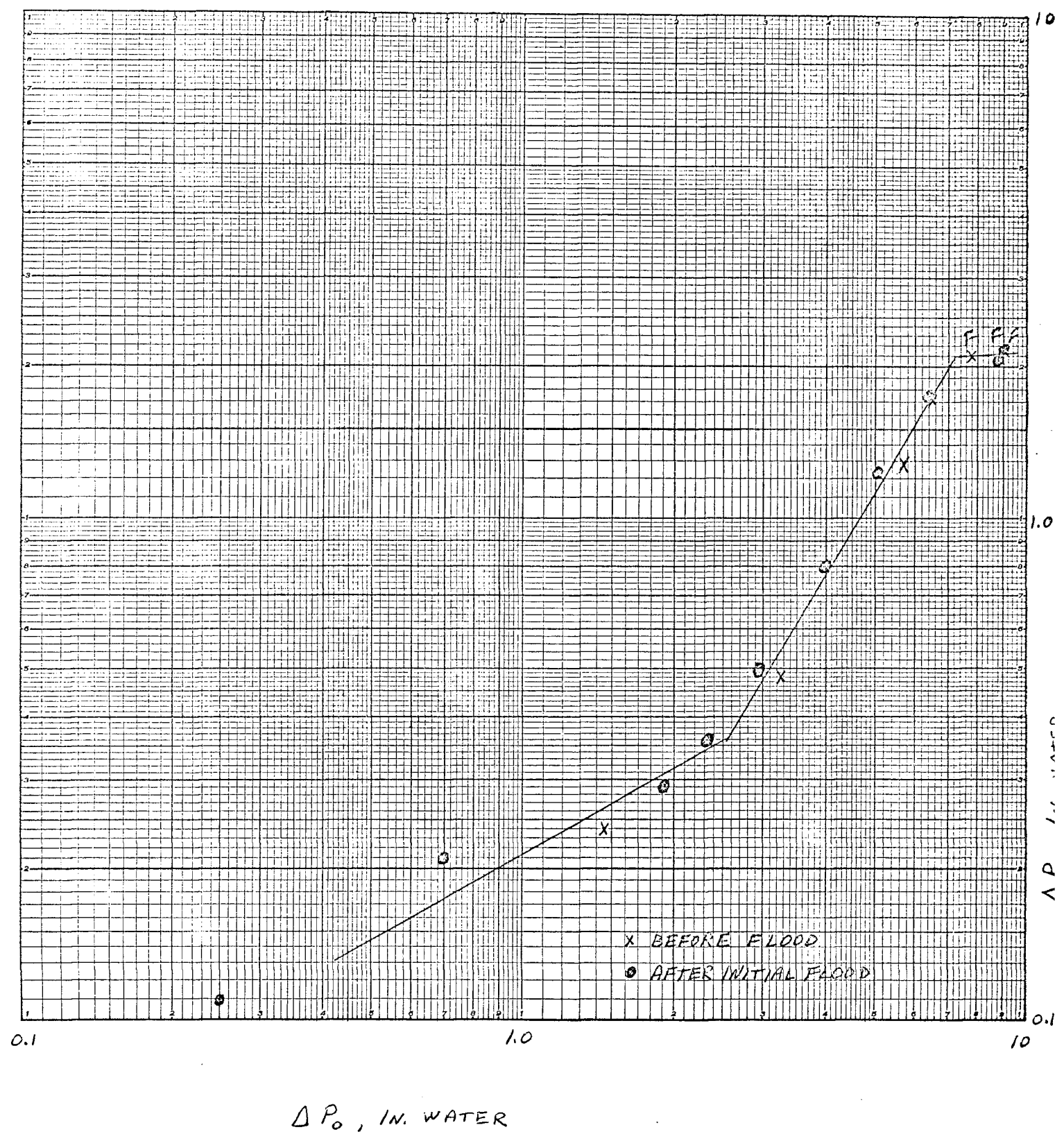


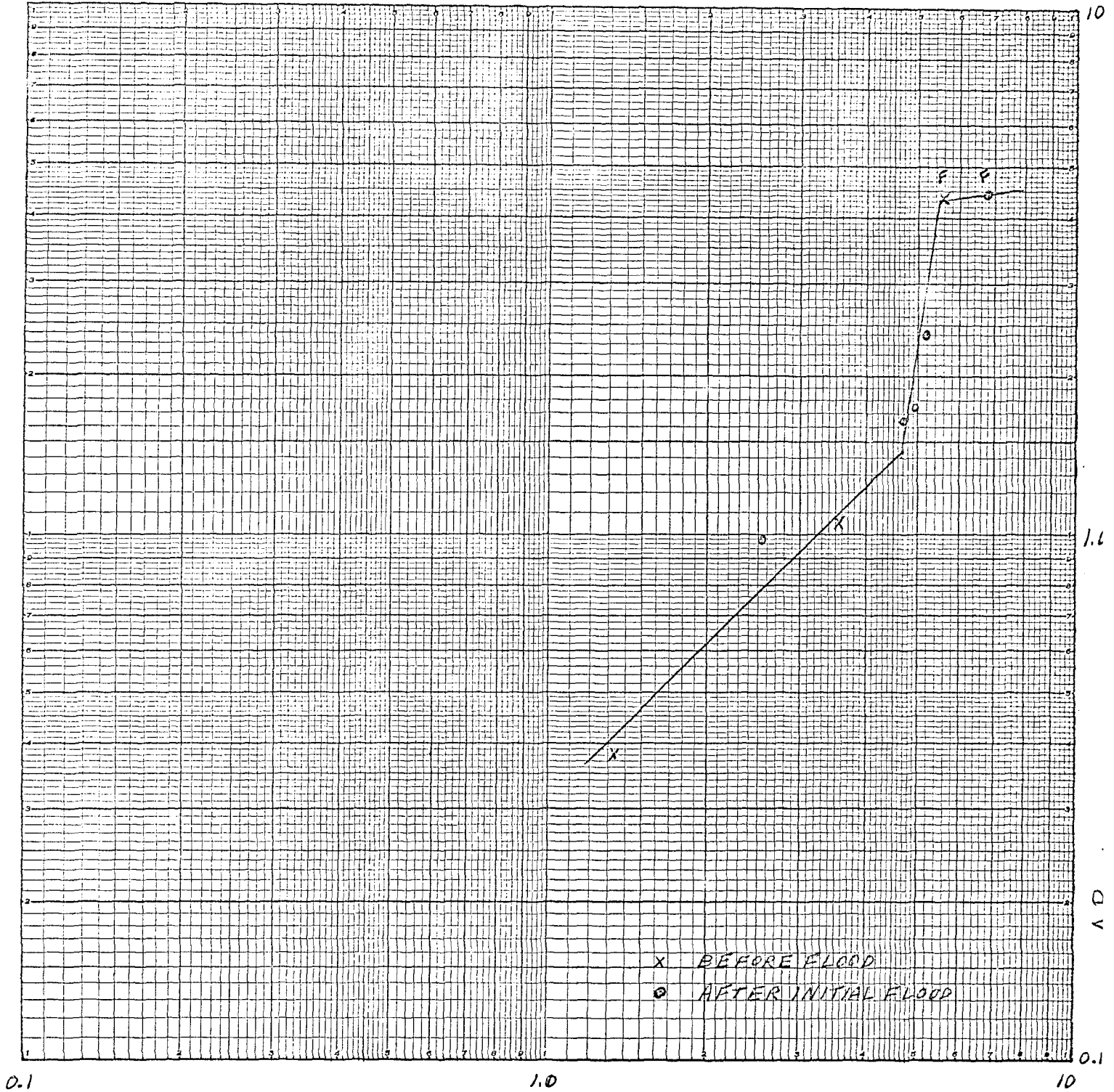
FIGURE B-5 EXPERIMENTAL DETERMINATION OF DEMISTER LOAD POINT AND FLOOD POINT

RUN NO. 6



EXPERIMENTAL DETERMINATION OF DEMISTER
LOAD POINT AND FLOOD POINT

RUN NO. 8

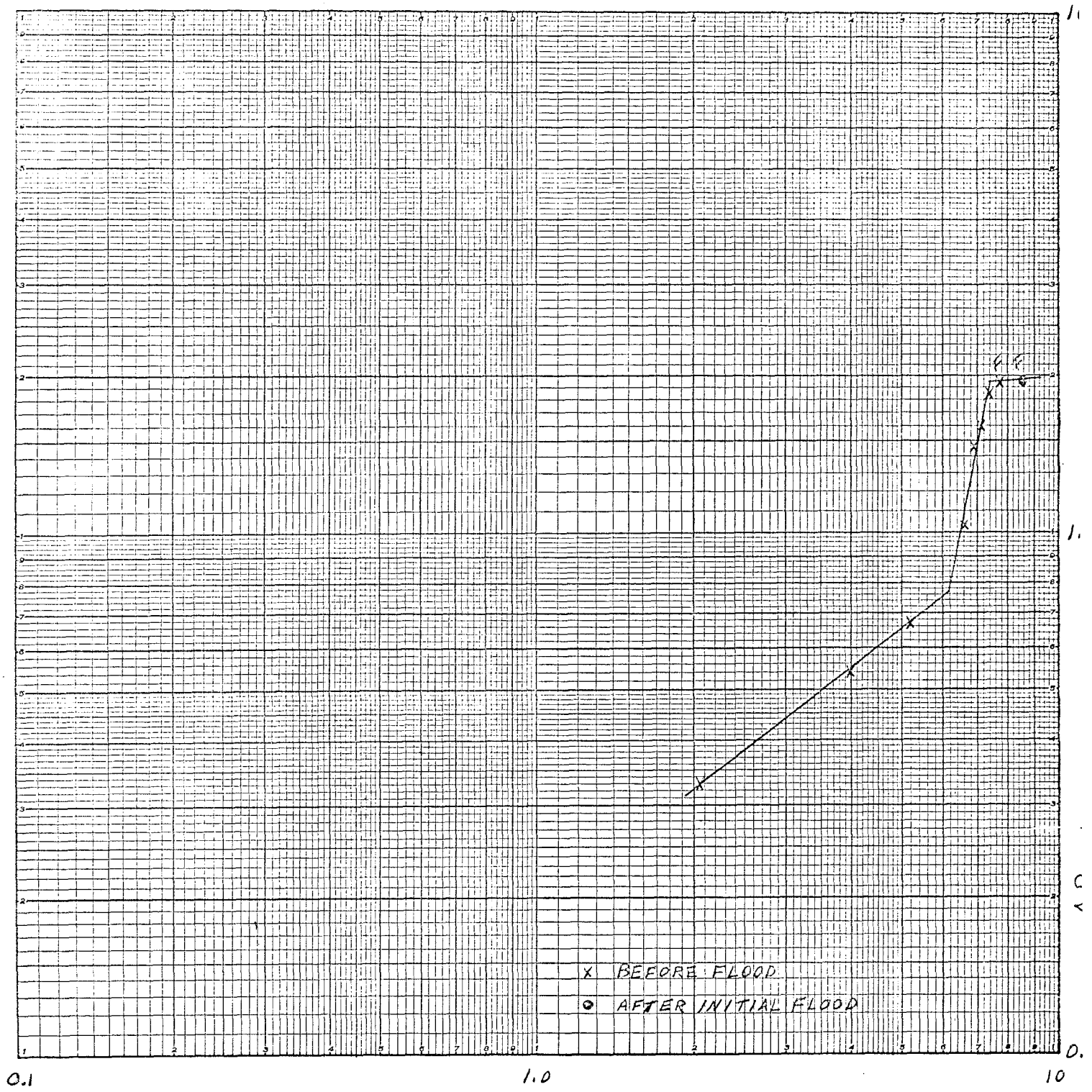


ΔP_0 , IN. WATER

FIGURE B-7

EXPERIMENTAL DETERMINATION OF DEMISTER LOAD POINT AND FLOOD POINT

RUN No. 9



$\Delta P_0, \text{ IN. WATER}$

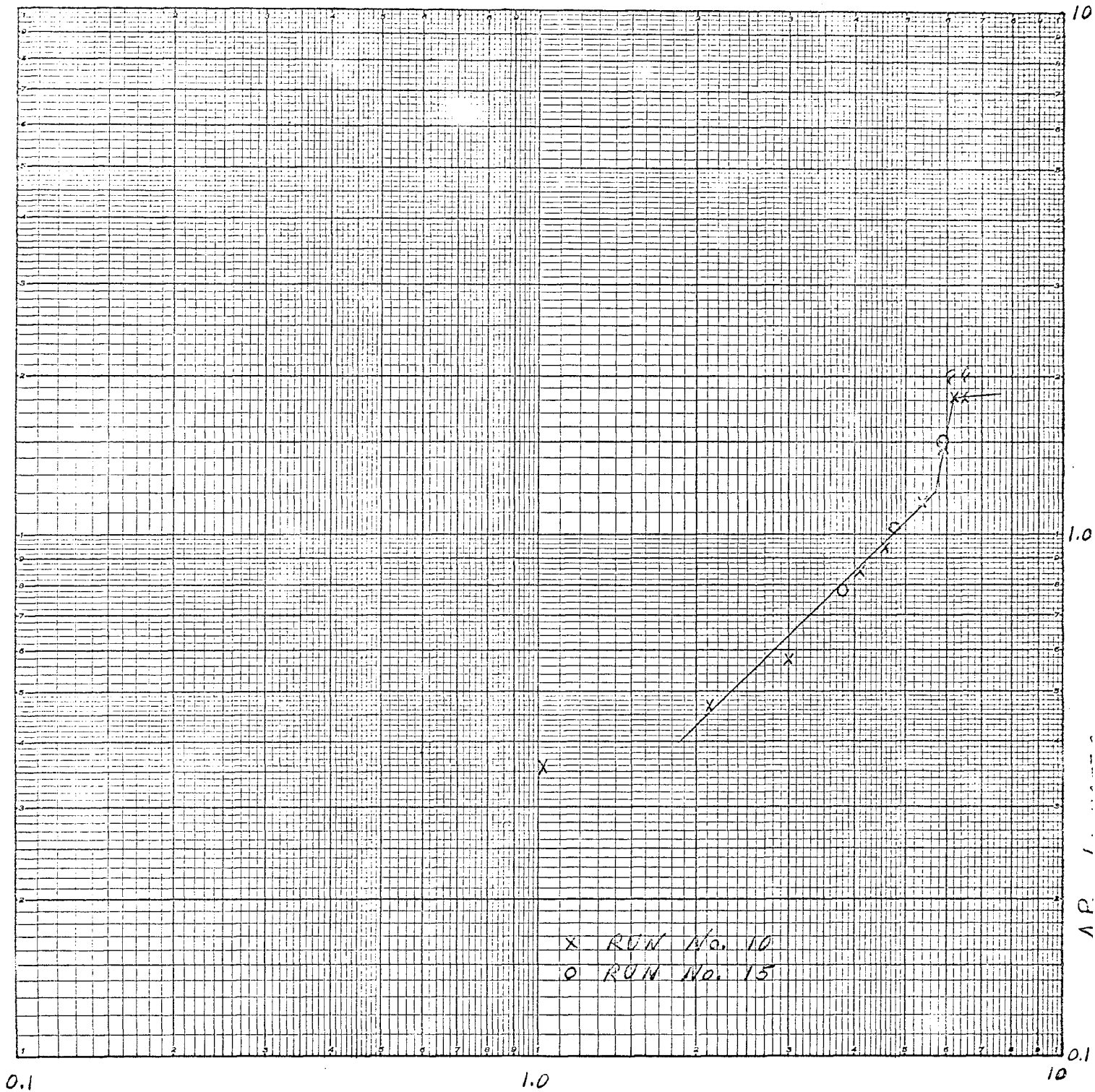
FIGURE B-8

(70)

EXPERIMENTAL DETERMINATION OF DEMISTER LOAD POINT AND FLOOD POINT

LOAD POINT AND FLOOD POINT

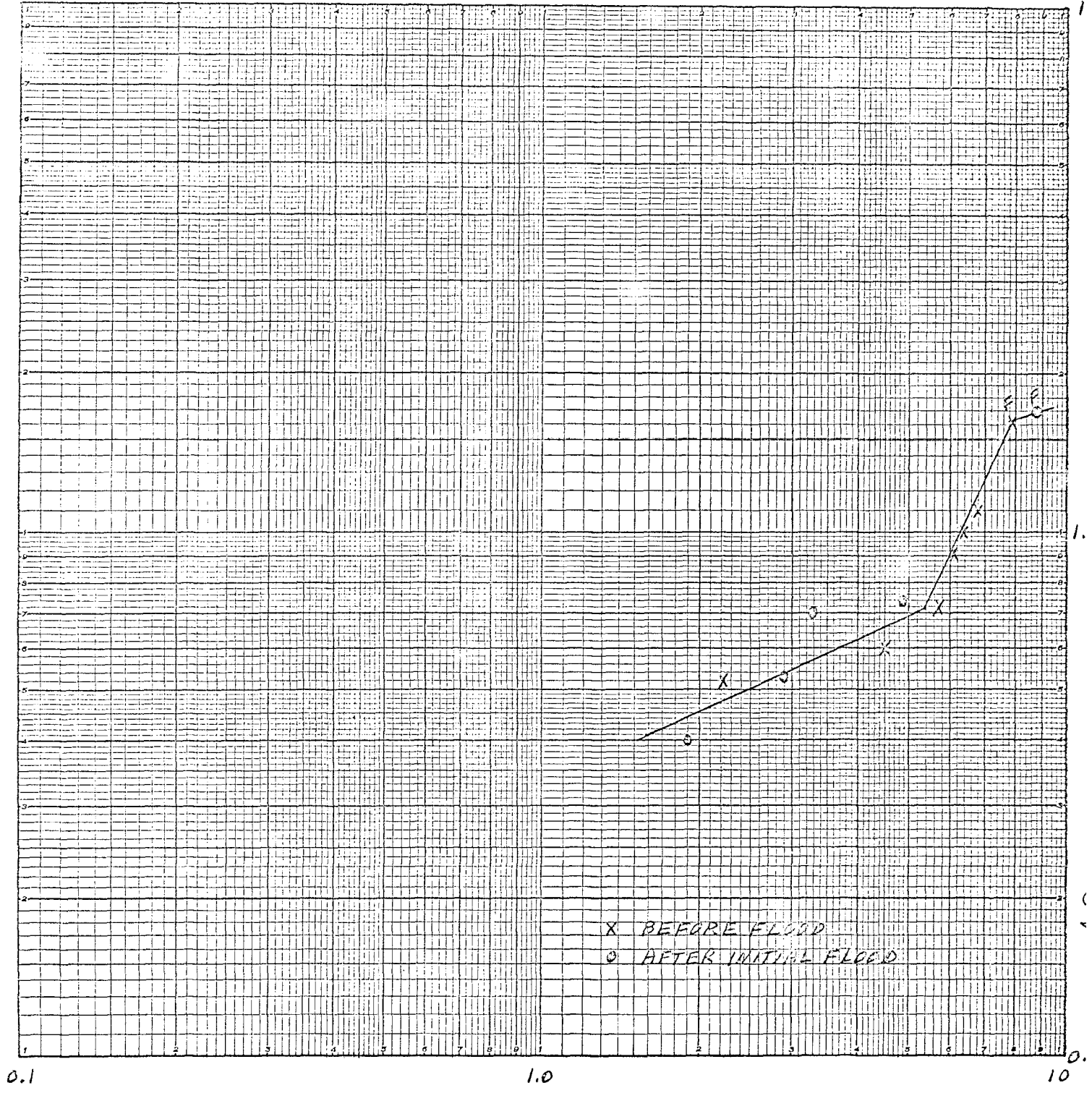
RUN NO. 10 & 15



$\Delta P_0, \text{ IN. WATER}$

EXPERIMENTAL DETERMINATION OF DEMISTER
LOAD POINT AND FLOOD POINT

RUN No. 11

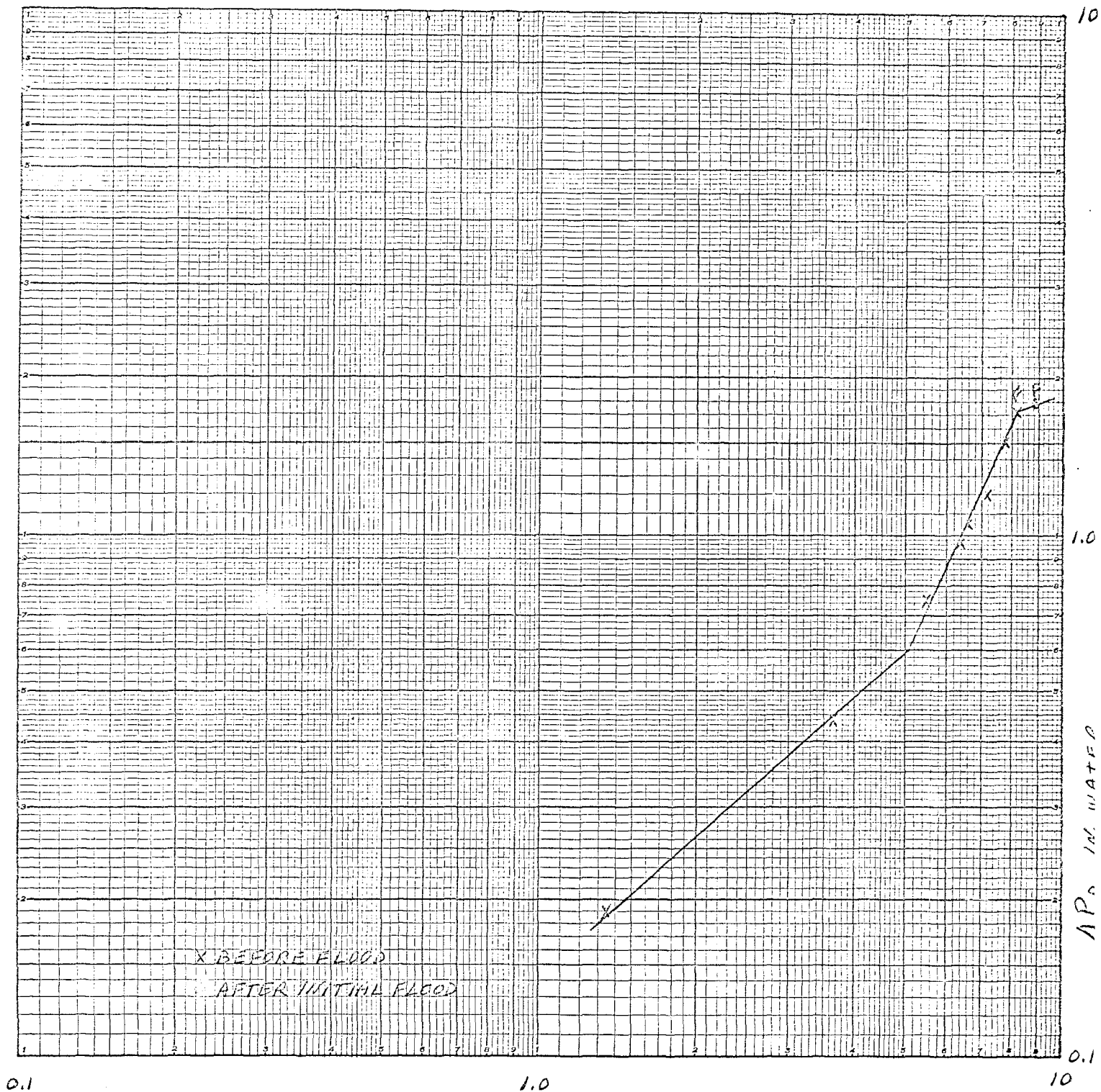


X BEFORE FLOOD
O AFTER INITIAL FLOOD

ΔP_0 , IN. WATER

EXPERIMENTAL DETERMINATION OF DEMISTER
LOAD POINT AND FLOOD POINT

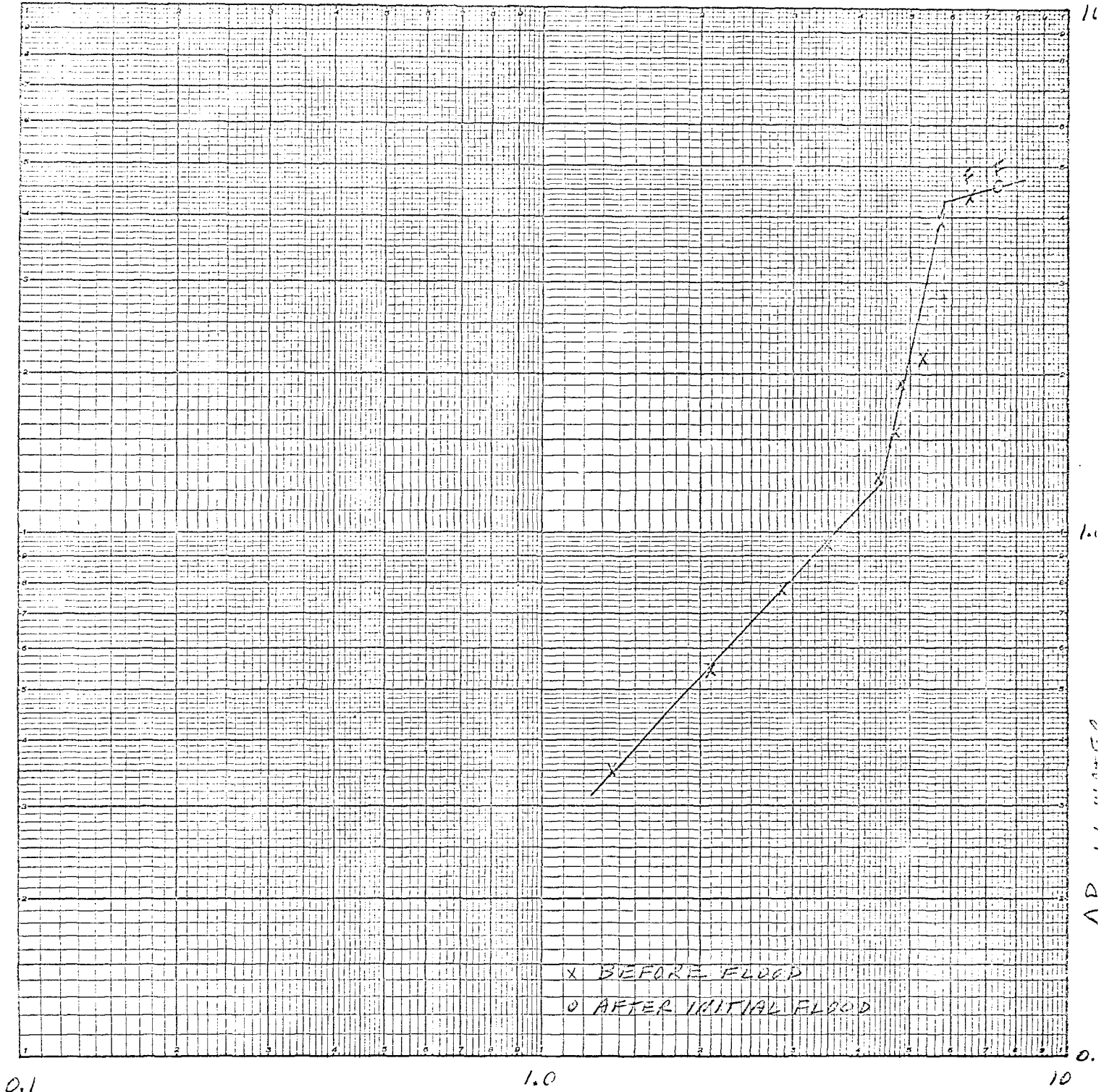
RUN NO. 12 (REPEAT OF RUN NO. 11)



ΔP_0 , IN. WATER

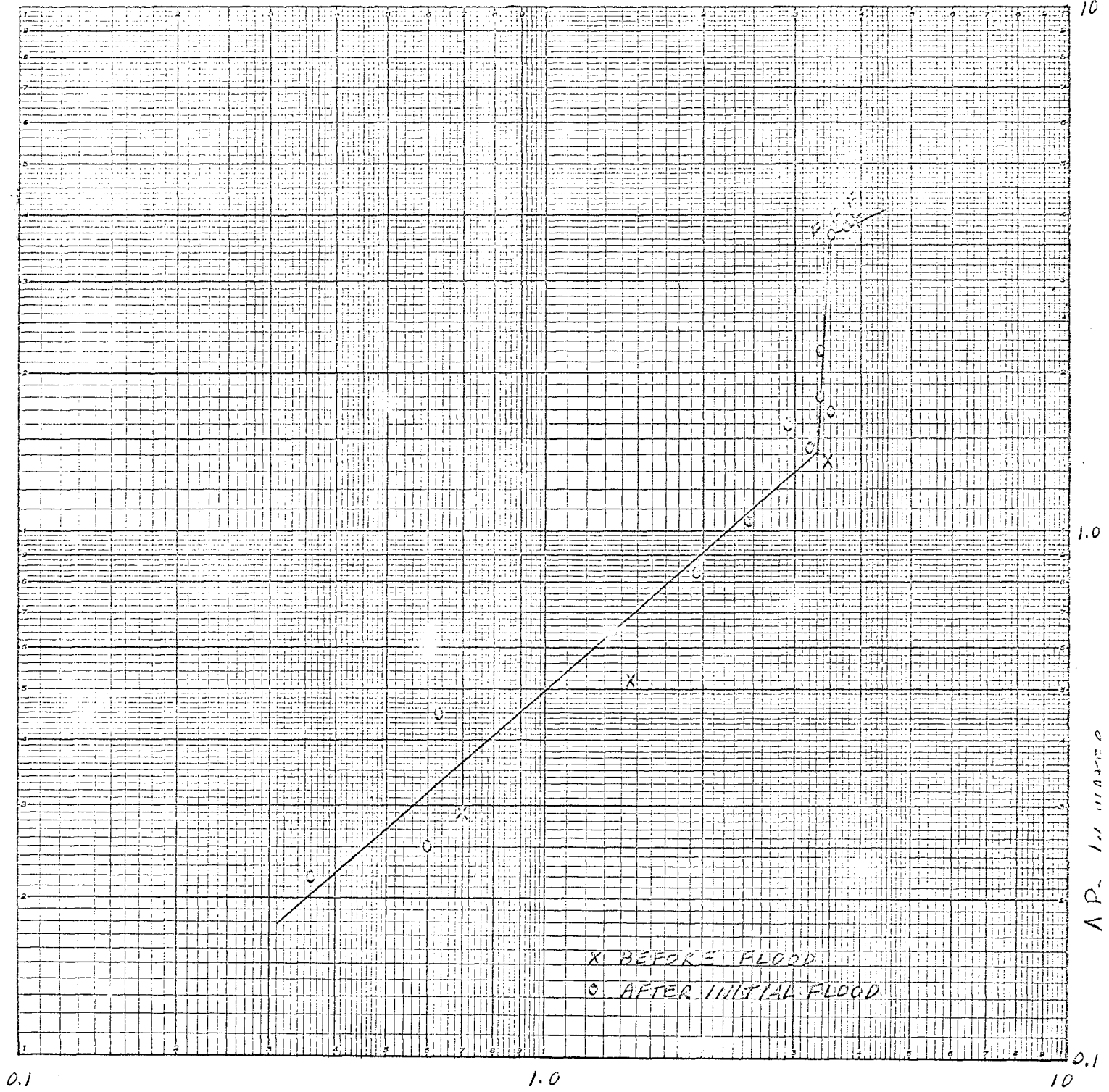
EXPERIMENTAL DETERMINATION OF DEMISTER
LOAD POINT AND FLOOD POINT

RUN NO. 13



EXPERIMENTAL DETERMINATION OF DEMISTER
LOAD POINT AND FLOOD POINT

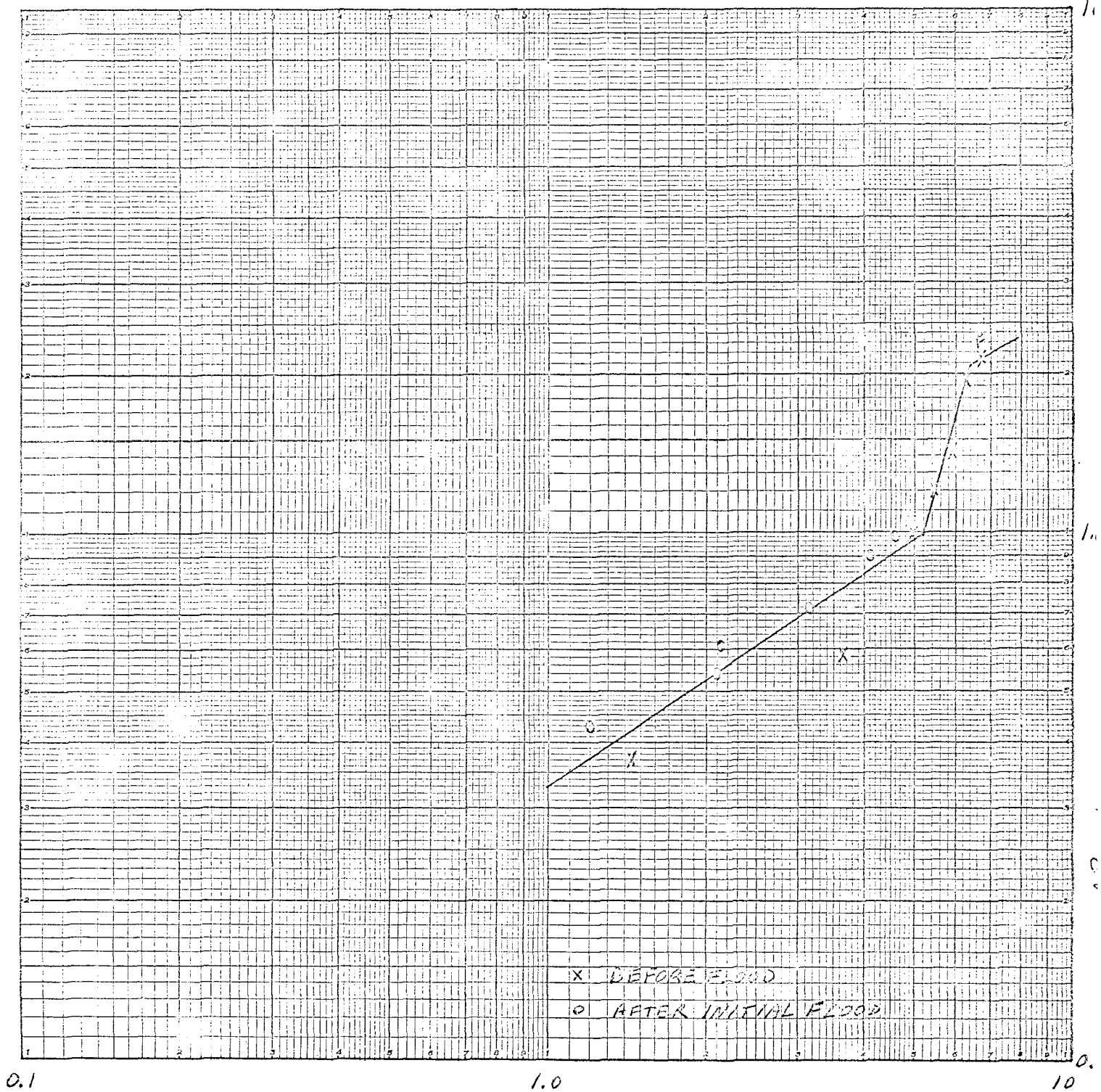
RUN NO. 14



ΔP_0 , IN. WATER

EXPERIMENTAL DETERMINATION OF DEMISTER
LOAD POINT AND FLOOD POINT

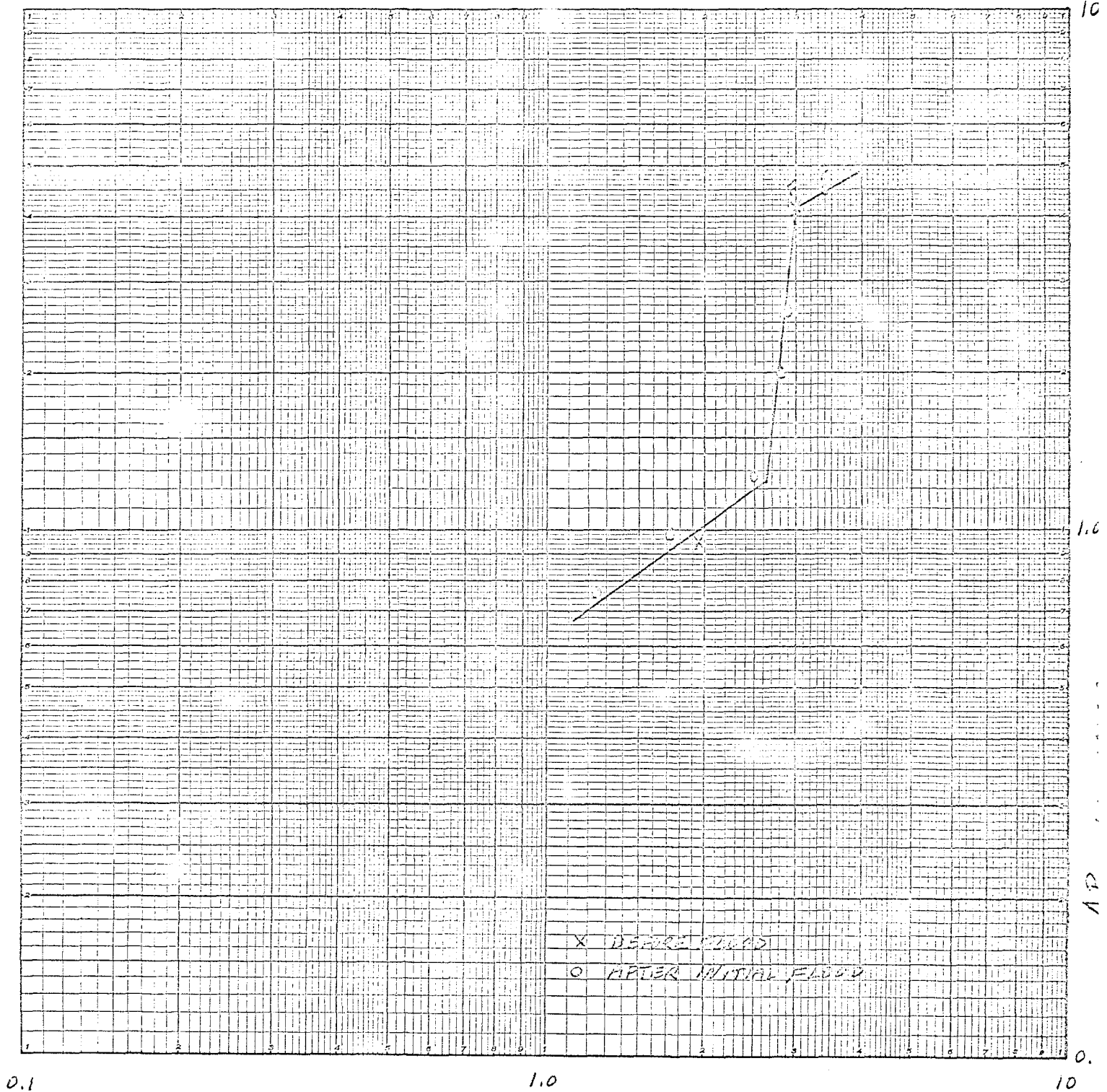
RUN No. 16



ΔP_0 , IN. WATER

EXPERIMENTAL DETERMINATION OF DEMISTER
LOAD POINT AND FLOOD POINT

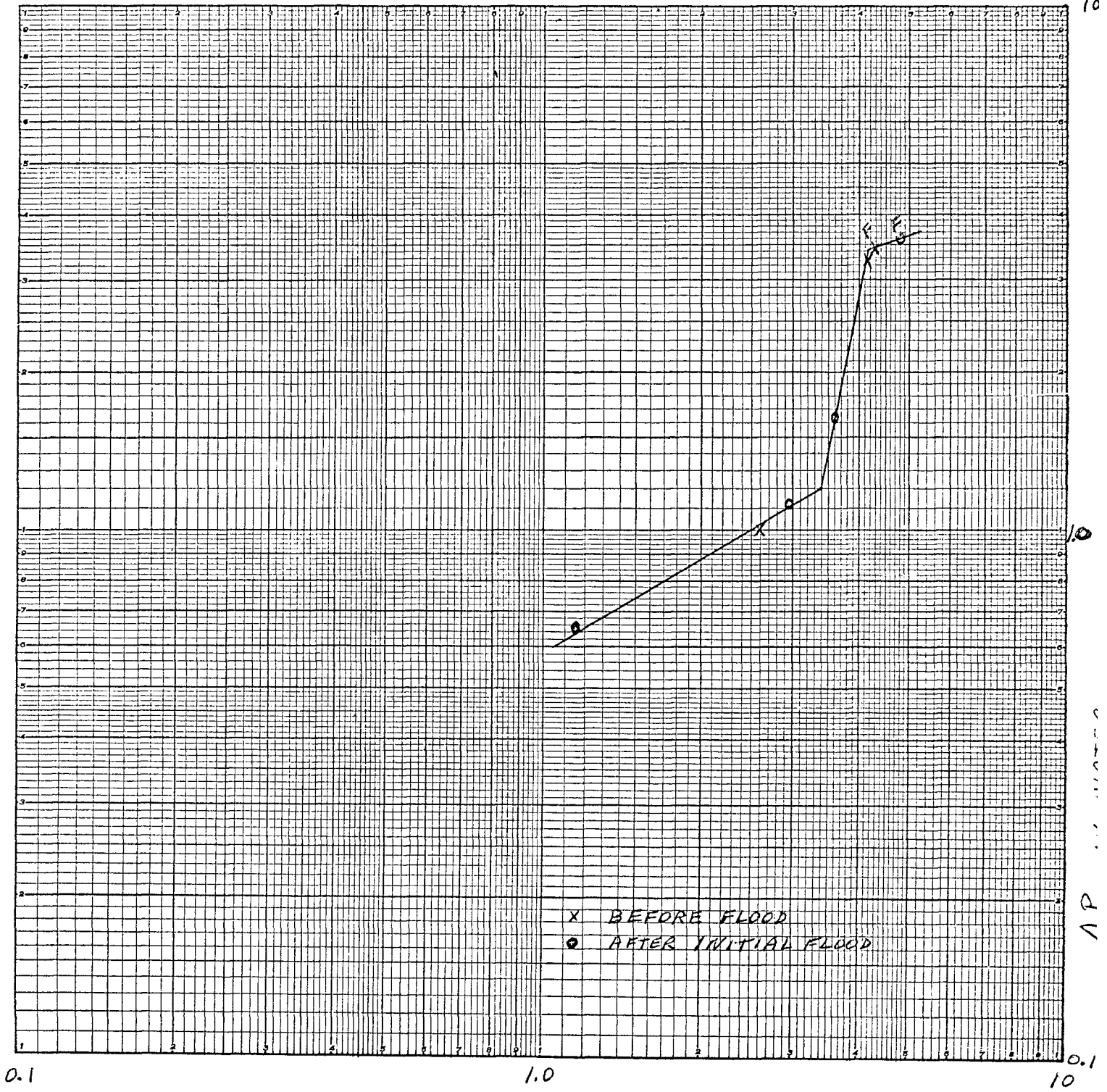
RUN No. 17



ΔP_0 , IN. WATER

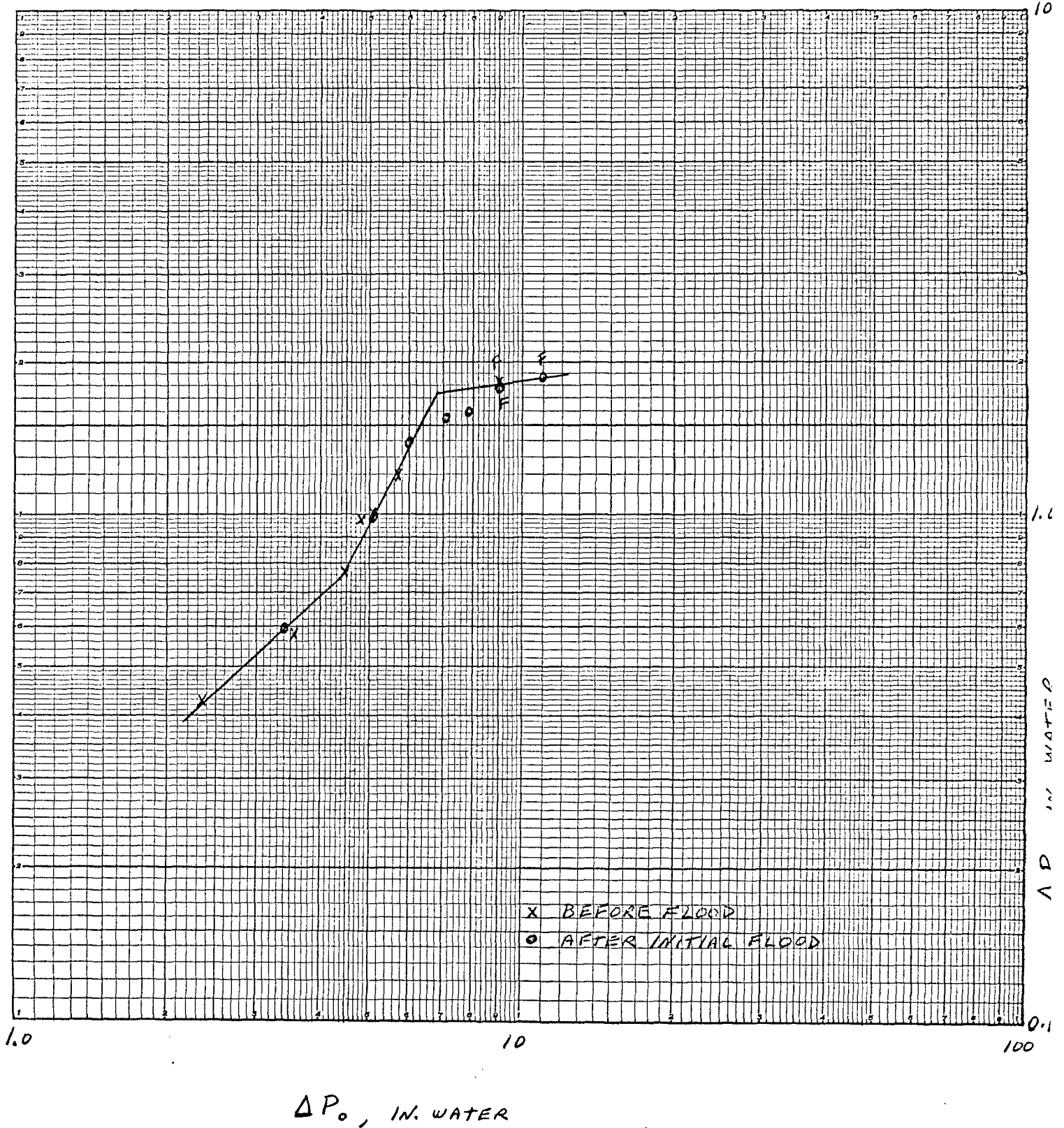
EXPERIMENTAL DETERMINATION OF DEMISTER
LOAD POINT AND FLOOD POINT

RUN NO. 18



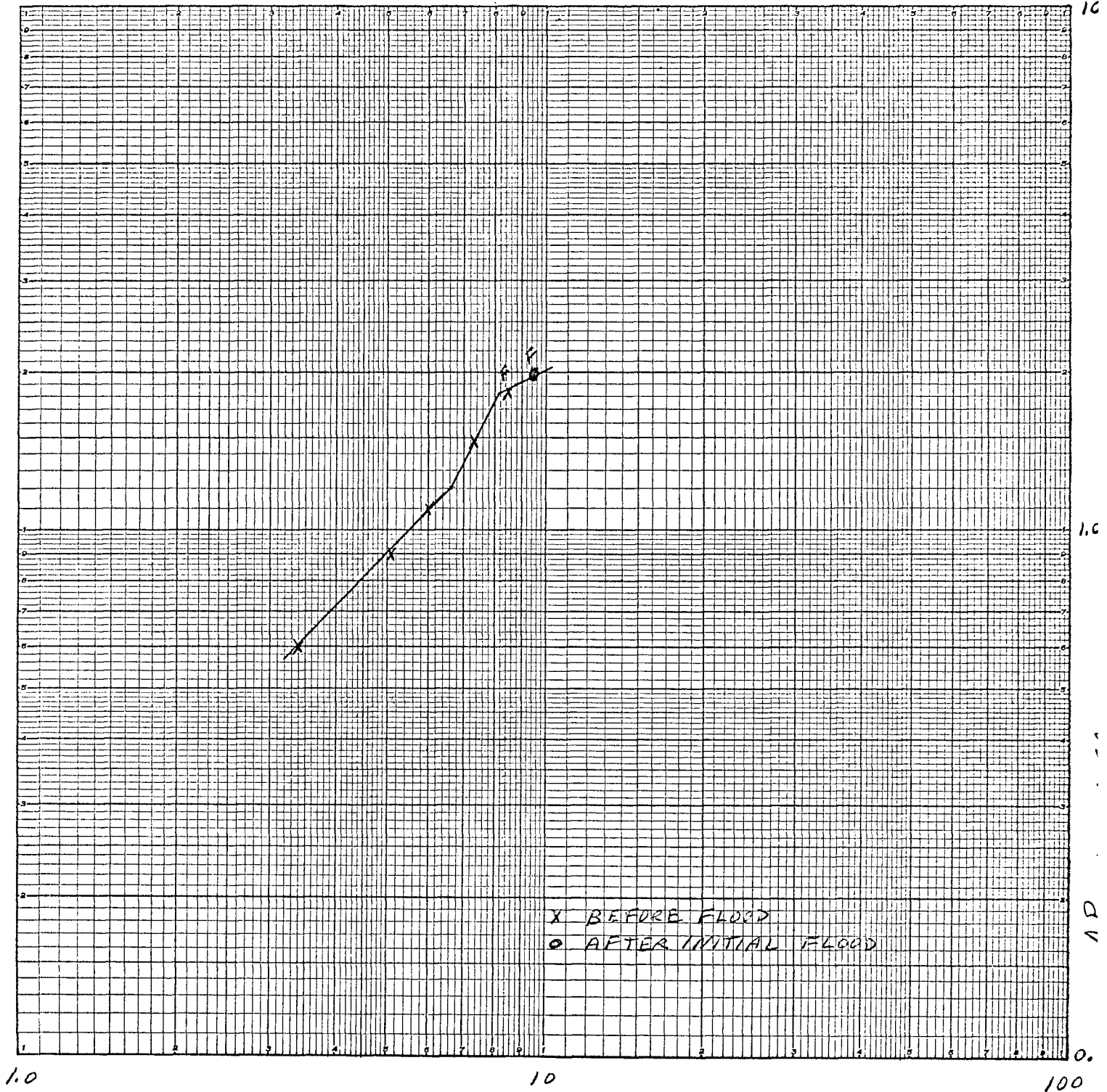
EXPERIMENTAL DETERMINATION OF DEMISTER
LOAD POINT AND FLOOD POINT

RUN No. 19



EXPERIMENTAL DETERMINATION OF DEMISTER
LOAD POINT AND FLOOD POINT

RUN No. 20

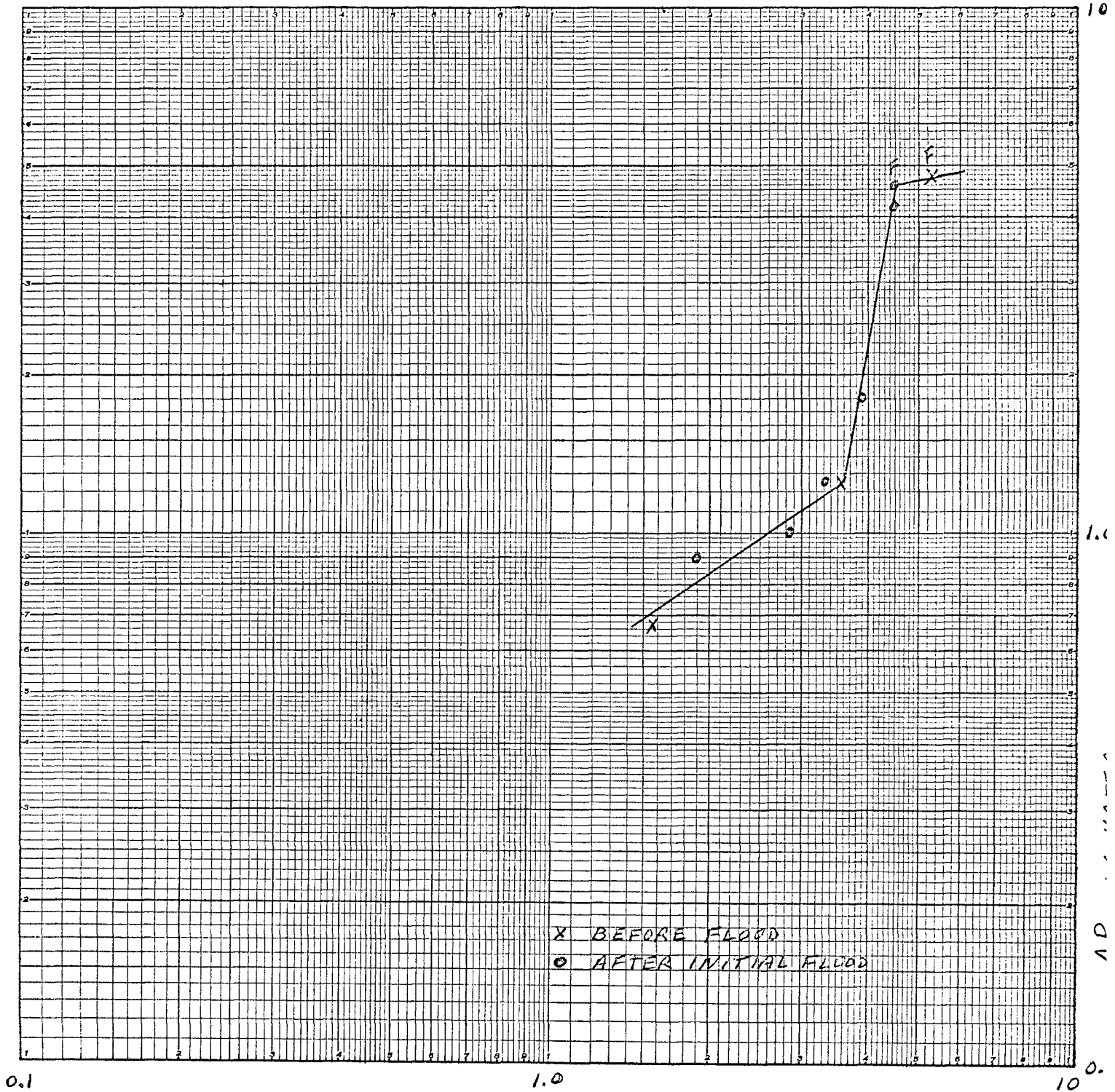


ΔP_0 , IN WATER

FIGURE B-18

EXPERIMENTAL DETERMINATION OF DEMISTER LOAD POINT AND FLOOD POINT

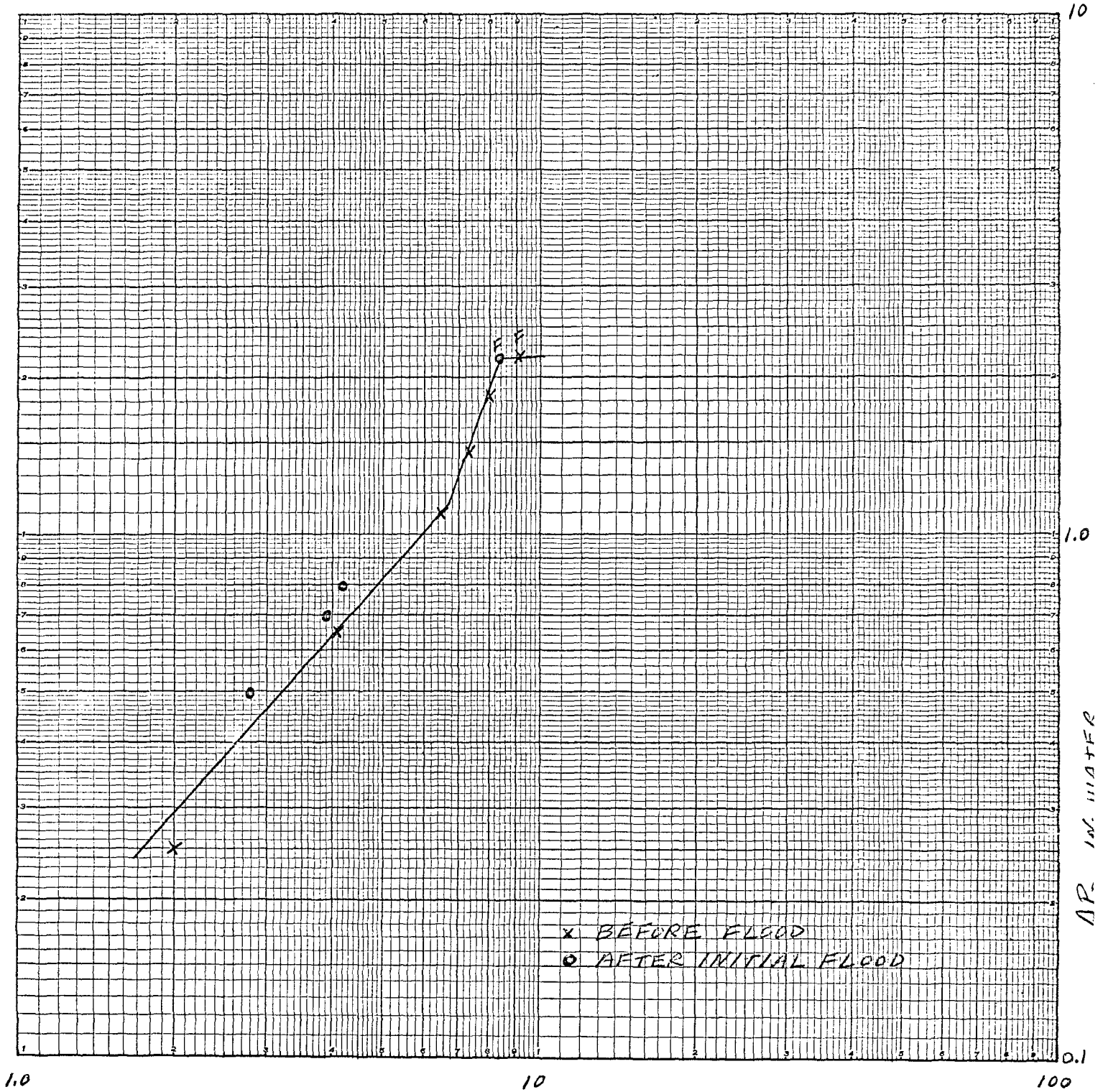
RUN No. 21



$\Delta P_0, \text{ IN. WATER}$

EXPERIMENTAL DETERMINATION OF DEMISTER
LOAD POINT AND FLOOD POINT

RUN No. 23



ΔPo, IN. WATER

EXPERIMENTAL DETERMINATION OF DEMISTER
LOAD POINT AND FLOOD POINT

RUN No. 24

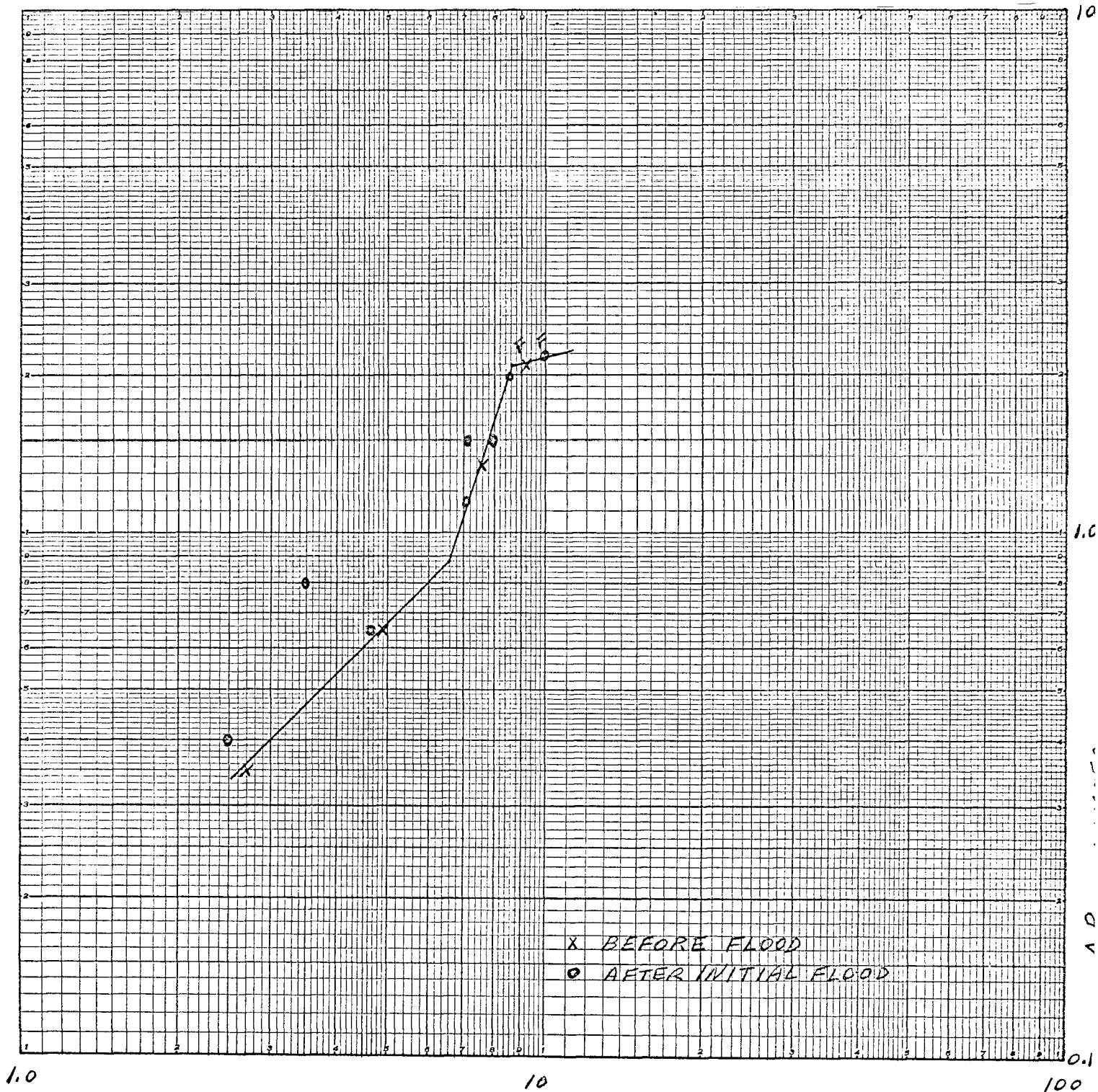
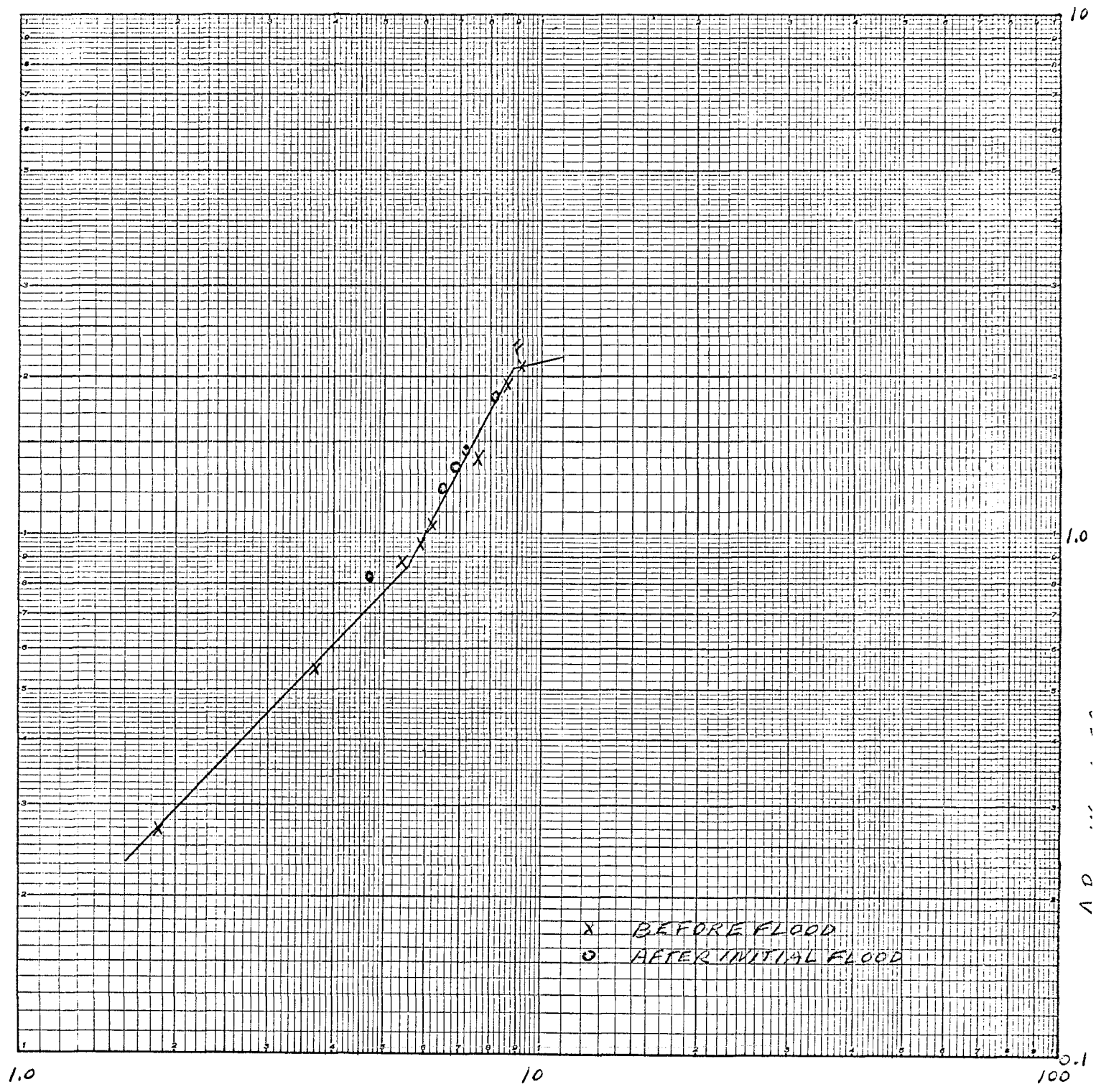


FIGURE B-22

EXPERIMENTAL DETERMINATION OF DEMISTER LOAD POINT AND FLOOD POINT

Run No. 25



ΔP_0 , IN. WATER

EXPERIMENTAL DETERMINATION OF DEMISTER
LOAD POINT AND FLOOD POINT

RUN No. 26

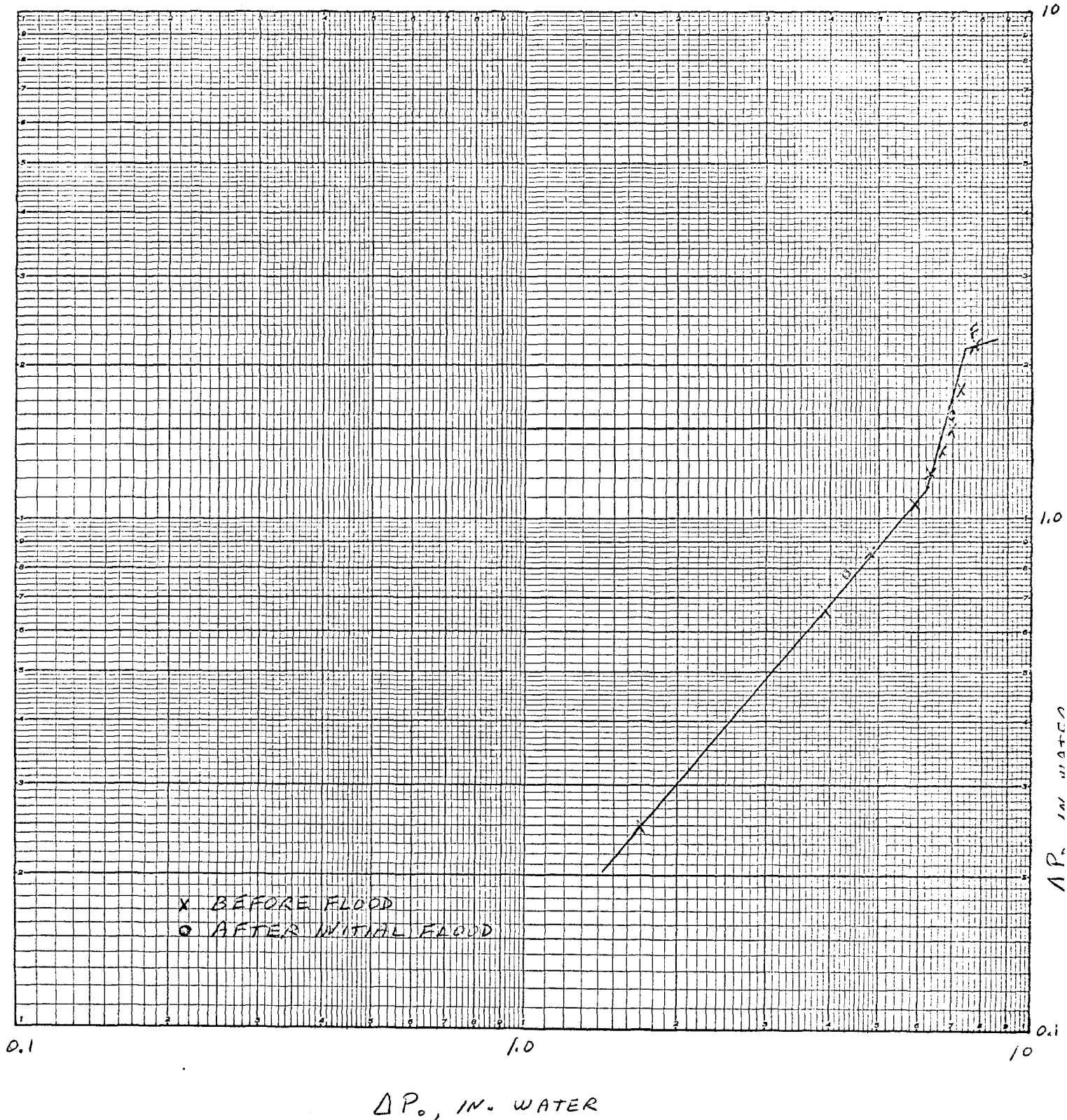
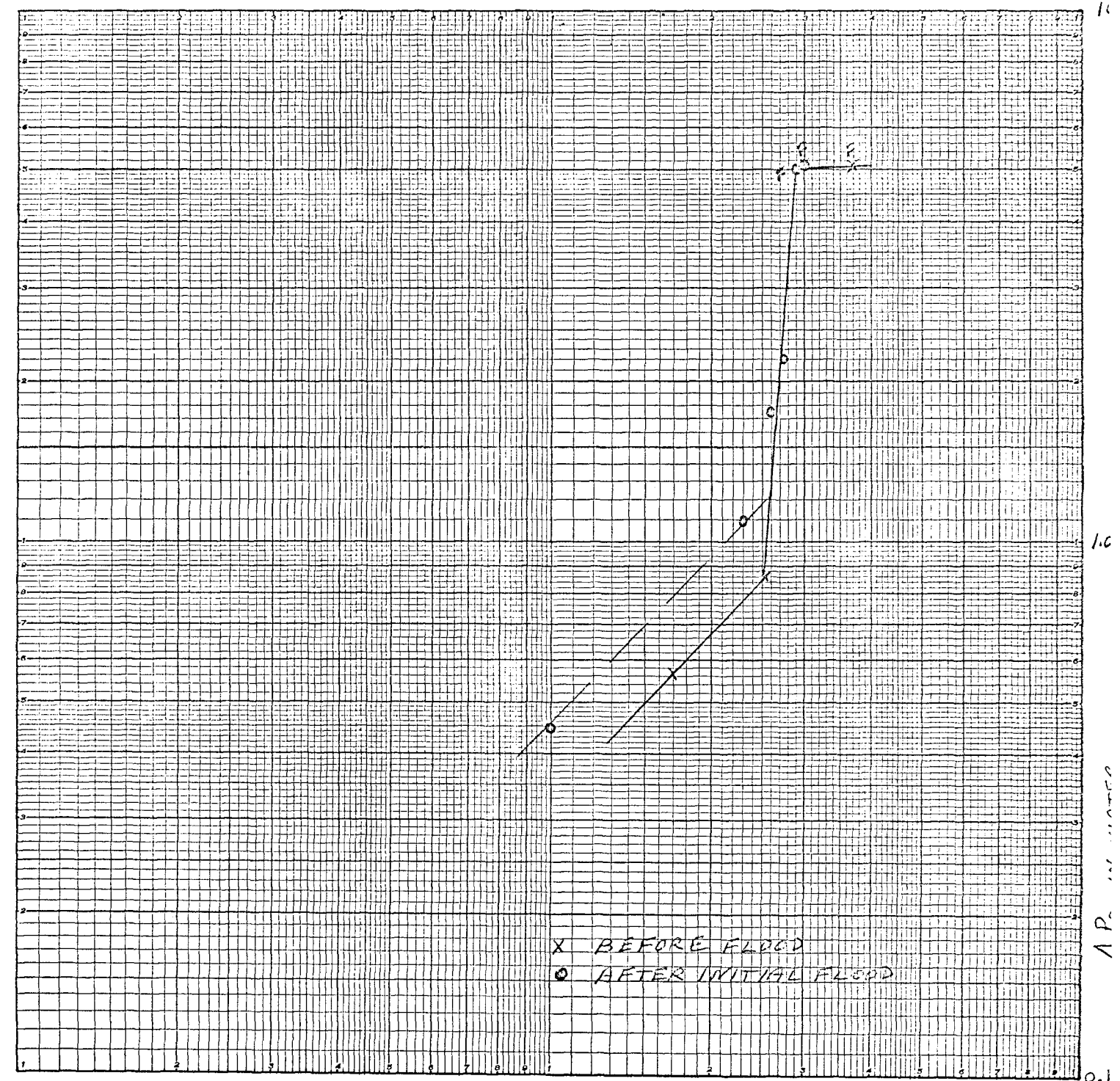


FIGURE B-24 EXPERIMENTAL DETERMINATION OF DEMISTER LOAD POINT AND FLOOD POINT

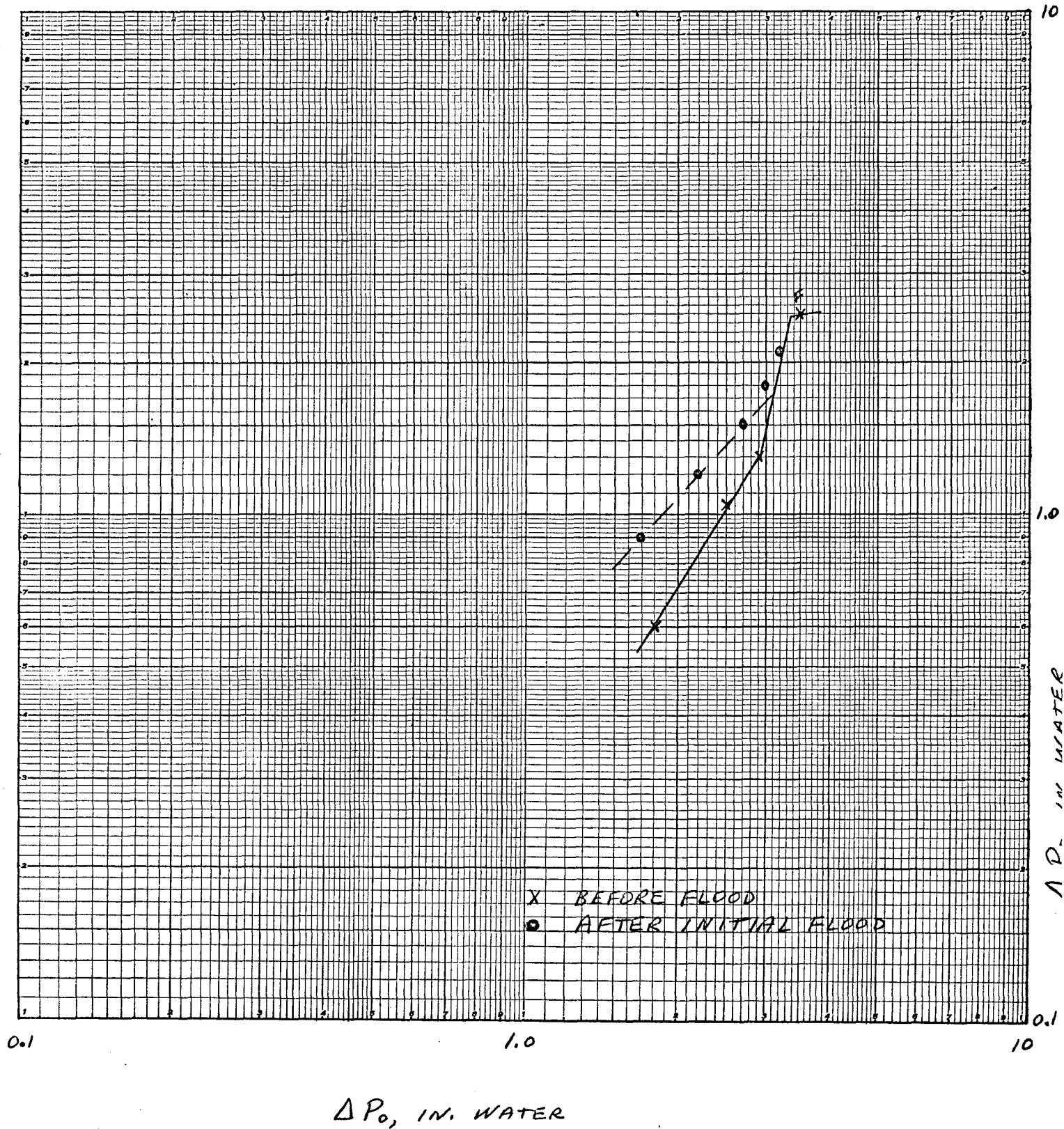
Run No. 27



ΔP_0 , IN. WATER

EXPERIMENTAL DETERMINATION OF DEMISTER
LOAD POINT AND FLOOD POINT

RUN No. 28



EXPERIMENTAL DETERMINATION OF DEMISTER
LOAD POINT AND FLOOD POINT

RUN No. 30

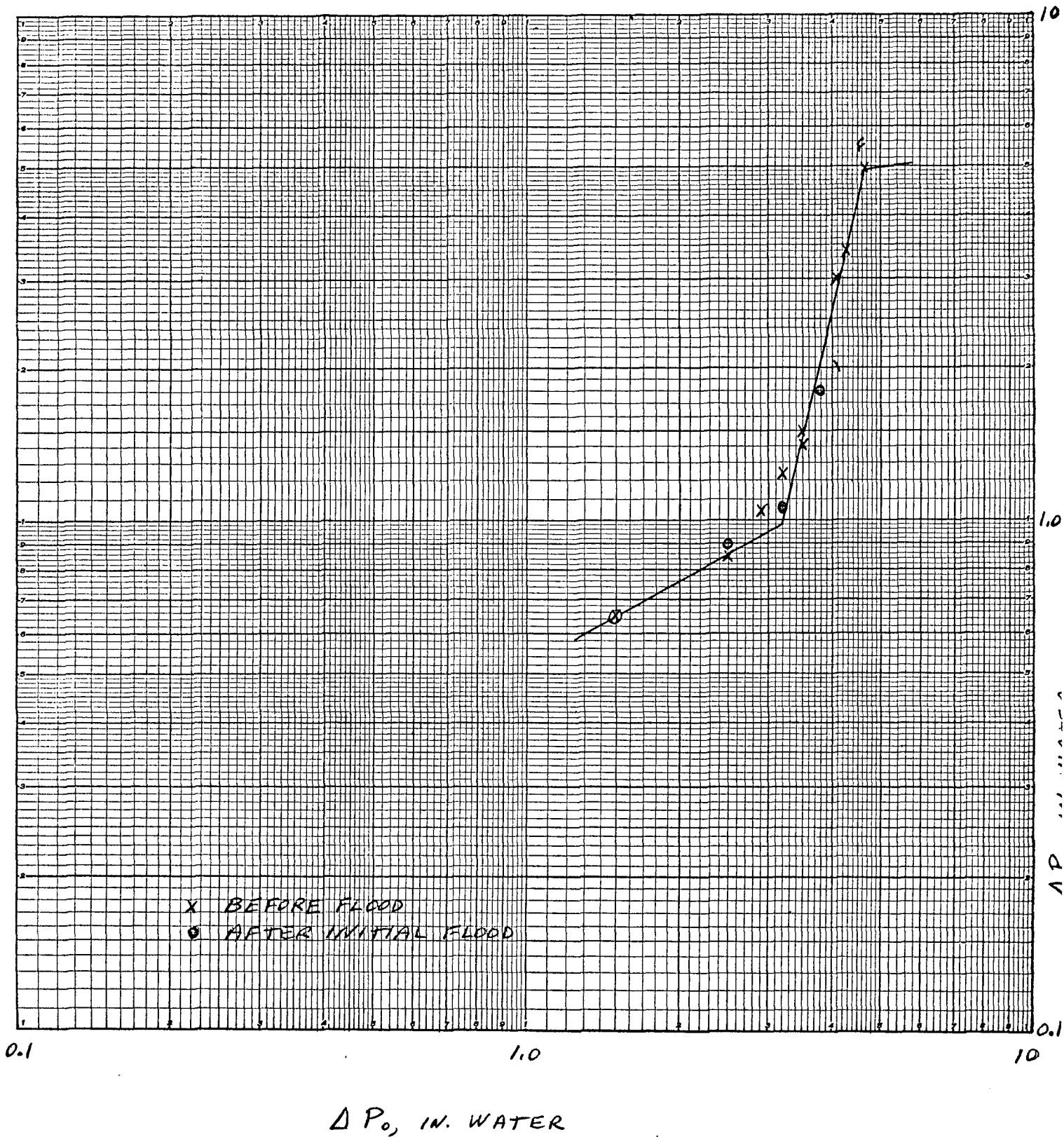
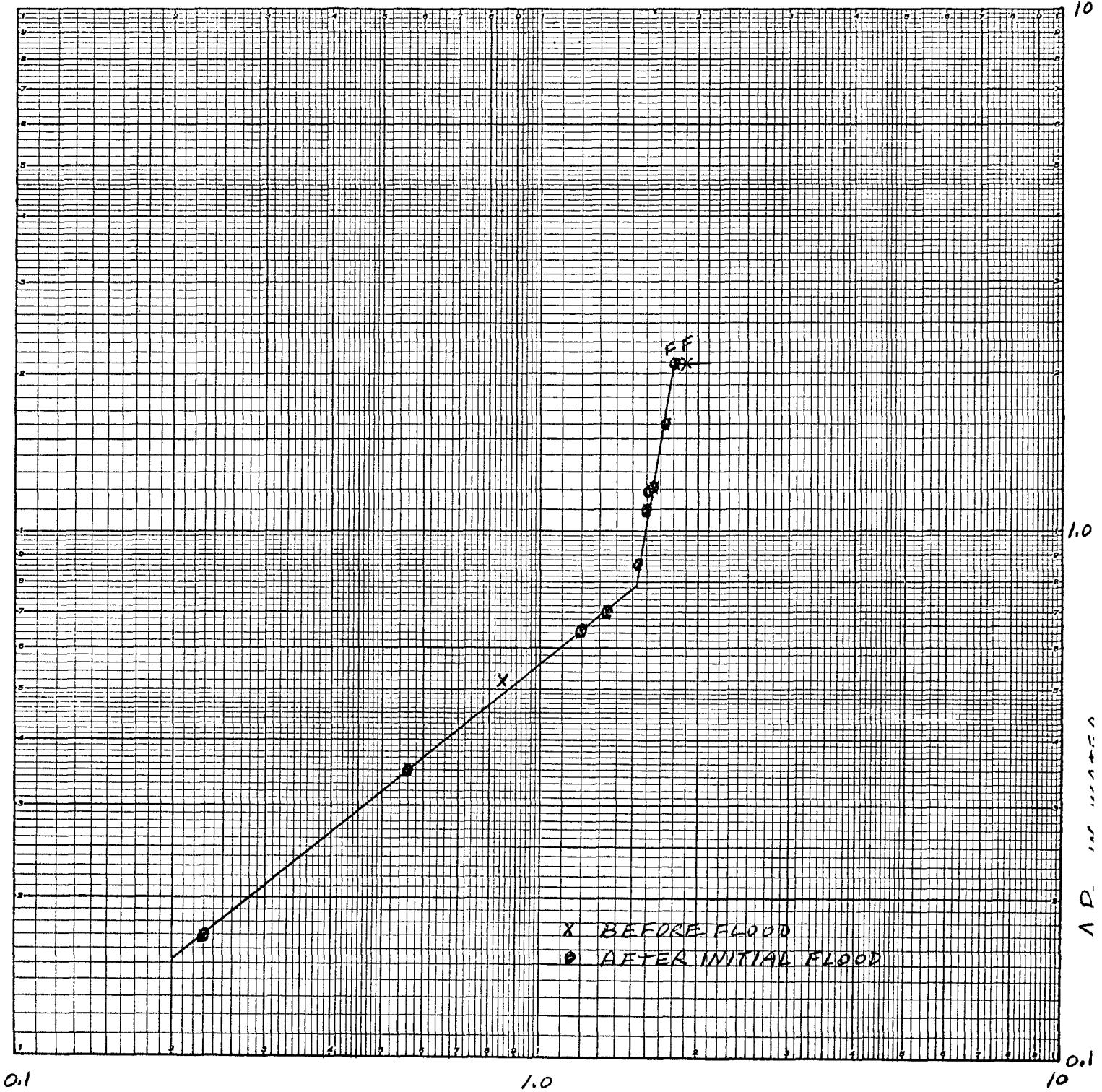


FIGURE B-27
EXPERIMENTAL DETERMINATION OF DEMISTER
LOAD POINT AND FLOOD POINT

RUN No. 31

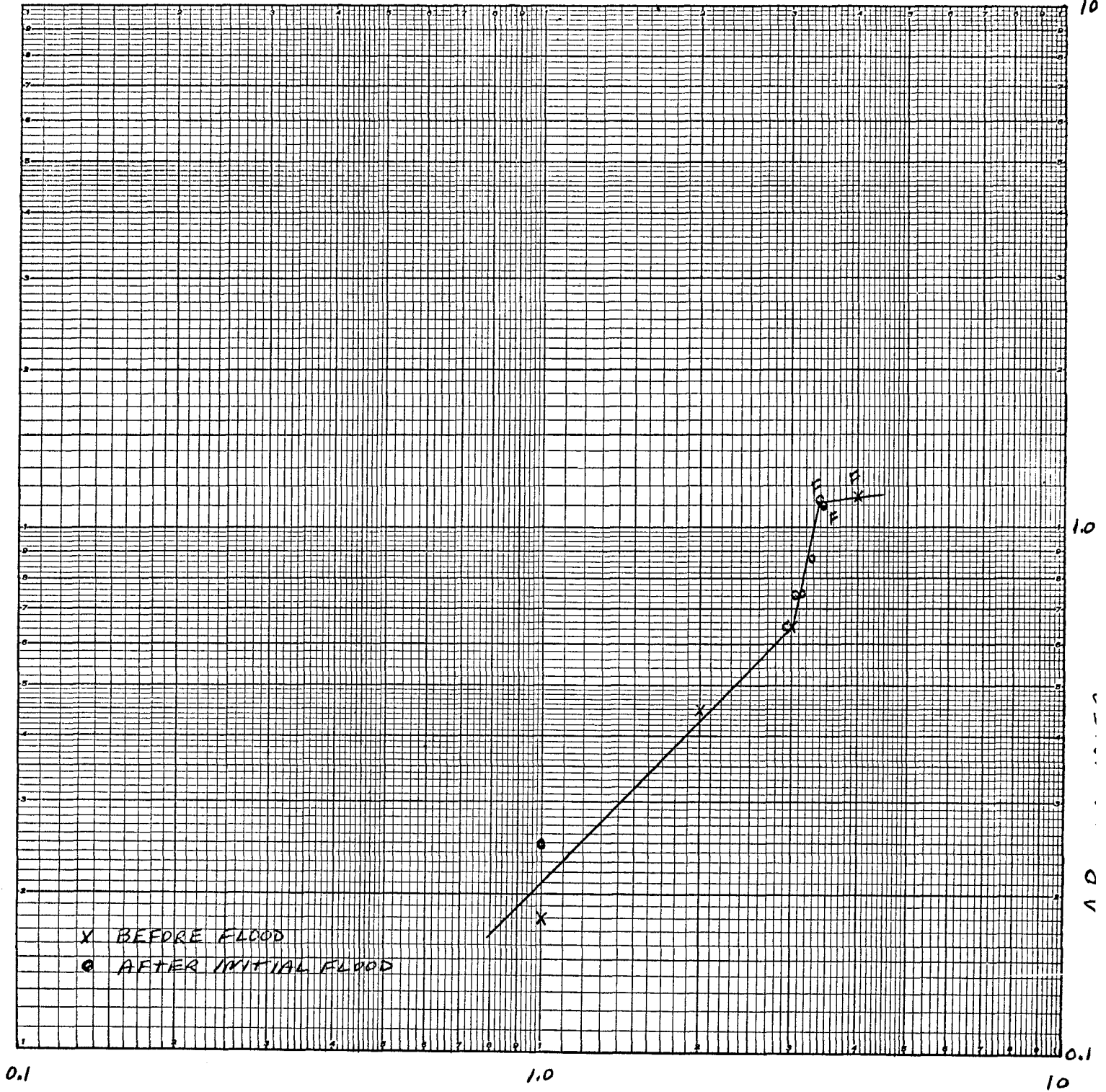


ΔP_o , IN. WATER

FIGURE B-28

EXPERIMENTAL DETERMINATION OF DEMISTER LOAD POINT AND FLOOD POINT

RUN No. 32

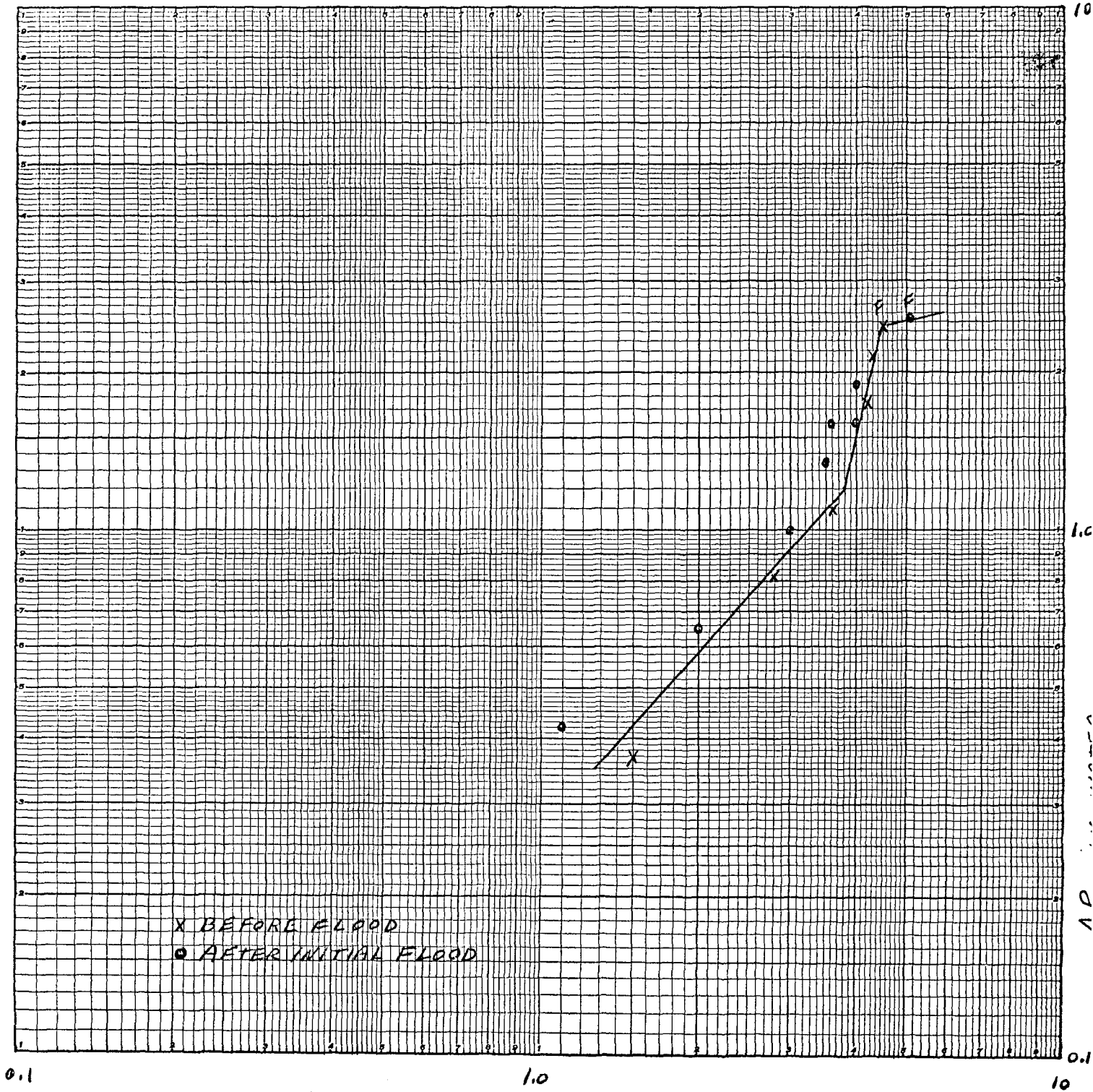


ΔP_0 , IN. WATER

FIGURE B-29

EXPERIMENTAL DETERMINATION OF DEMISTER LOAD POINT AND FLOOD POINT

RUN No. 33

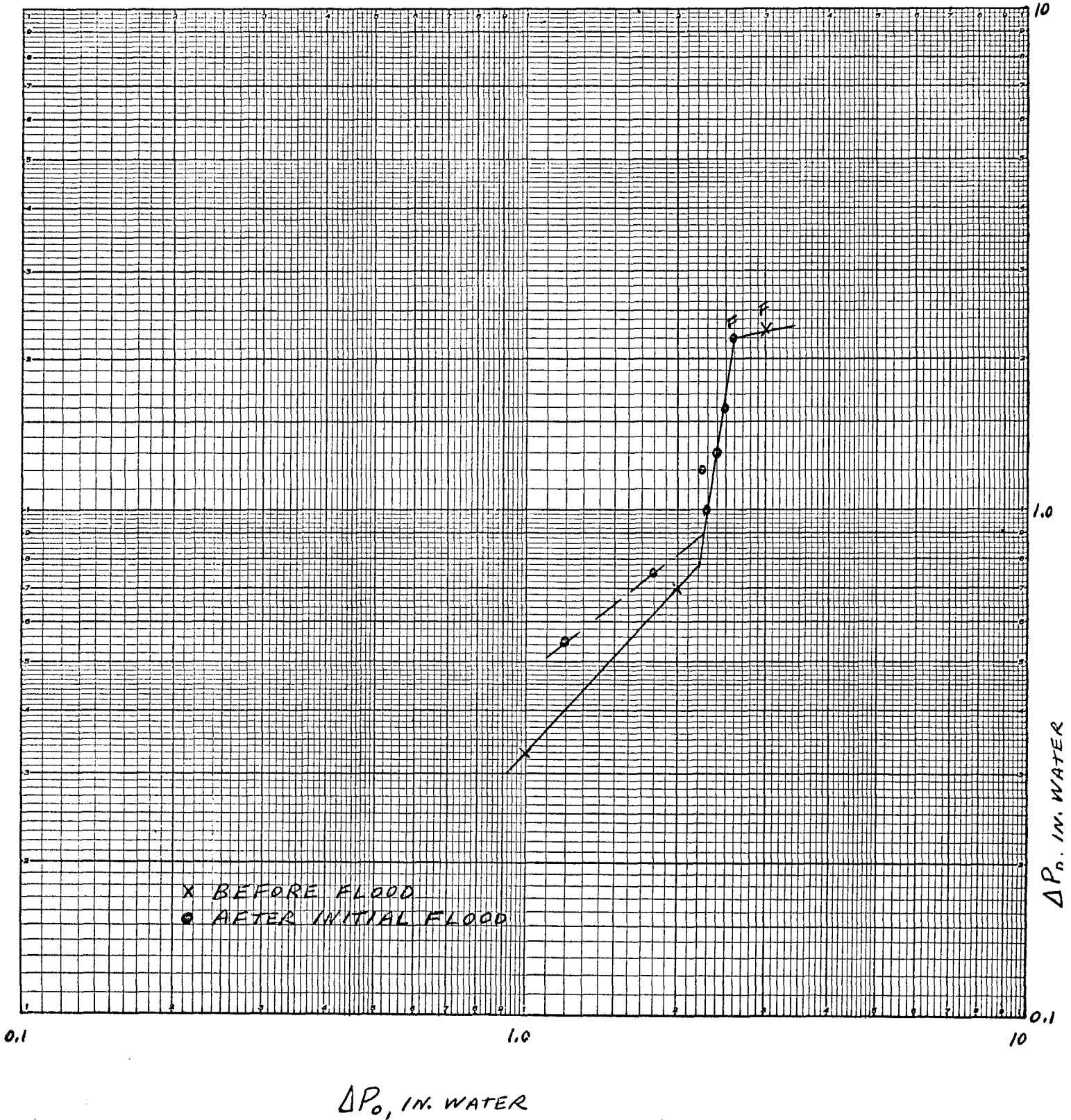


$\Delta P_o, \text{ IN. WATER}$

FIGURE B-30

EXPERIMENTAL DETERMINATION OF DEMISTER
LOAD POINT AND FLOOD POINT

RUN No. 34



EXPERIMENTAL DETERMINATION OF DEMISTER
LOAD POINT AND FLOOD POINT

RUN No. 35

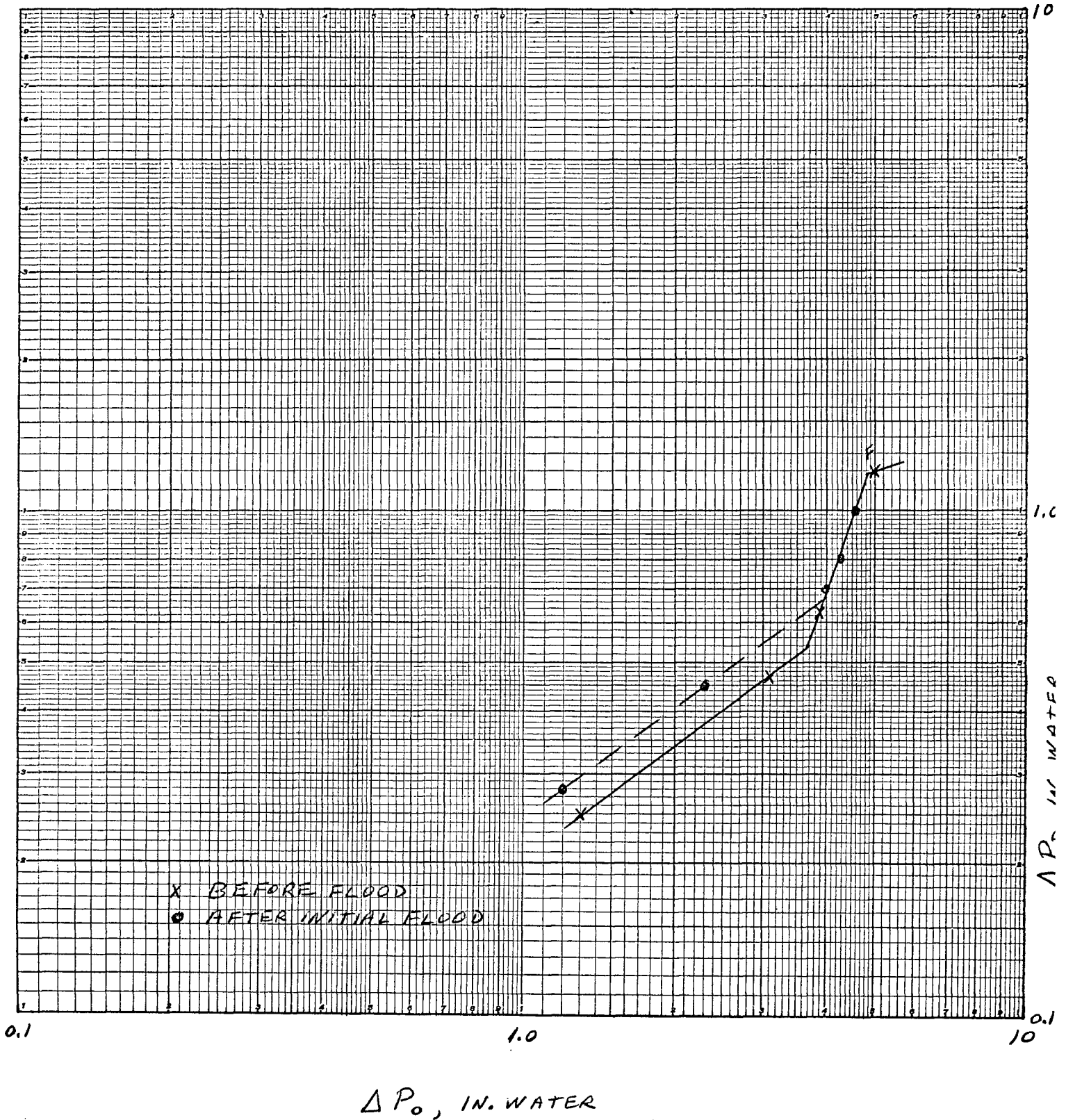
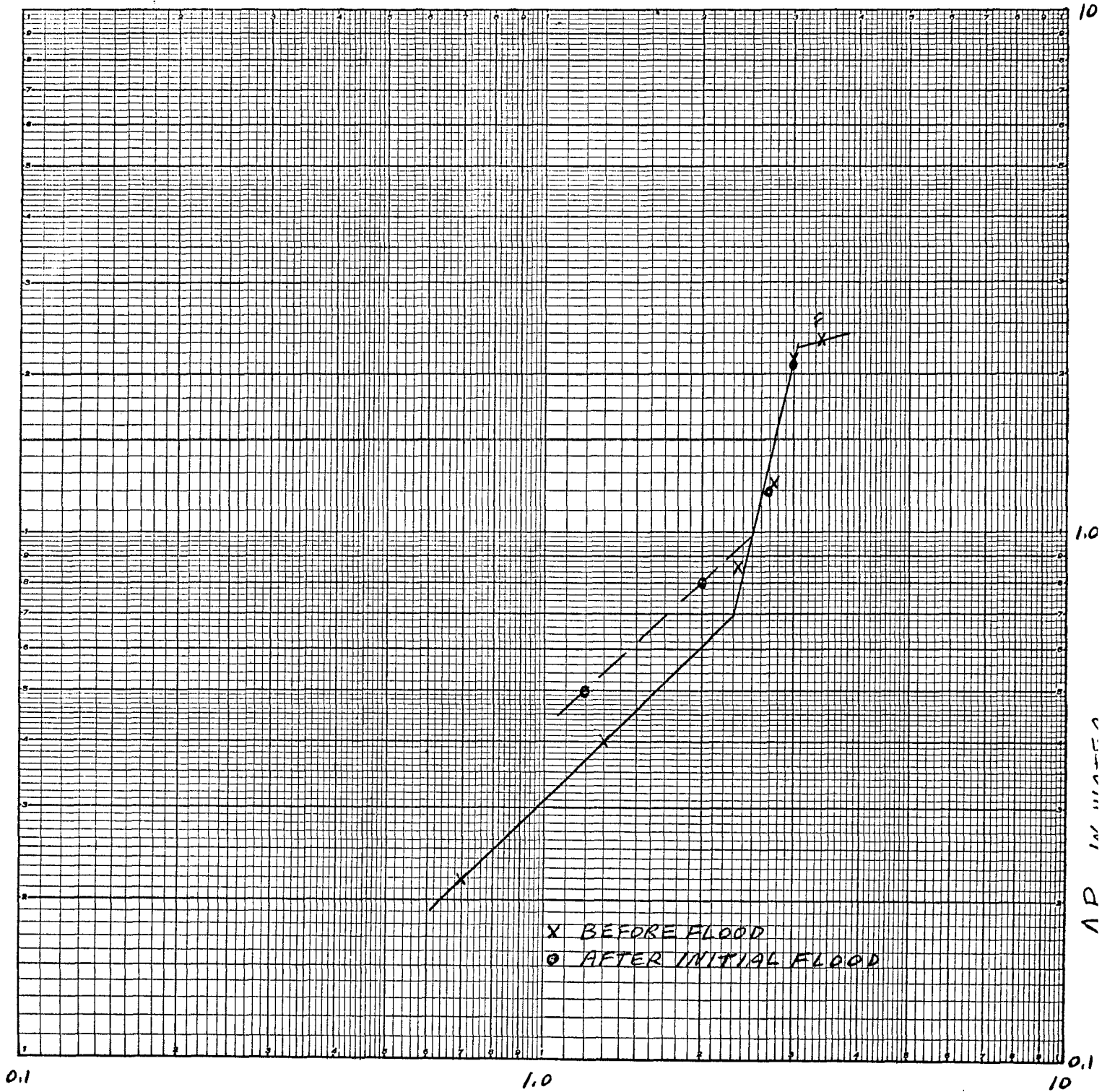


FIGURE B-32

EXPERIMENTAL DETERMINATION OF DEMISTER
LOAD POINT AND FLOOD POINT

RUN No. 36

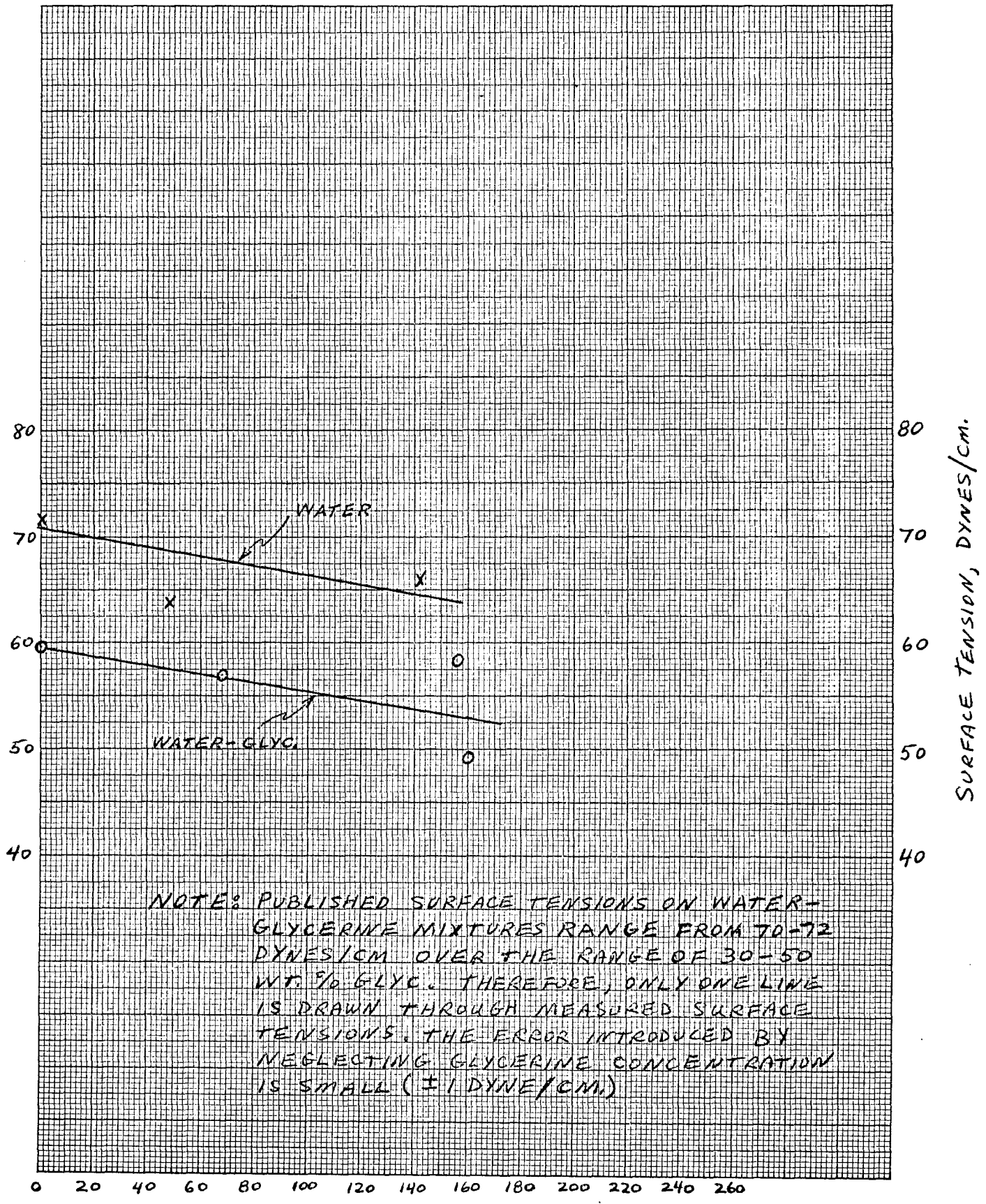


ΔP_0 , IN. WATER

APPENDIX C

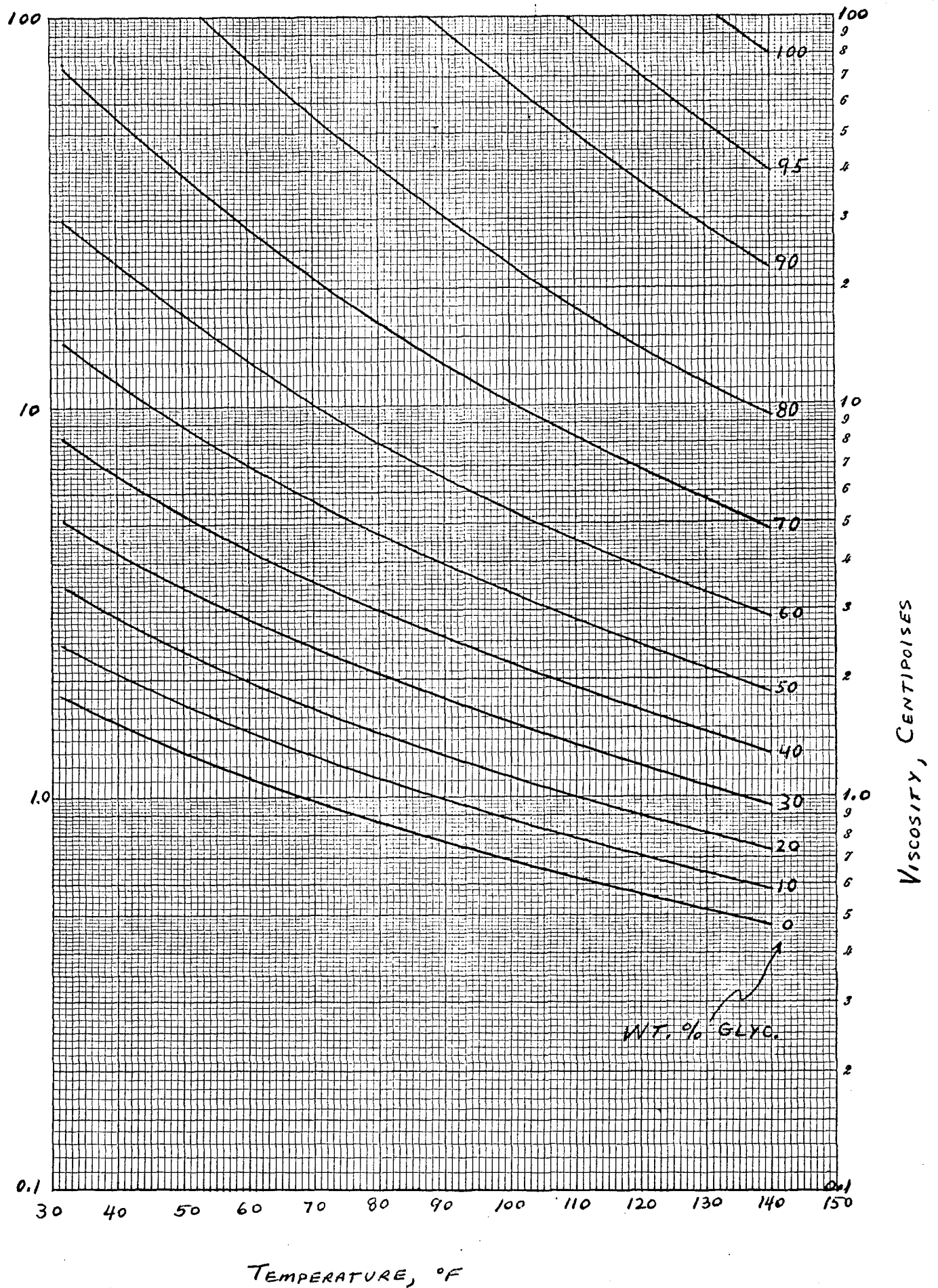
PHYSICAL PROPERTIES OF TEST LIQUIDS

FIGURE C-1
SURFACE TENSION OF TEST LIQUIDS



TIME ON SAMPLE, MINUTES

FIGURE C-2
VISCOSITY OF GLYCERINE-WATER MIXTURES



APPENDIX D

DATA CORRELATION

TABLE D-1
CALCULATED DATA FOR FIGURES 7 AND 8

RUN NO.	$\sqrt{\frac{P_L - P_G}{P_G}}$	K_L	K_F	$\frac{G_L}{G_G} \sqrt{\frac{P_G}{P_L}}$	$\frac{V_F^2 a P_G (\mu_L)^{0.2}}{32.2 E^3 P_L}$
1	29.6	0.33	0.38	0.00470	0.515*
2	29.6	0.34	0.37	0.00458	0.495*
5	29.6	0.37	0.41	0.00424	0.591*
6	29.6	0.31	0.52	0.00326	0.395
8	29.6	0.42	0.45	0.00108	0.748*
9	29.6	0.48	0.53	0.000910	0.411
10	29.6	0.47	0.48	0.00376	0.337
11	29.6	0.45	0.55	0.000447	0.432
12	29.6	0.44	0.56	0.000438	0.446
13	29.6	0.41	0.48	0.000515	0.795*
14	29.6	0.35	0.36	0.00490	0.478*
16	30.4	0.43	0.48	0.00340	0.382
17	30.7	0.30	0.32	0.00464	0.462*
18	30.7	0.35	0.38	0.000923	0.622*
19	30.8	0.39	0.49	0.000717	0.410
20	30.9	0.47	0.55	0.000788	0.547
21	31.1	0.35	0.39	0.00145	0.721*
22	31.4	0.36	0.38	0.00140	0.725*
23	31.6	0.47	0.53	0.000880	0.600
24	31.9	0.46	0.54	0.000285	0.683
25	31.7	0.43	0.55	0.000388	0.713
26	31.8	0.45	0.50	0.00203	0.583
27	32.0	0.29	0.31	0.00285	0.568*
28	32.0	0.31	0.33	0.00185	0.672*
30	30.8	0.33	0.41	0.00145	0.747*
31	27.1	0.26	0.28	0.00525	0.385*
32	27.1	0.34	0.40	0.00356	0.310
33	27.1	0.41	0.45	0.000292	0.976*
34	27.1	0.31	0.34	0.00147	0.560*
35	27.1	0.41	0.47	0.00107	0.422
36	27.1	0.32	0.38	0.00149	0.681*

*Denotes 421 demister, other data are for 931 demister.

TABLE D-2
 REGRESSION COEFFICIENTS FROM
 STEPWISE LINEAR REGRESSION ANALYSIS
 OF FLOODING VELOCITY

REGRESSION COEFFICIENTS (R.C.)
 AND STANDARD ERROR (S.E.) OF
 REGRESSION COEFFICIENTS

STEP NO.		$\ln(a/\epsilon^3)$	$\ln(\mu_1)$	$\ln(\rho_1)$	$\ln(G_2)$	$\ln(Y)$	$\ln(e)$	S.E. OF CORR.
1	R.C.	-	-	0.615	-	-	-	
	S.E.	-	-	0.008	-	-	-	0.193
2	R.C.	-0.308	-	0.938	-	-	-	
	S.E.	0.046	-	0.048	-	-	-	0.122
3	R.C.	-0.284	-	1.01	-0.079	-	-	
	S.E.	0.040	-	0.047	0.025	-	-	0.106
4	R.C.	-0.290	-0.087	1.07	-0.106	-	-	
	S.E.	0.028	0.015	0.034	0.017	-	-	0.072
5	R.C.	-0.302	-0.082	0.922	-0.106	-	0.646	
	S.E.	0.029	0.016	0.127	0.017	-	0.549	0.072
6	R.C.	-0.301	-0.036	0.466	-0.108	0.201	1.70	
	S.E.	0.029	0.044	0.429	0.017	0.181	1.09	0.072
7	R.C.	-0.301	-	0.144	-0.108	0.338	2.46	
	S.E.	0.029	-	0.156	0.017	0.062	0.56	0.071

FOR LOADING VELOCITY

1	R.C.	-	-	0.583	-	-	-	
	S.E.	-	-	0.007	-	-	-	0.170
2	R.C.	-0.238	-	0.832	-	-	-	
	S.E.	0.047	-	0.050	-	-	-	0.126
3	R.C.	-0.217	-	0.892	-0.068	-	-	
	S.E.	0.044	-	0.051	0.027	-	-	0.116
4	R.C.	-0.222	-0.063	0.935	-0.088	-	-	
	S.E.	0.039	0.021	0.048	0.025	-	-	0.102
5	R.C.	-0.226	-0.062	0.891	-0.088	-	0.196	
	S.E.	0.042	0.022	0.184	0.025	-	0.794	0.104
6	R.C.	-0.225	-0.033	0.608	-0.089	0.125	0.85	
	S.E.	0.043	0.065	0.633	0.026	0.267	1.61	0.106

REGRESSION OUTPUT, STEP 6, FLOODING VELOCITY

PREDICTED VS ACTUAL RESULTS

RUN NO.	ACTUAL		PREDICTED		DEVIATION	WEIGHT
	$\ln V_F$	V_F	$\ln V_F$	V_F	$\Delta \ln V_F$	
1	2.42480	11.3	2.40179	11.0	✓ 0.02301	1.00000
2	2.39334	10.9	2.40210	11.0	✓ -0.00876	1.00000
3 5	2.48657	12.0	2.40082	11.0	✓ 0.08575	1.00000
4 6	2.74084	15.5	2.68027	14.6	0.06057	1.00000
7 8	2.59077	13.3	2.53756	12.6	✓ 0.05320	1.00000
6 9	2.76254	15.9	2.81154	16.6	-0.04900	1.00000
7 10	2.66236	14.4	2.66527	14.4	-0.00291	1.00000
8 11	2.79117	14.3	2.88662	18.0	-0.09545	1.00000
9 12	2.80940	16.6	2.88482	18.0	-0.07542	1.00000
10 13	2.64688	14.2	2.60213	13.5	✓ 0.04475	1.00000
11 14	2.37304	10.7	2.39860	11.0	✓ -0.02555	1.00000
12 16	2.68102	14.6	2.64276	14.1	0.03826	1.00000
13 17	2.29556	9.9	2.37615	10.8	✓ -0.08059	1.00000
14 18	2.46130	11.7	2.52966	12.0	✓ -0.06836	1.00000
15 19	2.71403	15.1	2.79979	16.5	-0.08576	1.00000
16 20	2.83321	17.0	2.76942	16.0	0.06379	1.00000
17 21	2.50389	12.2	2.45761	11.7	✓ 0.04628	1.00000
18 22	2.47317	11.8	2.47441	11.9	✓ -0.00124	1.00000
19 23	2.82316	16.8	2.75472	15.7	0.06845	1.00000
20 24	2.84491	17.2	2.87034	17.6	-0.02543	1.00000
21 25	2.84955	17.3	2.82688	16.9	0.02267	1.00000
22 26	2.77384	16.0	2.66045	14.3	0.11339	1.00000
23 27	2.28544	9.9	2.39108	10.9	✓ -0.10564	1.00000
24 28	2.36462	10.6	2.42234	11.2	✓ -0.05772	1.00000
25 30	2.53052	12.6	2.47412	11.8	✓ 0.05640	1.00000
26 31	2.03732	7.7	2.14750	8.6	✓ -0.11018	1.00000
27 32	2.38601	10.9	2.42607	11.3	-0.04007	1.00000
28 33	2.50797	12.3	2.40773	11.1	✓ 0.10024	1.00000
29 34	2.23323	9.3	2.26393	9.6	✓ -0.03070	1.00000
30 35	2.54553	12.8	2.53858	12.6	0.00695	1.00000
31 36	2.33020	10.3	2.25112	9.5	✓ 0.07908	1.00000

✓ DENOTES 421 DEMISTER

REGRESSION OUTPUT, STEP 6, LOADING VELOCITY

PREDICTED VS ACTUAL RESULTS						
RUN NO.	ACTUAL		PREDICTED		DEVIATION	WEIGHT
	$\ln V_F$	V_F	$\ln V_F$	V_F	$\Delta \ln V_F$	
1	2.28238	9.8	2.29048	9.9	-0.00810	1.00000
2	2.31254	10.1	2.29145	9.9	0.02109	1.00000
3 5	2.39790	11.0	2.29085	9.9	0.10705	1.00000
4 6	2.20827	9.1	2.49885	12.2	-0.29057	1.00000
5 8	2.51770	12.4	2.40259	11.0	0.11511	1.00000
6 9	2.66026	14.3	2.60849	13.6	0.05177	1.00000
7 10	2.62467	13.8	2.48838	12.0	0.13629	1.00000
8 11	2.59525	13.4	2.67061	14.4	-0.07535	1.00000
9 12	2.56495	13.0	2.66975	14.4	-0.10480	1.00000
10 13	2.48491	12.0	2.45974	11.7	0.02517	1.00000
11 14	2.34181	10.4	2.28814	9.9	0.05367	1.00000
12 16	2.57261	13.1	2.48662	12.0	0.08599	1.00000
13 17	2.23001	9.3	2.29013	9.9	-0.06011	1.00000
14 18	2.36085	10.6	2.41831	11.2	-0.05746	1.00000
15 19	2.49321	12.1	2.62137	13.4	-0.12816	1.00000
16 20	2.67415	14.5	2.60179	13.5	0.07235	1.00000
17 21	2.38876	10.9	2.36797	10.7	0.02079	1.00000
18 22	2.42480	11.3	2.37972	10.8	0.04508	1.00000
19 23	2.70136	14.9	2.59292	13.4	0.10844	1.00000
20 24	2.69463	14.8	2.68891	14.8	0.00572	1.00000
21 25	2.60269	13.5	2.65367	14.2	-0.05098	1.00000
22 26	2.66723	14.4	2.51753	12.4	0.14970	1.00000
23 27	2.21920	9.2	2.31891	10.2	-0.09970	1.00000
24 28	2.28238	9.8	2.34582	10.4	-0.06344	1.00000
25 30	2.31254	10.1	2.37443	10.7	-0.06189	1.00000
26 31	1.94591	7.0	2.07050	7.9	-0.12459	1.00000
27 32	2.29253	9.9	2.27889	9.8	0.01365	1.00000
28 33	2.41591	11.2	2.28565	9.8	0.13027	1.00000
29 34	2.12823	8.4	2.16676	8.7	-0.03853	1.00000
30 35	2.39790	11.0	2.37191	10.7	0.02599	1.00000
31 36	2.15176	8.6	2.15617	8.6	-0.00441	1.00000

✓ DENOTES 421 DEMISTER

REFERENCES

1. Schroeder, H.F., Masters Thesis, Newark College of Engineering, June, 1962.
2. Poppele, E.W., Masters Thesis, Newark College of Engineering, June, 1958.
3. York, O.H., Chemical Engineering Progress, Vol.50, 1954.
4. York, O.H., and Poppele, E.W., Wire Mesh Mist Eliminators, Chemical Engineering Progress, Vol 59, June, 1963.
5. Sherwood, T.K., Shipley, G.H., and Holloway, F.A.L., Flooding Velocities in Packed Columns, Industrial and Engineering Chemistry, Vol 30, July, 1938.
6. Souders, M., and Brown, G.G., Industrial and Engineering Chemistry, Vol 26, 1934.
7. Perry, J.H., ed., Chemical Engineers' Handbook, Third Edition, pages 597-98, 840, 1017-1020, Mc Graw-Hill Book Company, Inc. 1950.
8. Stearns, Jackson, Johnson and Larson, Flow Measurement with Orifice Meters, D. Van Nostrand Company, Inc., 1951.